



NTNU – Trondheim
Norwegian University of
Science and Technology

Design and measurement of a CO₂ refrigeration system with integrated propane subcooler at high air temperature operations

Synne Kathinka Bertelsen
Stine Børslid Haugsdal

Master of Science in Mechanical Engineering

Submission date: June 2015

Supervisor: Trygve Magne Eikevik, EPT

Co-supervisor: Ignat Tolstorebrov, EPT
Inge Håvard Rekstad, EPT
Sigmund Jenssen, Cadio AS

Norwegian University of Science and Technology
Department of Energy and Process Engineering

EPT-M-2015-10

MASTER THESIS

for

Student Synne Kathinka Bertelsen
and student Stine Børslid Haugsdal

Spring 2015

**Design and measurement of a CO₂ refrigeration system with integrated
propane subcooler at high air temperatures operations***Design og målinger på et CO₂ kuldeanlegg med integrert propan kjøler for drift ved høye
lufttemperaturer***Background and objective**

The project is in cooperation with the Cadio AS in Trondheim. The company is developing energy efficient heat pumping system with environmentally friendly working fluids.

The aim of the company is to build module based refrigeration units from 18-20 kW and upwards. These units will be based on standard components, but to be able to deliver units to different climatic zones it is necessary to increase the energy efficiency of the system. Such a solution is to make a new gas cooler for the CO₂ system with integrated condenser for the propane system. One of the challenges is to find the optimal distribution between the two working fluids.

In this thesis the focus will be on optimization of the design and running conditions of the CO₂/propane system at different outdoor air temperatures and find the point/temperature where the propane system starts to operate. It is built a prototype system at Cadio AS production facilities at Heimdal. In the thesis it could be necessary to do some extended measurements on the system to complement the measurements done in the project work.

The following tasks are to be considered:

1. Literature review of CO₂ refrigeration system within the scope of work
2. Plan and perform necessary extended measurements on the prototype system
3. Further developing of a simulation model of the CO₂/propane system
4. Optimization of energy efficiency of the integrated system with focus on the gas cooler/condenser at different ambient temperatures (climate zones)
5. Make proposal of improvement of the existing system and recommendations of operational conditions
6. Write a scientific paper from the main results of the work
7. Make proposals for further work

Within 14 days of receiving the written text on the master thesis, the candidate shall submit a research plan for his project to the department.

When the thesis is evaluated, emphasis is put on processing of the results, and that they are presented in tabular and/or graphic form in a clear manner, and that they are analyzed carefully.

The thesis should be formulated as a research report with summary both in English and Norwegian, conclusion, literature references, table of contents etc. During the preparation of the text, the candidate should make an effort to produce a well-structured and easily readable report. In order to ease the evaluation of the thesis, it is important that the cross-references are correct. In the making of the report, strong emphasis should be placed on both a thorough discussion of the results and an orderly presentation.

The candidate is requested to initiate and keep close contact with his/her academic supervisor(s) throughout the working period. The candidate must follow the rules and regulations of NTNU as well as passive directions given by the Department of Energy and Process Engineering.

Risk assessment of the candidate's work shall be carried out according to the department's procedures. The risk assessment must be documented and included as part of the final report. Events related to the candidate's work adversely affecting the health, safety or security, must be documented and included as part of the final report. If the documentation on risk assessment represents a large number of pages, the full version is to be submitted electronically to the supervisor and an excerpt is included in the report.

Pursuant to "Regulations concerning the supplementary provisions to the technology study program/Master of Science" at NTNU §20, the Department reserves the permission to utilize all the results and data for teaching and research purposes as well as in future publications.

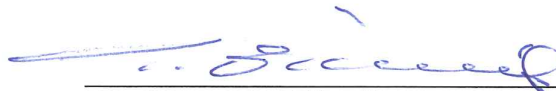
The final report is to be submitted digitally in DAIM. An executive summary of the thesis including title, student's name, supervisor's name, year, department name, and NTNU's logo and name, shall be submitted to the department as a separate pdf file. Based on an agreement with the supervisor, the final report and other material and documents must be given to the supervisor in digital format. All relevant data collected and produced during the project shall be delivered to the supervisor on a Memory stick at the end of the project.

- Work to be done in lab (Water power lab, Fluids engineering lab, Thermal engineering lab)
 Field work

Department of Energy and Process Engineering, January 12th 2015



Prof. Olav Bolland
Department Head



Prof Trygve M. Eikevik
Academic Supervisor
e-mail: trygve.m.eikevik@ntnu.no

Co-Supervisor(s):
Sigmund Jensen, Cadio AS
Ignat Tolstorebrov
Håvard Rekstad, NTNU

e-mail(s)
sigmund@cadio-as.com
ignat.tolstorebrov@ntnu.no
havard.rekstad@ntnu.no

Preface

This master thesis is a part of the Mechanical Engineering study programme at the Norwegian University of Science and Technology (NTNU). The thesis has been written for the Department for Energy and Process Engineering at NTNU, during the spring of 2015.

This project has been a collaboration between NTNU and Cadio AS.

We would like to thank Professor Trygve Magne Eikevik for great guidance and for his dedication to the project and Armin Hafner for helpful advice with improvements. We would also use this opportunity to thank Trond Andresen for useful assistance with HXsim and Inge Håvard Rekstad for advantageous consultations.

We would like to acknowledge the help from Sigmund Jenssen at Cadio AS for good academic discussions and guidance. Finally yet importantly, we thank Roger Tellefsen for useful help with the prototype system.

Trondheim, 2015-06-05

Synne Bertelsen, Stine Haugsdal

Summary

After the rediscovery of CO₂ as a prominent, environmentally benign working fluid, several technological modifications for the basic CO₂ refrigeration cycle has been reviewed. These have been presented as solutions to the low Coefficient of Performance experienced in high air temperature operations. This is due to the great correlation between the ambient air temperature and the enthalpy after the gas cooler in the CO₂ refrigeration cycle. Economisers, mechanical subcoolers, ejectors, expanders, CO₂ integrated systems, parallel and auxiliary compression for flash vapour compression and evaporative cooling are technology solutions that mainly is implemented to reduce the energy consumption and the enthalpy before throttling in the basic CO₂ cycles.

Cadio AS has developed a CO₂ system with a secondary propane cycle for operation at higher ambient temperatures. The system has a CO₂ gas cooler with integrated propane condenser and a propane subcooler that condenses the CO₂. This allows subcritical operation at all ambient temperatures.

A prototype unit in a production facility at Heimdal was instrumented and tested during the project thesis work. Measurement data were corrected and the optimal point for start of the propane operation was found at an ambient temperature of 23,5°C. Further, these measurement data has been compared to results from a simulation model developed using the Heat Exchanger simulation program (HXsim) and the Engineering Equation Solver (EES). Simulations showed that a propane set point corresponding to an ambient temperature of 19,4°C provides the best Coefficient of Performance. However, when the propane system is not in operation, the refrigeration capacity starts to drop significantly from an ambient temperature of 15°C.

Several different modifications of the integrated condenser/gas cooler has been tested in HXsim. A minimum increase of 9 % in the Coefficient of Performance can be achieved when implementing an improved CO₂ condenser design at an ambient temperature of 19°C. By implementing a new propane condenser, the systems Coefficient of Performance can increase with 16,2 % at an ambient temperature of 40°C. By rising the fan speed, the performance of the system can be increased even further. When implementing the improved propane condenser, a smaller propane

compressor can be applied, thus energy savings on the propane system can be achieved.

Performance of the system was tested for different European capitals. The seasonal performance in Madrid was found to be 2,85 in comparison to 3,22 in Oslo. The propane system also have almost three more months of operation in Madrid than Oslo, which clarifies the importance of the set point and efficient high temperature operations.

Various system modifications has been investigated and simulated in EES. The modified system that gave the best seasonal performance for the capitals with the warmest climates proved to be the mechanical subcooling system, even though the prototype system provided the best Coefficient of Performance at high ambient temperatures. The mechanical subcooling system also provided the best refrigeration capacity up to an ambient temperature of 37°C, where the prototype system competes when it comes to refrigeration capacity. The transcritical system with an internal heat exchanger had an improved refrigeration capacity of 5-6% at high temperature operation compared to the simple transcritical system. This indicates a simple and cost-effective method for improving the refrigeration capacity of the system.

Sammendrag

Etter gjenoppdagelsen av CO₂ som et fremtredende og miljøvennlig kjølemedium, har flere teknologiske modifikasjoner for den grunnleggende CO₂ kjølesyklusen blitt undersøkt. Disse er blitt presentert som løsningen på den lave kuldefaktoren for CO₂ kjølesystemer i varme omgivelser. Dette er grunnet den sterke korrelasjonen mellom utetemperaturen og entalpien etter gasskjøleren i CO₂ kjølesyklusen. Economisere, mekanisk underkjøling, ejektorer, expandere, CO₂ integrerte systemer, hjelpe- og parallellkompressorer for kompresjon av flash damp og fordamningskjøling er teknologiske løsninger som hovedsakelig som er foreslått for å redusere energibehovet og entalpien før struping i den grunnleggende CO₂ kjølesyklusen.

Cadio AS har utviklet et CO₂ system med en propan sekundærdel for operasjon ved høye utetemperaturer. Systemet har en integrert CO₂ gasskjøler med en propan-kondensator, samt en propan- underkjøler som absorberer varme fra CO₂-enheten. Dette tillater subkritisk operasjon ved alle utetemperaturer.

Prototypen, lokalisert i et produksjonslokale på Heimdal, har blitt instrumentert og testet for videre analysering under prosjektarbeidet. Måledataene har blitt korrigerte og det optimale startpunkt for propansystem ble funnet ved en utetemperatur på 23,5 °C. Videre ble disse måledataene sammenlignet med resultater fra et simuleringsprogram for varmevekslere (HXsim) og et termodynamisk programmeringsspråk (EES). Simuleringer viste at et innslagspunkt for propansystemet ved en utetemperatur på 19,4 °C ga den beste kuldefaktoren. Når propansystemet ikke kjører vil kuldeytelsen avta betydelig fra en utetemperatur på 15 °C.

Flere ulike modifikasjoner av den integrerte kondensator/gasskjøleren ble testet i HXsim. Hvis det foreslåtte kondensatordesiget blir implementert, kan systemet oppleve en økning i kuldefaktoren på minimum 9 %. Dette er ved en omgivelsestemperatur på 19 °C. Ved å implementere en ny propankondensator, kan kuldefaktoren økes med 16,2% ved en utetemperatur på 40 °C. Ved å øke viftehastigheten kan kuldefaktoren til systemet heves med 15 %. Hvis den foreslåtte propankondensatoren blir implementert, kan en mindre propankompressor tas i bruk.

Systemets ytelse ble testet i ulike europeiske hovedsteder. Den sesongmessige kuldefaktoren i Madrid var 2,85 sammenlignet med 3,22 i Oslo. Propansystemet opererer i nærmere tre måneder

mer i Madrid enn i Oslo. Dette understreker betydningen av innslagspunktet samt en velfungerende høytemperaturoperasjon.

Ulike systemmodifikasjoner ble undersøkt og testet i EES. Den systemmodifikasjonen som ga best SCOP for hovedstedene med varmest klima var mekanisk underkjøling, til tross for at prototypesystemet hadde den beste kuldefaktoren ved høye utetemperaturer. Systemet med mekanisk underkjøling viste best kjølekapasitet opp til en utetemperatur på 37°C, hvor prototypesystemet kan konkurrere med tanke på kjølekapasitet. Det transkritiske systemet med en internvarmeveksler fikk en forbedret kjølekapasitet på 5-6% ved høytemperaturoperasjon sammenlignet med det enkle transkritiske systemet. Dette er en enkel metode for å forbedre kjølekapasiteten til systemet.

Contents

Preface	iii
Summary	iv
Sammendrag	vi
Table of Contents	x
List of Tables	xii
List of Figures	xvi
Nomenclature	xvii
Abbreviations	xviii
1 Introduction	1
2 Objectives	3
3 Literature survey	5
3.1 CO ₂ as a refrigerant	5
3.1.1 Internal heat exchangers	8
3.1.2 Expanders	9
3.1.3 Booster systems	10
3.1.4 Economisers	11
3.1.5 Auxiliary or parallel compressors for flash vapour compression	11

3.1.6	Ejectors	13
3.1.7	Subcooling	15
3.1.8	Evaporative Cooling	16
3.1.9	Optimisation of the transcritical cycle	17
3.1.10	Summary	17
4	Theory	19
4.1	Physical and thermophysical properties of CO ₂	19
4.2	Basic refrigeration cycle	21
4.3	Heat transport	25
4.4	Air cooled tube-and-fin CO ₂ heat exchangers	26
4.5	Description of the system	28
5	Analysis	35
5.1	Initial plan for simulation and optimisation of the prototype system	35
5.2	Simulation model of prototype system	36
5.2.1	Fundamental simulation model	38
5.2.2	Simulation in EES with restrictions developed in HXsim	42
5.3	Optimisation of energy efficiency	47
5.3.1	Modifications condenser and gas cooler	47
5.3.2	Modifications overall system	60
6	Results	63
6.1	Measurements and simulation model	63
6.1.1	System operation in European capitals	68
6.2	Modification condenser and gas cooler	70
6.2.1	Modification of the CO ₂ condenser	70
6.2.2	Modification of the CO ₂ gas cooler	73
6.2.3	Modifications of the propane condenser	74
6.2.4	Fan modifications	77
6.3	Modifications overall system	78

7 Discussion	83
7.1 Measurements and simulation model	83
7.1.1 Comparison of measurements and simulation	84
7.1.2 Prototype simulation	86
7.1.3 System operation in some selected European capital cities	88
7.2 Modification of the condenser and gas cooler	89
7.2.1 Modification of the CO ₂ condenser	89
7.2.2 Modification of the CO ₂ gas cooler	91
7.2.3 Modification of the propane condenser	92
7.2.4 Fan modifications	94
7.3 Modifications overall system	95
8 Conclusion	99
9 Proposal for further work	101
Reference list	103
A Additional Information	107
A.1 Files on flash drive	107
A.2 Scientific paper	108
A.3 List of instrumentation components	118
A.4 Modifications condenser and gas cooler	119
A.5 System operation in European capitals	122
A.6 EES scripts	126

List of Tables

4.1	Data from design point (Cadio AS).	30
4.2	Set point refrigeration unit described by R744 high side pressure.	32
4.3	Overview of the system components.	33
5.1	Conditions for performed tests during project thesis.	36
5.2	Assumptions and restrictions for simulation model.	37
5.3	Specifications simulation HXsim.	43
5.4	Modifications CO ₂ condenser at a T_{amb} of 18,7°C.	53
5.5	Modifications propane condenser at a T_{amb} of 40°C.	54
5.6	Modifications CO ₂ gas cooler at a T_{amb} of 40°C.	54
6.1	Obtained Q_o , COP and T_a from tests performed during project thesis.	64
6.2	Set point for start of propane operation.	67
6.3	System performance in different climates.	68
6.4	Best CO ₂ condenser configuration modifications at a T_{amb} of 18,7°C.	70
6.5	Increase in Q_o and COP as a result of CO ₂ subcooling.	73
6.6	Subcooling calculated as a decrease in work including an increase in Q_o .	73
6.7	Increase in COP when the work/condensing pressure is decreased.	73
6.8	Best CO ₂ gas cooler configurations at a T_{amb} of 40°C. Enhancement factor 0,7.	74
6.9	Best propane condenser configurations at a T_{amb} of 40°C.	74
6.10	Propane subcooling calculated as an increase in Q_o and an increase in COP for the overall system.	76

6.11 Propane subcooling calculated as a decrease in work including an increase in Q_o for the overall system.	76
6.12 Increase in the overall systems COP when work is decreased as a result of improved propane condenser.	76
6.13 The best CO ₂ condenser configurations with suggested integrated propane condensers.	77
6.14 Seasonal performance and yearly energy consumption for modifications.	80
7.1 Comparison of optimal start of propane operation for the best COP.	88
7.2 System performance in different climates.	88
7.3 Seasonal performance and yearly energy consumption for modifications.	96
A.1 Overview of instrumentation component	118

List of Figures

3.1	Refrigeration system with suction line heat exchanger.	8
3.2	Simple expander cycle (Hafner, Hemmingsen, and Van de Ven 2014).	9
3.3	Standard R744 booster system (Hafner, Hemmingsen, and Van de Ven 2014). . . .	10
3.4	Economiser(Hafner, Hemmingsen, and Van de Ven 2014).	12
3.5	Two stage throttling using an auxiliary compressor (Fornasieri, Zilio, et al. 2009). .	12
3.6	Transcritical R744 booster system using parallel compression with and without ejector support (Hafner, Schonenberger, et al. 2014).	14
3.7	Simplified transcritical R744 refrigeration system with mechanical subcooler unit (Hafner, Hemmingsen, and Van de Ven 2014).	16
3.8	Evaporative cooling of a gas cooler (Fornasieri, Zilio, et al. 2009).	17
4.1	Temperature loss versus pressure loss for CO ₂ compared to other refrigerants (Eike- vik 2015).	20
4.2	Influence of gas cooler pressure and exit temperature on COP (Eikevik 2015). . . .	21
4.3	Influence of the temperature before expansion and gas cooler pressure on the re- frigeration capacity (Eikevik 2015).	21
4.4	Basic refrigeration cycle.	22
4.5	R744 refrigeration cycles.	23
4.6	Flow chart CO ₂ refrigeration system with integrated propane subcooler.	29
4.7	Location of instrumentation components.	31
4.8	Heat exchange subcooler.	31
4.9	The R744/R290 gas cooler (Cadio AS).	32

4.10 The R744/R290 unit (Cadio AS).	34
4.11 Application envelope for the CO ₂ compressor (Dorin 2014).	34
5.1 Volumetric and isentropic efficiency for the CO ₂ compressor.	38
5.2 Volume flow air as a function of condensing temperature.	39
5.3 Flow chart for obtaining correlations from HXsim.	41
5.4 Integrated CO ₂ and propane condenser seen from above.	42
5.5 Hxsim models of CO ₂ condenser and propane condenser.	43
5.6 LMTD as a function of CO ₂ condensing temperature.	44
5.7 U-value for CO ₂ condenser as a function of ambient temperature.	44
5.8 Process flow chart of simulation model in EES with input variables T_{amb} and propane operational variable ON/OFF	46
5.9 Original configuration with propane condenser (6-1-7) and CO ₂ gas cooler (6-2-7). The air flow is represented by the blue arrow.	48
5.10 Example of a 6-3-2 condenser.	49
5.11 Condenser modification with propane in the middle pipeline row, and CO ₂ in the two outer pipelines.	50
5.12 CO ₂ front row, shared last row.	51
5.13 Condenser modification with propane condenser tubes at the bottom and CO ₂ tubes at the top.	51
5.14 Original gas cooler configuration with an enhancement factor of 1,1 at a T_{amb} of 22°C.	55
5.15 Original gas cooler configuration with an enhancement factor of 0,7 at a T_{amb} of 22°C.	56
5.16 Temperature plot for the CO ₂ 15-2-3 gas cooler configuration with 45°C inlet air temperature. 8 % heat balance deviation.	56
5.17 Temperature plot for the CO ₂ 15-2-3 gas cooler configuration at 22°C inlet air tem- perature and normal simulation control.	57
5.18 Temperature plot for the CO ₂ 15-2-3 gas cooler configuration with 6°C inlet air temperature.	58

5.19 Temperature plot for the CO ₂ 9·3·3 gas cooler configuration with 6°C inlet air temperature.	58
5.20 Temperature plot for the CO ₂ 15·2·3 gas cooler configuration with 15,5°C inlet air temperature.	59
5.21 Temperature plot for the CO ₂ 9·3·3 gas cooler configuration with 15,5°C inlet air temperature.	59
5.22 Transcritical CO ₂ refrigeration system.	60
5.23 Transcritical CO ₂ refrigeration unit with internal heat exchanger.	61
5.24 CO ₂ refrigeration system with mechanical subcooling using propane.	62
6.1 COP from measurements.	64
6.2 Refrigeration capacity from measurements.	64
6.3 Comparison of Q _o without propane operation.	65
6.4 Comparison of COP without propane operation.	65
6.5 Comparison of Q _o with propane operation.	65
6.6 Comparison of COP with propane operation.	66
6.7 Simulated refrigeration capacity with and without propane.	66
6.8 Simulated COP with and without propane.	67
6.9 Log p-h diagram for the prototype system at T _{amb} = 35°C.	68
6.10 Ambient temperature versus refrigeration capacity in Madrid 2005.	69
6.11 Ambient temperature versus COP in Madrid 2005.	69
6.12 Subcooling for the best CO ₂ configurations.	71
6.13 Performance improvement for the CO ₂ condenser as subcooling and reduced pressure.	71
6.14 Refrigeration capacity including CO ₂ subcooling.	72
6.15 COP including CO ₂ subcooling.	72
6.16 Subcooling for the best propane configurations.	75
6.17 Refrigeration capacity when including propane subcooling.	75
6.18 COP when including propane subcooling.	75
6.19 Subcooling for integrated propane condenser options.	77

6.20	New fan set points for the 12·3·2 configuration with zero subcooling.	78
6.21	Effect on COP for original CO ₂ condenser when fan speed is doubled.	78
6.22	Comparison of refrigeration capacity for the modifications.	79
6.23	Comparison of COP for the modifications.	79
6.24	R744 log(p)-h diagram for the transcritical system at $T_{amb} = 35^{\circ}\text{C}$	81
6.25	R744 log(p)-h diagram for the transcritical system with internal heat exchanger at $T_{amb} = 35^{\circ}\text{C}$	81
6.26	Log(p)-h diagram for the mechanical subcooling system at $T_{amb} = 35^{\circ}\text{C}$	82
7.1	Comparison of Q_o and COP from measurements.	84
7.2	Comparison of Q_o and COP from measurements and simulations without propane operation.	86
7.3	Comparison of Q_o and COP from measurements and simulations with propane operation.	86
7.4	Subcooling for the best CO ₂ configurations.	90
7.5	Subcooling for the best propane configurations.	93
7.6	Effect on COP for original CO ₂ condenser when fan speed is doubled.	95
A.1	CO ₂ condenser configurations with four rows and different vertical duplications. . .	119
A.2	CO ₂ condenser configurations with new pipe dimension.	119
A.3	CO ₂ condenser configurations with two/ three rows and different vertical duplica- tions.	120
A.4	Propane condenser configurations with different vertical duplications.	121
A.5	Ambient temperature versus refrigeration capacity in Oslo 2005.	122
A.6	Ambient temperature versus COP in Oslo 2005.	122
A.7	Ambient temperature versus refrigeration capacity in London 2005.	123
A.8	Ambient temperature versus COP in London 2005.	123
A.9	Ambient temperature versus refrigeration capacity in Paris 2005.	124
A.10	Ambient temperature versus COP in Paris 2005.	124
A.11	Ambient temperature versus refrigeration capacity in Budapest 2005.	125
A.12	Ambient temperature versus COP in Budapest 2005.	125

Nomenclature

A	Heat transfer area	m^2
c_p	Specific heat capacity	$\frac{J}{kg \cdot K}$
h	enthalpy	$\frac{kJ}{kg}$
\dot{m}	mass flow rate	$\frac{kg}{s}$
P	Pressure	bar
\dot{Q}	Heat transfer rate	kW
Q_o	Refrigeration capacity	kW
T	Temperature	$^{\circ}C$
ΔT	Temperature difference	K
ΔT_{LMTD}	Log mean temperature difference	K
U	Heat transfer coefficient	$\frac{W}{m^2 K}$
V_{suc}	Suction volume	$\frac{m^3}{s}$
V_s	Swept volume	$\frac{m^3}{s}$
ν	Specific volume	$\frac{m^3}{kg}$
\dot{W}	Work	kW
W_{theo}	Theoretical work	kW
η_{is}	isentropic efficiency	-
π	Pressure ratio	-
λ	Volumetric efficiency	-

Subscripts

a	approach
amb	ambient
p	propane

Abbreviations

BC	Bypass Compressor
CFC	Chlorofluorocarbons
CFD	Computational fluid dynamics
COP	Coefficient Of Performance
CSC	Combined Secondary Cascade
DX	Direct Expansion
EES	Engineering equation solver
EU	European Union
GWP	Global Warming Potential
HCFC	Hydrochlorofluorocarbons
HFC	Hydrofluorocarbons
IHX	Internal Heat Exchangers
LMTD	Logarithmic Mean Temperature Difference
MT	Medium temperature
ODP	Ozone Depletion Potential
R134a	1,1,1,2-Tetrafluoroethane
R22	Chlorodifluoromethane
R290	Propane
R404a	R-125/143a/134a (44±2/52±1/4±2)
R414a	1,1-Dichloro-2-fluoroethane
R610	Ethyl ether
R744	Carbon dioxide
Rnlib	Refrigerant Routine Library
SCOP	Seasonal Coefficient of Performance
SLHX	Suction Line Heat Exchangers

Chapter 1

Introduction

The development of CO₂ as a refrigerant has been intriguing. From being discovered as a natural working fluid at the 19th century, nearly abandoned during the second world war to later be rediscovered at the end of the 20th century. This ideal refrigerant as described by Gustav Lorentzen is environmentally benign with zero Global Warming Potential (GWP) and zero Ozone Depletion Potential (ODP), safe, cheap and compatible with normal machine construction. The prevalence of R744 refrigeration is experiencing a steady increase. This trend is especially seen in northern climates, due to the reduced efficiency of the basic CO₂ cycle in warmer climates when compared to other synthetic refrigerants.

When the ambient temperature is increasing, the basic CO₂ cycle experience a decrease in the refrigeration capacity (Q_o), thus the Coefficient of Performance (COP). The challenge is to keep both the gas cooler outlet enthalpy and the power consumption as low as possible. Today, an array of technology solutions are available that improve the system efficiency in higher ambient temperatures, including but not limited to economisers, mechanical subcoolers, ejectors, expanders, CO₂ integrated systems, parallel compression and auxiliary compressors for flash vapour compression and evaporator overfeed.

Cadio AS approach to the problem is a CO₂ system with integrated propane subcooler for high air temperatures operations. This subcooler is only in operation above a certain temperature, due to the extra compressor work of the propane cycle. During the project work in 2014, in-

strumentation and testing of Cadio's prototype was performed. During the development of the master thesis in spring 2015, the performance of the prototype system has been identified using simulation programs HXsim and EES. The integrated CO₂ and propane condenser has been simulated in HXsim, and compared to other configurations in order to optimise the heat exchanger. Further on, an operational optimisation has been performed, testing various system designs in EES.

Chapter 2

Objectives

Cadio AS has developed a CO₂ system with integrated propane subcooler. The subcooler will only operate when the high CO₂ side pressure reaches 67 bar. The operation of the system will be further investigated in the master thesis. The main objectives of the thesis are

- Literature review of CO₂ refrigeration system that operates efficiently in warmer climates.
- Plan and perform necessary measurements on the prototype system if necessary.
- Map the performance of the integrated CO₂/propane condenser/gas cooler in HXsim.
- Develop a simulation model in EES with implemented HXsim correlations.
- Simulate the performance of the system over a one year period and compare the seasonal coefficient of performance and average cooling capacity for different set points and climates.
- Optimisation of energy efficiency of the system with focus on the condenser/gas cooler at different ambient temperatures (climate zones).
- Make proposal of improvement of the existing system and recommendations of operational conditions.
- Write a scientific paper from the main results of the work.
- Make proposals for further work.

Chapter 3

Literature survey

3.1 CO₂ as a refrigerant

The first commercial refrigeration system was invented by Jacob Perkins in 1834, using ethyl ether (R610) (Dincer 2003). A few years later in 1866 Thaddeus invented an ice production machine using CO₂ (R744) as a refrigerant (Thevenot 1979). Later over 50 chemical substances has been used as refrigerants in commercial systems. In the early 1930's, chlorofluorocarbons (CFC) was introduced to refrigerant and air-conditioning systems. The main advantages put forward in their favor were harmlessness to the environment and comprehensive safety. This led to a drastic decline in the use of natural refrigerants such as CO₂. Despite the fact that the CFC and hydrochlorofluorocarbons (HCFC) refrigerants were stated to be some of the most useful chemical substances ever developed, the consumption was heavily reduced during the 1990's (Dincer 2003). This was due to the revelation of their high Ozone Depleting Potential (ODP) and Global Warming Potential (GWP). Two governing environmental issues. In 1993 Gustav Lorentzen emphasised the fact that CO₂ was as close to an ideal refrigerant as possible (Lorentzen 1993). CO₂ as a working fluid is environmentally benign with zero GWP and zero ODP. CO₂ is also safe, cheap and compatible with normal machine construction. Later it was shown that CO₂ was a viable refrigerant for mobile air conditioning (Lorentzen and Pettersen 31 July 1992), heat pump water heaters, heat pumps for space conditioning, heat pump dryers, as well as a commercial

refrigerant.

CO₂ has a low critical temperature of 31,3°C and high critical pressure of 73,8 bar. Standard transcritical CO₂ systems achieves the highest Coefficient of Performance (COP) in northern climates, due to the fact that CO₂ refrigeration systems are sensitive to increased ambient temperatures. The gas cooler outlet enthalpy is principally dependent on the inlet temperature of the coolant, but is also influenced by the high side pressure. For the subcritical cycle, the enthalpy is mainly dependent on the temperature. While in transcritical operation the enthalpy is also dependant on the gas cooler pressure. This can be seen as S-shaped isotherm in the supercritical region. This results in a need for pressure control in the supercritical region. When conventional refrigeration system has a decrease in the COP after an increase in discharge pressure, this is not the case for the CO₂ transcritical cycle. Due to high throttling loss and the gliding heat rejection temperature, the COP for a CO₂ system is notably sensible to the gas cooler exit temperature. To be able to achieve requested refrigeration capacity it is important that the enthalpy before the throttling is as low as possible. In warmer climates this aspect has challenged the commercialisation of CO₂ refrigeration systems, due to a considerable lower COP compared to other conventional systems. During the last decades several methods have been developed and researched in order improve the efficiency of CO₂ refrigeration systems.

The supply of CO₂ systems is increasing rapidly, especially in the Northern and Southern part of Europe. The CO₂ equator is being moved further and further south. Commercial refrigeration systems have experienced a penetration rate of 64 % (ATMOsphere 2015). Europe has experienced an increase of 117 % CO₂ transcritical supermarket over the last two years (shecco 2014). There are also 1,639 stores using CO₂/HFC cascade systems in Europe, an addition to the 2885 transcritical R744 stores. However, in warmer countries the amount of transcritical R744 systems are way less common. Japan also has an increased market share with more than 600 food retails using CO₂, and marked predictions claims that China and North America soon will follow these trends (shecco 2014).

There is a clear tendency towards developing all-natural solutions for warm climates in order to expand the uptake of CO₂ in commercial refrigeration to the southern part of Europe. Today, an array of technology solutions are available that improve the system efficiency in higher ambient

temperatures, including but not limited to economisers, mechanical subcoolers, ejectors, expanders, CO₂ integrated systems, parallel and auxiliary compression for flash vapour compression and evaporator cooling. However, these systems still have great potential when it comes to increasing energy and cost efficiency. The European Union (EU) “20-20-20” target sets three objectives for year 2020. This includes a 20 % reduction in EU’s greenhouse gas emissions and a 20 % improvement in the EU’s energy efficiency (Comission [2014](#)). EU has also implemented the F-gas regulation in order to reduce HFC emissions from the HVAC and refrigeration industry. New stricter measures is expected from EU in the future, in order to phase down HFC’s and ban fluorinated greenhouse gases. Denmark has even stricter regulations than the EU policy, and is today a leader in the use of CO₂ refrigeration technology with 712 transcritical stores (shecco [2014](#)). This is the highest number of transcritical R744 stores in Europe. Refrigeration systems represents a great part of today’s energy consumption and an optimisation of these systems can play an important role in reaching the climate targets in Europe, but also in other continents.

A review of the most promising technologies for CO₂ systems at high air temperature operations is provided below.

- Internal heat exchangers
- Expanders
- Auxiliary compressors for flash vapour compression
- Booster systems
- Economisers
- Ejectors
- Subcooling
- Parallel Compression
- Evaporative Cooling

3.1.1 Internal heat exchangers

For some refrigerants it is beneficial to include an internal heat exchanger (IHX) between the suction line and the gas cooler outlet. These are often referred to as suction line heat exchangers (SLHX). Implementation results in two effects; increased refrigeration capacity due to subcooling and increased compressor work due to increased suction temperature. The impact on the systems overall efficiency depends on the operating conditions and the refrigerant used. For refrigerants like chlorodifluoromethane and tetrafluoroethane (R22 and R134a), the implementation of an internal heat exchanger will have a negative effect on the overall efficiency. However, for CO₂ there are prominent benefits because the optimal pressure is lowered when including an internal heat exchanger and the throttling losses are reduced (Kima, Pettersen, and Bullard 2004). Implementation of an SLHX improves the COP in a range from 2 to 4 % for the conventional R744 cycle (Kadam, Padalkar, and Walekar 2013). This COP yield is calculated when the ambient temperature exceeds 35 °C. When this system was tested with a rise in evaporating temperature, the COP increased rapidly. A 12 % increase in cooling capacity for transcritical R744 cycles with high gas cooler outlet temperatures has been achieved (Torella et al. 2011). However, it has also been discovered an increase in compressor discharge temperature, to 10 °C at an evaporating temperature of 15 °C. This limits the operation of the plant at low evaporating levels.

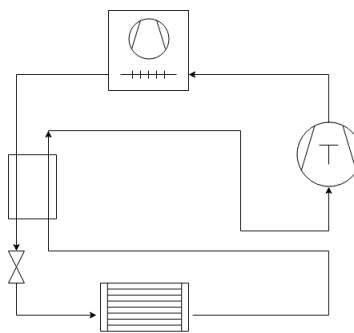


Figure 3.1: Refrigeration system with suction line heat exchanger.

3.1.2 Expanders

CO₂ cycles have much greater throttling loss compared to conventional refrigerants, due to the large pressure change in the expansion process. Thus, the benefits of including an expander have a greater impact compared to cycles with other working media. The advantages include increased refrigeration capacity and decreased compression work as a result of recovered expansion work. The amount of recovered work depends on the isentropic efficiency of the expander. In transcritical cycles the efficiency is better compared to subcritical cycles, since most of the expansion occur in the dense gas phase where the friction is less than in the two-phase region. A great amount of research has been directed to CO₂ transcritical cycles using expanders. The COP of a system with an expander is 6-10 % higher compared to systems without expanders (Maa, Liu, and Tian 2013). At the Technical University of Dresden expander design has been developed from laboratory work since 1994 (Nickl et al. 2005). One expander developed, has been used for transcritical operation in a supermarket in Switzerland. Later on an expander/compressor in subcritical operation has been shown to be possible. The cost of the expander/compressor was less than 30 % of the associated main compressor. Operational cost, in terms of power savings, will easily cover these costs (Riha, Quack, and Nickl 2006). In the laboratory at the Technical University of Dresden, it was also shown that that a system with three-stage expander would increase the COP by 40 % in comparison to a using a throttling valve. The maturity of expander in commercial systems has not been proven yet and need further research to be implemented in commercial cycles (Hafner, Hemmingsen, and Van de Ven 2014).

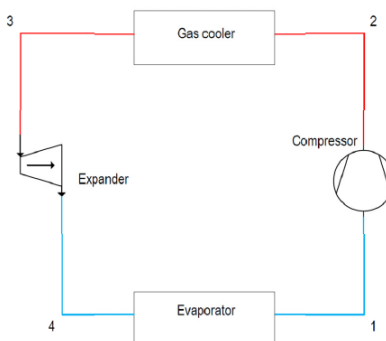


Figure 3.2: Simple expander cycle (Hafner, Hemmingsen, and Van de Ven 2014).

3.1.3 Booster systems

There are different configurations of the booster system, the standard R744 booster system is seen in figure 3.3. The main part of the currently installed CO₂ refrigeration systems in Northern Europe are standard R744 booster systems with bypass control from the flash tank to the suction line. Only the medium pressure level is included in the figure, since the low temperature part are similar. The system consist of three pressure levels, four pressures including the low temperature freezing unit. The high pressure level is not located in the same area, but outside the refrigeration area. The standard booster system is installed with a small capacity subcooling device, if system shut down should occur. This is connected to the flash tank and maintains the pressure level above blow out limit for the safety valve (Hafner, Hemmingsen, and Van de Ven 2014).

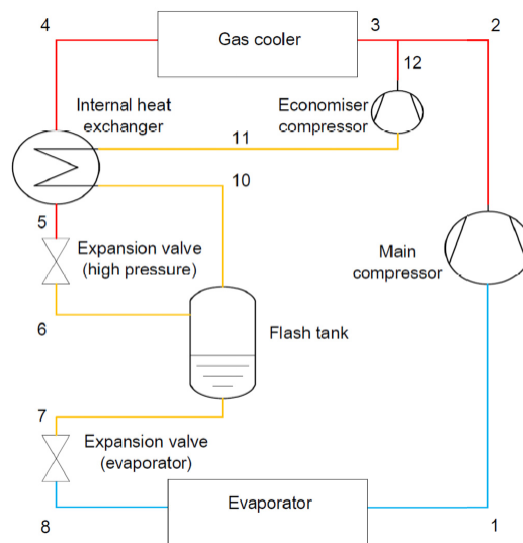


Figure 3.3: Standard R744 booster system (Hafner, Hemmingsen, and Van de Ven 2014).

In a study presented in (Sharma, Fricke, and Bansal 2014), a transcritical R744 booster system with a bypass compressor was compared to a HFC R404A multiplex direct expansion (DX) system and a combined secondary cascade (CSC) system using R744 and R404A. All systems were operating subcritically. The systems performances were simulated for the climate in 88 cities from all climate zones in Southeast Asia. It was found that the transcritical booster system performed better or equal to the R-404A multiplex DX system in the northern regions of Southeast Asia (China and Japan). In the southern regions of Southeast Asia (India, Bangladesh, Burma),

the R404A multiplex DX and the CSC systems achieved a better performance than the booster system. The booster R744 system achieved the highest COP for temperatures below 10°C, but at temperatures between 22°C to 33°C, the COP were comparable for the R744 and the R404A systems.

3.1.4 Economisers

A further technique to reduce the energy consumption in a R744 system is by utilising an intermediate heat exchanger, referred to as economisers. These heat exchangers usually expand a small part of the liquid at intermediate pressure to further subcool the main stream before it enters the second part of throttling. In figure 3.4, an economiser configurations described by (Hafner, Hemmingsen, and Van de Ven 2014) is presented. An economiser expansion valve is connected to an internal heat exchanger and provides subcooling to the main refrigerant from the gas cooler before it is compressed to the high pressure side. The control strategy for the expansion valve occurs in two operations; The economiser expansion valve is only in operation when the ambient temperature exceeds 20°C. When the ambient temperature reaches 40°C the economiser circuit will be able to lower the temperature entering the expansion valve before the evaporator to 25°C (Hafner, Hemmingsen, and Van de Ven 2014).

R744 system architectures with economisers are becoming widespread in Europe and have a significantly improved efficiency compared to the standard booster systems. However, at very high ambient temperatures additional equipment must be installed for the economiser system to be able to compete with mechanical subcooling that provides additional equipment and installation cost (Hafner, Hemmingsen, and Van de Ven 2014).

3.1.5 Auxiliary or parallel compressors for flash vapour compression

The simple cycle is extended by using an auxiliary compressor that removes the vapour appearing in the open flash tank after the first expansion. The remaining liquid is throttled to evaporator pressure, where it is further evaporated and compressed. The process is illustrated in

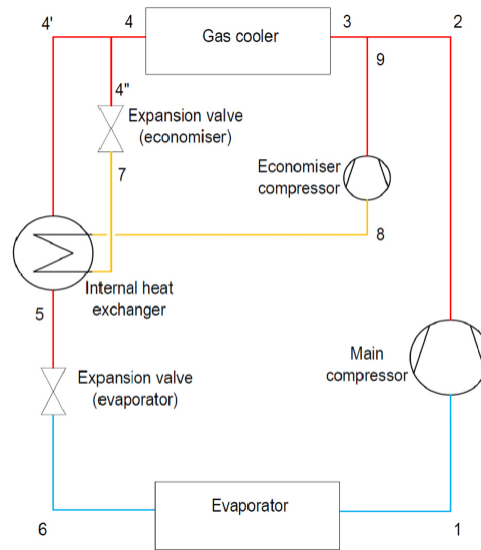


Figure 3.4: Economiser (Hafner, Hemmingsen, and Van de Ven 2014).

figure 3.5. The advantages with an auxiliary compressors cycle arise from the two-stage throttling since the vapour appearing in the flash tank is compressed directly from the intermediate to the high pressure level, and thereby saving compressor work and expansion losses. This cycle is advantageous when the temperature level in the evaporator is not too low, where optimum compressor ratio and efficiency is attainable. In this manner, the cycle will improve the energy efficiency and larger refrigeration capacities are achievable (Fornasieri, Zilio, et al. 2009). Problems with oil recovery at the crankcases of the compressor, limits the operation of this cycle. This is due to the operation at different pressures and the oil level equalisation by gravity is not achieved. A solution to this issue, is the parallel compression cycle.

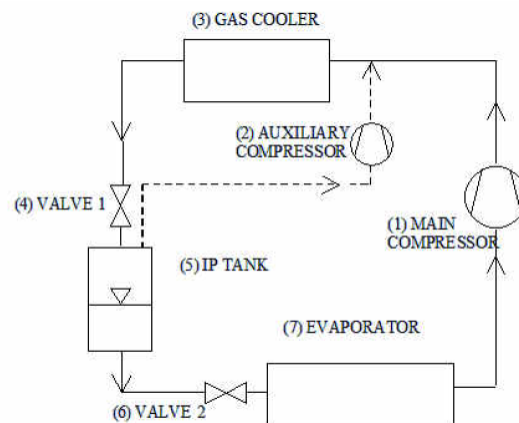


Figure 3.5: Two stage throttling using an auxiliary compressor (Fornasieri, Zilio, et al. 2009).

The parallel compression technology has been implemented in high end facilities since 2010 (Hafner, Schonenberger, et al. 2014) and is commonly used in combination with ejectors, as seen in figure 3.6b. In figure 3.6a, the transcritical booster system using parallel compression without ejectors is shown. The expansion of the flash gas from the separator, downstream of the high pressure valve, is mainly avoided. This is due to the parallel compressors controlling the pressure level in the separator accumulating the liquid refrigerant before distributed at high pressure to the display cabinets.

In seasons when ambient temperature is low, cycles that are utilising ejectors can experience that the ejector lift capability is limited. For this reason, an additional parallel compressor can be implemented in the cycle, to compress some of the vapour returning to the gas cooler. The first architecture using this concept, achieved a 12 % efficiency increase (Hafner, Schonenberger, et al. 2014).

3.1.6 Ejectors

Replacing the throttling valve with an ejector in a transcritical R744 cycle is highly advantageous, especially when operating in warm climates. The ejector utilises the pressure difference usually dissipated in the throttling valve for energy recovery and optimises the COP by actively controlling the high pressure according to the ambient temperature or load requirements. This is done by throttling the refrigerant in a motive nozzle inside the ejector. In some designs, the ejectors use the expansion work to transfer liquid and vapour from a low-pressure receiver back to the separator. As mentioned, implementation of an additional parallel compressor to compress some of the vapour returning to the gas cooler is beneficial in seasons with lower ambient temperatures.

The first field installation of a R744 booster system with both full optional ejector support and parallel compression was implemented in a Swiss supermarket during the summer of 2013 (Hafner, Schonenberger, et al. 2014). The design is compared to the standard booster system with parallel compression in figure 3.6. Three ejectors are implemented; the first ejector implemented to transfer liquid accumulated downstream the medium temperature (MT) receiver,

back to the separator. Two additional ejectors are connected to a low pressure receiver, acting as a precompression mechanism of the vapour. These apply expansion work to compress MT vapour to the separator pressure level, which is controlled by parallel compressors. These ejectors are especially relevant during summer operation. Compared to the MT compressors, the pressure lift and the pressure ratio of the parallel compressors are much smaller, in other words the power consumption of the system can be notably reduced. An important feature of the ejector is the ability to operate at very high ambient temperatures.

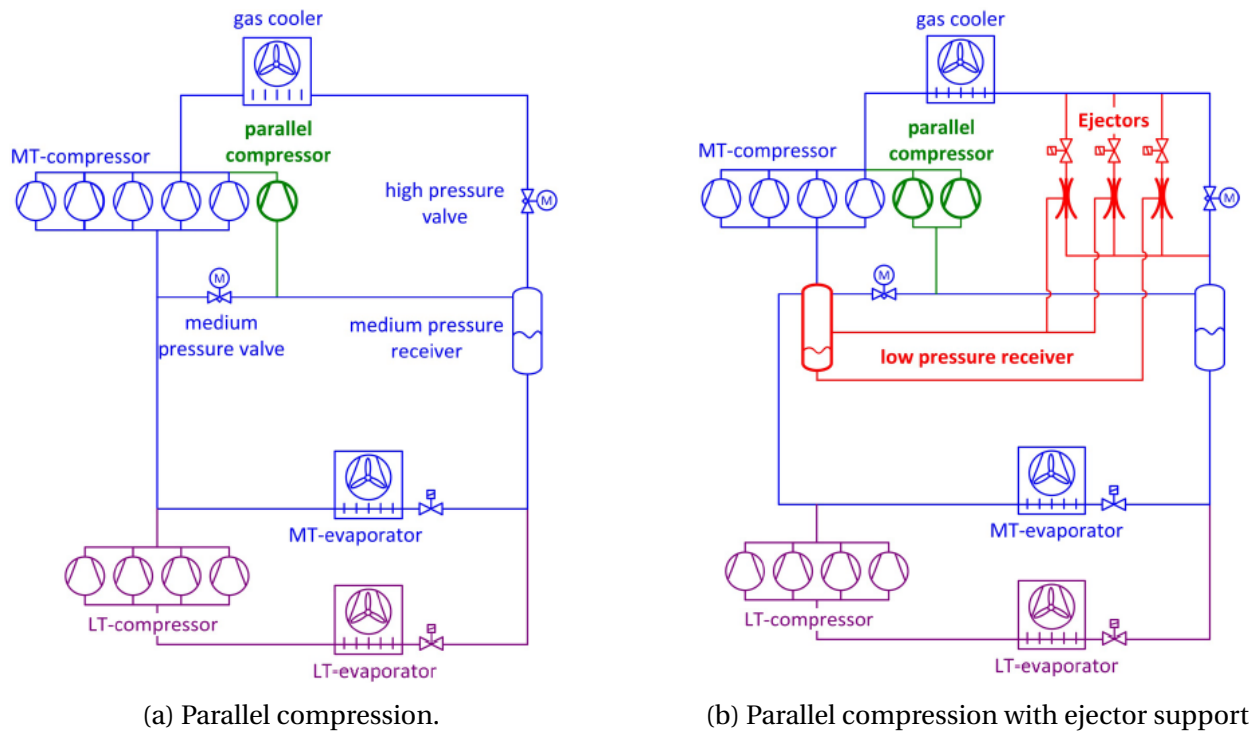


Figure 3.6: Transcritical R744 booster system using parallel compression with and without ejector support (Hafner, Schonenberger, et al. 2014).

Taking the climate into consideration, a 12 % increase in energy efficiency was achieved for this system, compared to the common R744 booster architecture with parallel compression. System simulations has shown that the COP for supermarket refrigeration systems installed with an ejector, increases significantly by up to 20 % (Hafner, Schonenberger, et al. 2014).

In simulations done by (Hafner, Forsterling, and Banasiak 2014) of a R744 system using the similar multi-ejector concept was set in comparison to an R744 reference booster system and tested for various climate conditions in Europe. Typical COP increase 17 % in Athens, 16 % in Frankfurt

and 5 % in Trondheim was achieved during summer conditions.

Transcritical R744 systems using ejectors has been analysed theoretically and experimentally for some years. Several empirical, mathematical and thermodynamic models has been presented, in order to find parameters that can optimise the ejector efficiency. A computational fluid dynamics (CFD) investigation done by (Banasiak et al. 2014), focused on understanding the fluid dynamic phenomena that affect ejector performance. Simulation and experimental results by (Elbel and Hrnjak 2008) affirm that the use of an ejector in CO₂ high ambient transcritical systems provides a 10% higher COP and an 8% improvement in cooling capacity. This COP yield can be further boosted, in combination with an IHX.

(Minetto et al. 2015) looks in to various methods of application of ejectors, and some improvements are presented. Here an interchangeable layout of the main and auxiliary compressor for a system utilising both auxiliary compressors and ejectors are suggested. The system design allows utilising the auxiliary compressor only when the ambient air temperature is increasing.

3.1.7 Subcooling

An efficiency increase can also be achieved by cooling the refrigerant further to lower temperatures than those supplied by the gas cooler. This can be accomplished by either providing an external chiller or by integrating the CO₂ cycle into a multi-stage cycle. A higher capacity mechanical subcooling device is able to reduce the refrigerant temperature downstream the gas cooler. By using a mechanical subcooler, the R744 system can operate at much lower high side pressure than the traditional R744 cycle.

Both machine-made subcooling by an external refrigerating machine and internal CO₂ subcooling increase energy efficiency extensively (Petrač 2013). System simulations on a pilot plant in Spain has been performed, where mechanical subcooling technology is used in R744 booster systems (Hafner, Hemmingsen, and Van de Ven 2014). Here propane (R290) is applied in the subcooling devices. A cooling capacity of 60 kW was achieved. The COP obtained was slightly less compared to the parallel compression unit with ejectors.

In a study of Chinese cities presented in (Hafner, Hemmingsen, and Neksa 2014), a R404A sys-

tem was used as a reference compared to three R744 systems using the standard booster architecture, the ejector system and R290 mechanical subcooling. The R744 ejector supported units with parallel compression had the highest energy efficiency values (25 % saving) compared to a R404A unit. 16 % saving was achieved by the standard booster system equipped with an external mechanical subcooling system. Due to the high ambient temperatures in southern China, energy savings of 5-10 % was be obtained when replacing R404A units with a standard R744 booster system. Their conclusion was that these innovative R744 architectures soon will outperform all HFC refrigeration systems in the future.

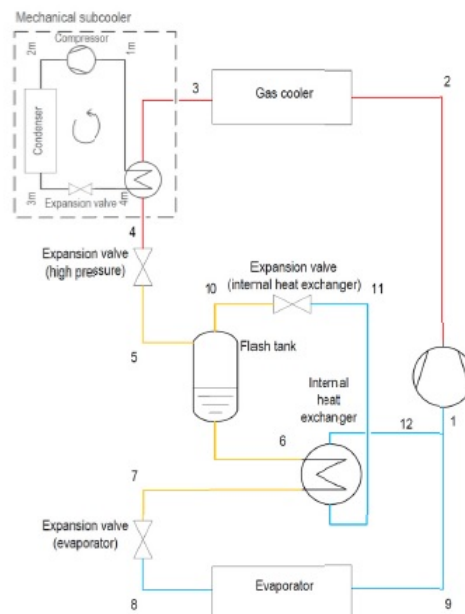


Figure 3.7: Simplified transcritical R744 refrigeration system with mechanical subcooler unit (Hafner, Hemmingsen, and Van de Ven 2014).

3.1.8 Evaporative Cooling

Increased COP when facing peak temperatures, can also be achieved by staged compression and expansion combined with evaporative cooling. Evaporative cooling of air at the gas cooler inlet, using adiabatic saturation is a general way to improve efficiency in vapour compression cycles. As mentioned, heat rejection in the gas cooler is ideally an isobaric, not isothermal process, so evaporative cooling only for a part of the total air stream cooling of the gas cooler is sufficient.

The beneficial results using this implementation, depends on the difference between the dry and wet temperature, or on the amount of humidity in air. The humidity content of air will in some tropical climates be close to its maximum value and the cooling efficiency will be very low. (Fornasieri, Girotto, and Minetto 2008) discovered that it is worth considering this method also in humid climates, especially when the ambient temperature exceeds 35°C. This is due to a higher achievable drop in air temperature, and consequently a better COP yield. A possible modification of evaporative cooling to a fin and tube gas cooler is shown in figure 3.8. Here 100 % of the air entering the gas cooler is pre-cooled.

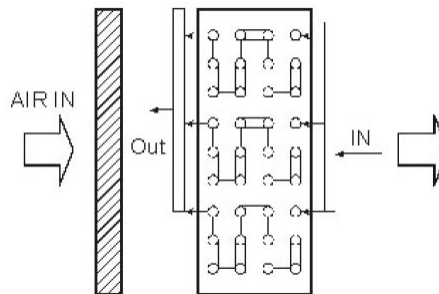


Figure 3.8: Evaporative cooling of a gas cooler (Fornasieri, Zilio, et al. 2009).

3.1.9 Optimisation of the transcritical cycle

(Penarrocha et al. 2014) has recently proposed a control strategy, based on a control algorithm, for CO₂ transcritical refrigeration plants. This is done by controlling the opening degree of the back pressure valve and manipulating the speed of the compressor, applying a variable-frequency driver. Feedback is given to the control system from three measuring devices, measuring pressure, temperature and power consumption. Using this approach helped the system operate at optimal high side pressure, thus maximising the COP.

3.1.10 Summary

Since the revival of CO₂ as a natural, environmentally benign working fluid in refrigeration systems, performance enhancement of the CO₂ cycle has been attained through modification of

the basic cycle, but also by replacement and addition of components in the systems. Today, an array of technology solutions are available that improves the system efficiency in higher ambient temperatures, including but not limited to economisers, mechanical subcoolers, ejectors, expanders, CO₂ integrated systems, parallel compression, auxiliary compressors for flash vapour compression and evaporative cooling.

A positive yield in COP for internal heat exchangers, evaporative cooling, auxiliary compressors and parallel compressors has been proven. Still, there are some limitations to these components. Economiser systems has also shown great potential, but might need to be assisted by ejectors at high ambient temperatures. Several studies has proved that the ejector with a supported parallel compression unit, achieves a COP yield up to 20 %, compared to other systems like the standard booster system with mechanical subcooling. The former systems might provide a COP yield up to 17%.

There is no doubt that a special interest for the ejector and expanders has been developed the last years. Knowledge on how the parameters affect the efficiency contributes to optimise ejector performance and in turn improving the COP of the CO₂ refrigeration systems. An important feature of the ejector, is its ability to operate at very high ambient temperatures. While the ejector is commercially available, the expander is not yet applied in basic refrigeration systems.

The ejector and expander systems can increase the efficiency significantly, but the economiser systems are limited for further efficiency improvement. The overall energy efficiency of a system depends on the selected concept, but also on the performance of the components. The selection of an efficient system depends on the potential future improvement, including the feasibility and reliability of the systems.

Today, CO₂ refrigeration systems are becoming more and more competitive. With more suppliers offering CO₂ refrigeration solutions, the southern European countries will discover a great growth over the next few years. Denmark is seen as a shining example considering their strict HFC restrictions, and use of refrigerants with low GWP. Future development of the R744 systems is dependent on further optimisation of existing solutions, or development of new untested system designs. Most importantly this development can be boosted with even stricter restrictions and tax arrangements by different governments, following in the foot steps of the Danish policy.

Chapter 4

Theory

In this chapter basic theory on CO₂ as a refrigerant and the basic CO₂ refrigeration cycle is given. Further on, the basic heat transfer equations are presented. Characteristics on the specific CA-DIO AS refrigeration system is disclosed, as well as general theory on air cooled tube-and-fin heat exchangers.

4.1 Physical and thermophysical properties of CO₂

CO₂ has a low critical temperature of 31,3°C and high critical pressure of 73,8 bar. The operating pressure of CO₂ is typically 5-10 times higher than systems using conventional refrigerants (Kima, Pettersen, and Bullard 2004). The CO₂ vapour density is remarkably high, which results in a high volumetric heating capacity, a moderate discharge temperature and a small compressor volume. Due to the high operating pressures of CO₂ systems, the pressure ratio is relatively low, resulting in high compressor efficiencies. The steep pressure curve, $\frac{\Delta t}{\Delta p}$ for CO₂ illustrated in figure 4.1, gives low temperature loss per unit pressure loss. Due to this feature, R744 systems can be designed for higher pressure losses compared to conventional systems, without harming the energy efficiency. The low viscosity, the steep pressure curve and the high vapour density results in small component dimensions. CO₂ has superior heat transfer properties due to low surface tension, low viscosity, low $\frac{\Delta t}{\Delta p}$ and efficient pool boiling in the evaporator. As a result of

the better heat transfer efficiency, a lower LMTD-value is possible. CO₂ has very high throttling loss due to high specific heat value.

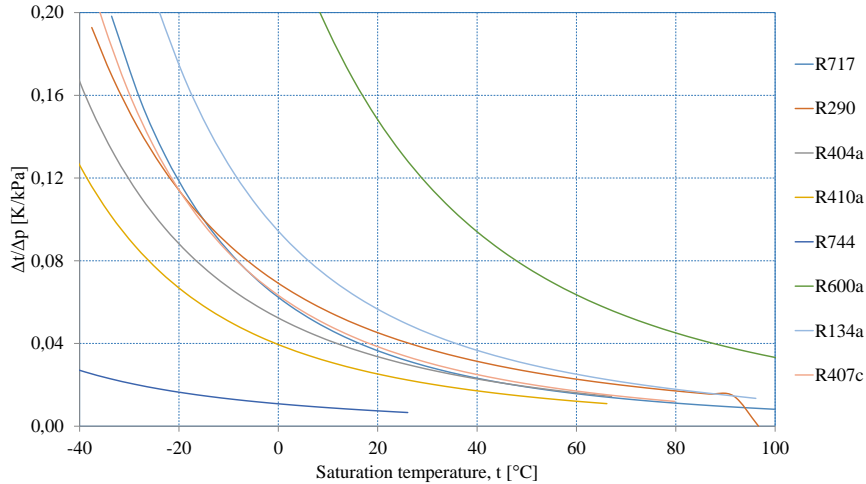


Figure 4.1: Temperature loss versus pressure loss for CO₂ compared to other refrigerants (Eikevik 2015).

The practical upper limit of condensation, refers to a condensing temperature of 28°C for subcritical operation (Haukaas 2005). The transcritical operation is the most prevalent, due to the temperature of the heat sink being too high for subcritical operation.

Figure 4.2 shows the pressure and exit temperature influence on the COP in a CO₂ gas cooler. The figure is shown for an evaporating temperature of -10°C. Above the critical point at 73,8 bar, the temperature curves are steep, and an increase in pressure results in a significant increase in COP. This is explained by the gentle slope of the isotherms just above the critical point. The optimum gas cooler pressure is determined by the pressure that gives the maximum COP for the system. Figure 4.3 shows how the refrigeration capacity changes with temperature before expansion and gas cooler pressure. The figure is shown for an evaporating temperature of -10°C, and for an ideal compressor with a swept volume of $10 \frac{m^3}{h}$. As the temperature before the throttling valve increases, the refrigeration capacity drops significantly if the pressure is not kept high enough. The COP and the refrigeration capacity is to a large extent determined by the CO₂ gas cooler exit temperature.

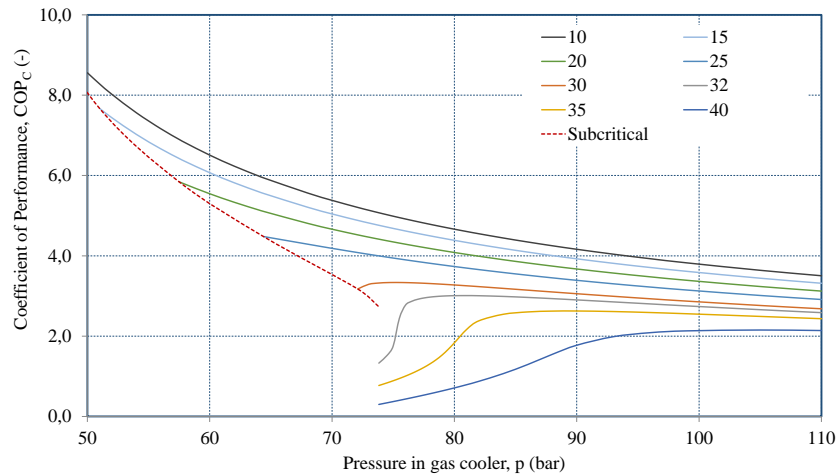


Figure 4.2: Influence of gas cooler pressure and exit temperature on COP (Eikevik 2015).

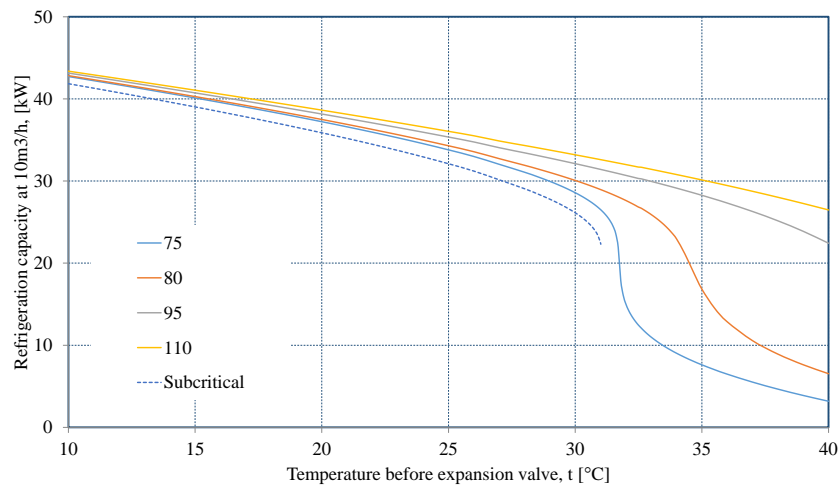


Figure 4.3: Influence of the temperature before expansion and gas cooler pressure on the refrigeration capacity (Eikevik 2015).

4.2 Basic refrigeration cycle

A basic refrigeration cycle is given in figure 4.4. In the basic cycle, the refrigerant is compressed to a higher pressure level in the compressor (1-2) and work to the compressor is required. Depending on the ambient temperature and the high pressure side of the cycle, the cycle will be in subcritical or transcritical operation. Figures 4.5a and 4.5b shows the subcritical and transcritical process in a $\log(p)$ - h diagram. At pressures below the critical pressure, operation will be in the subcritical area and heat rejection will occur at a constant temperature during conden-

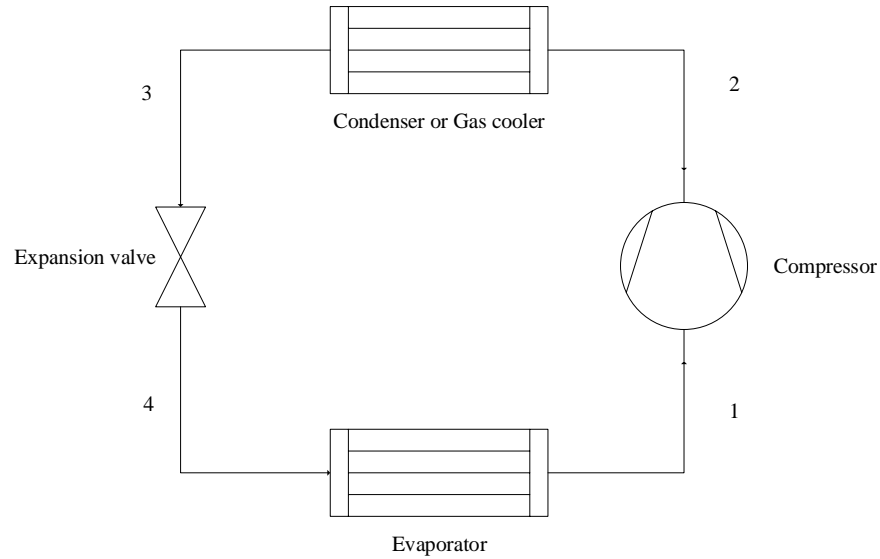


Figure 4.4: Basic refrigeration cycle.

sation in the condenser (2-3). When the pressure is above the critical pressure, the refrigerant will be in the supercritical area and no condensation will occur since the refrigerant will only be in one phase, namely gas. The heat rejection will occur at gliding temperatures in a gas cooler (2-3), due to the independent temperature and pressure in the supercritical region. Following, the refrigerant will be expanded in the throttling valve (3-4). After the throttling, heat is absorbed in the evaporator, the refrigerant is evaporated (4-1) and cooling is provided. The heat rejected in the gas cooler or the condenser equals the work supplied to the compressor and the heat absorbed in the evaporator. The coefficient of performance of the system is defined as the refrigeration capacity divided by the compressor work supplied.

$$Q_{gc} = Q_o + W \quad (4.1)$$

$$COP = \frac{Q_o}{W} \quad (4.2)$$

The refrigeration capacity of the system is obtained at constant pressure and temperature in the subcritical region. It is calculated by the amount of refrigerant circulated in the system and the enthalpy difference before and after the evaporator.

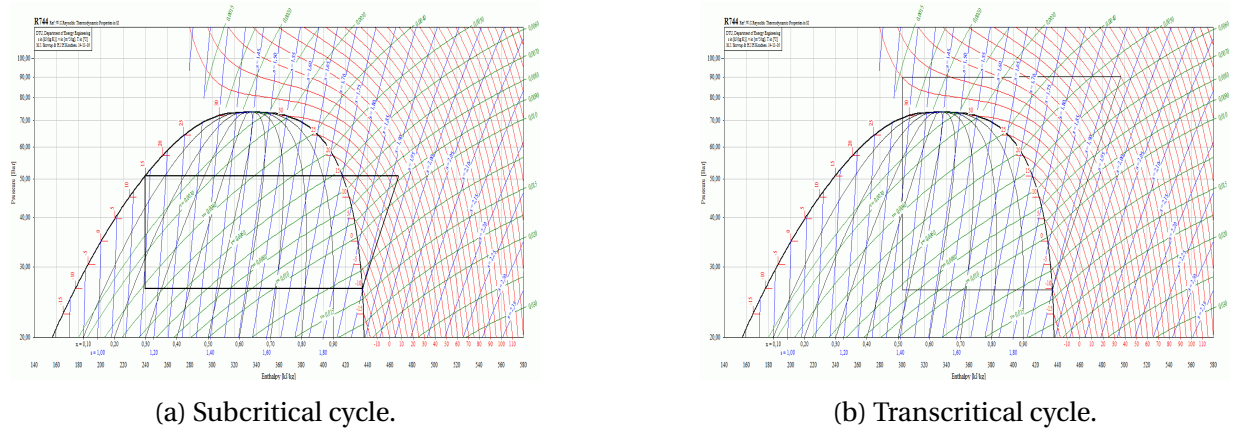


Figure 4.5: R744 refrigeration cycles.

$$\dot{Q}_o = \dot{m} \cdot (h_1 - h_4) \quad (4.3)$$

The size of the compressor is determined by the volume flow of the refrigerant required to achieve the desired refrigeration capacity. The suction volume is the volume that needs to be removed from the evaporator, see equation 4.4. But due to volumetric losses, the required volume of the compressor also known as the swept volume, is larger than the suction volume. The volumetric efficiency of the compressor is defined as the ratio between the suction and swept volume, see equation 4.5. However, the volumetric losses are not the only losses that influences the efficiency of the compressor and the cycle. Energy losses in the compressor results in a higher power demand than the theoretical demand. The energy losses are given by the isentropic efficiency as seen in equation 4.7.

$$V_{suc} = \dot{m} \cdot v_1 \quad (4.4)$$

$$\lambda = \frac{V_{suc}}{V_s} = \frac{\dot{m} \cdot v_1}{V_s} \quad (4.5)$$

$$\dot{W}_{theo} = \dot{m} \cdot (h_{2,is} - h_1) \quad (4.6)$$

$$\eta_{is} = \frac{W_{theo}}{W} \quad (4.7)$$

When heat loss from the compressor is included, then two different discharge enthalpies have to be calculated, as seen in equation 4.8 and 4.9. The reason for this is that energy can not dissipate or arise from nowhere. The heat is produced among other factors by friction in the compressor which results in an increased compressor work. In terms of the condenser or gas cooler it means that less heat needs to be removed.

$$h_2 = h_1 + \frac{h_{2,is} - h_1}{\eta_{is}} \quad (4.8)$$

$$h_2^* = h_1 + \frac{h_{2,is} - h_1}{\eta_{is}} \cdot (1 - Q_{heatloss}) \quad (4.9)$$

The compressor work is calculated with the enthalpy difference excluding the heat loss as seen in equation 4.10.

$$\dot{W} = \dot{m} \cdot (h_2 - h_1) \quad (4.10)$$

For a system comprising of an air cooled condenser with a fan, the fan power is described in equation 4.11, where η_{fan} is the efficiency of the fan, ΔP_{tot} is the total pressure drop in [kPa] over the fan and \dot{V} is the airflow rate in [$\frac{m^3}{s}$].

$$\dot{W}_{fan} = \frac{\dot{V} \cdot \Delta P_{tot}}{\eta_{fan}} \quad (4.11)$$

For a system consisting of two compressors, the COP of the system will be defined as the refrigeration capacity divided by total power, including the fan work.

4.3 Heat transport

Heat is energy and the equations for heat transfer are based on conservation of energy. Equation 4.12 describes how much heat that is rejected from the working medium in the condenser or how much that is absorbed in the evaporator. Δh for a condenser is the difference between the inlet enthalpy described in equation 4.9 and the outlet enthalpy of the condenser.

$$\dot{Q} = \dot{m} \cdot \Delta h \quad (4.12)$$

Equation 4.13 describes the amount heat transported to or from a medium. The equation shows that the temperature difference in the heat source or sink is proportional to the heat transported.

$$\dot{Q} = \dot{m} \cdot c_p \cdot \Delta T \quad (4.13)$$

The heat transferred within a heat exchanger where one of the media experience a change in temperature, can be calculated with equation 4.14. A is the heat transfer area, U is the overall heat transfer coefficient and ΔT_{LMTD} is the log mean temperature difference. However, for transcritical operations, equation 4.15 cannot be used to calculate the logarithmic temperature difference, due to the changing specific heat capacity in the gas phase. Equation 4.15 shows the ΔT_{LMTD} for a counterflow heat exchanger.

$$\dot{Q} = U \cdot A \cdot \Delta T_{LMTD} \quad (4.14)$$

$$\Delta T_{LMTD} = \frac{\Delta T_{in} - \Delta T_{out}}{\ln \frac{\Delta T_{in}}{\Delta T_{out}}} \quad (4.15)$$

T_{in} and T_{out} is defined in equations 4.16 and 4.17 for the condenser. T_c is the condensing temperature for the CO_2 , $T_{air,in}$ is the inlet heat sink temperature and $T_{air,out}$ is the outlet heat sink temperature, were the heat sink in this case is ambient air.

$$\Delta T_{in} = T_c - T_{air,in} \quad (4.16)$$

$$\Delta T_{out} = T_c - T_{air,out} \quad (4.17)$$

Energy balance in the heat exchange is required. This means that the heat absorbed or rejected by the heat source or sink must be equal to the heat rejected or absorbed by the refrigerant and the temperature difference in the heat exchanger. By combining equation 4.12, 4.13 and 4.14, equation 4.18 is obtained.

$$\dot{Q} = \dot{m} \cdot \Delta h = \dot{m} \cdot c_p \cdot \Delta T = U \cdot A \cdot \Delta T_{LMTD} \quad (4.18)$$

4.4 Air cooled tube-and-fin CO₂ heat exchangers

A heat exchanger transfers heat from a hot fluid to a colder fluid, without mixing the two fluids. There are several different types of heat exchangers, where shell-and-tube is the most common. Air cooled tube-and-fin heat exchangers consists of tubes with fins in order to increase the heat exchange area, thus the heat transfer. The temperature difference between the hot and the cold fluid will vary through the heat exchanger, if not both of the fluids undergoes a phase transition.

A good heat exchanger design is important in order to reduce the compressor work. A good design is also essential in order to cool the fluid as much as possible, thus maximising the thermal performance of the system. Also reducing the throttling loss and minimising the entropy generation are important when designing a heat exchanger. Parameters such as space, economics, safety, fluid and metal properties are important parameters to contemplate when designing the heat exchanger.

The point where the temperature difference between the hot and cold streams reaches its minimum, is termed as the pinch point. In order to obtain an efficient heat exchanger, it is important that the pinch point is located at the cold stream outlet. Pinch at the centre of the heat exchanger

characterises a bad heat transfer between the two working fluids, hence a poor heat exchanger design.

In a basic CO₂ refrigeration cycle, the ambient air temperature will decide whether the operation is transcritical or subcritical. Consequently, the air cooled CO₂ heat exchanger will act both as a condenser and as a gas cooler. When optimising the CO₂ heat exchanger, this feature needs to be taken into account in order to enhance the performance of the system. (Ge et al. 2015) identified that 90 % of the temperature drop occurs in the first 17 % of the total circuit pipe. 90 % of the total heat transfer rate drop occurs in the first row of the heat exchanger. Furthermore it was discovered that that variation of air flow rate is the most effective way to control and minimise the approach temperature. If the air flow rate was highly increased, a great effect on the refrigerant temperature was discovered. It was shown that the COP was not penalised as much by the extra fan work compared to the significant increase in refrigeration capacity.

When operating as a condenser it is important to ensure that the liquid is fully condensed at the inlet of evaporator for proper operation. As the refrigerant flows through the condenser there is a phase change where a drop in velocity occurs (American Society of Heating, Refrigerating, and Air-Conditioning Engineers 2008). A decrease in velocity will lead to an increase in the laminar boundary layer against the pipe wall and a larger temperature difference over the boundary layer. By allowing a pressure drop when designing the condenser, the velocity is increased through the pipe, hence a thinner boundary layer is obtained, providing a more effective heat transport. However, a pressure loss through the condenser leads to a loss in temperature, which can result in flashing in the liquid line and a decrease in the system efficiency. A large pressure loss will result in a higher pressure ratio, thus an increased compressor work. By subcooling the liquid sufficiently, flashing in the liquid line can be prevented. Subcooling is also an efficient way to increase the refrigeration capacity or to decrease the compressor size. The normal procedure when designing an air-cooled condenser is to provide a heat transfer area and a pressure drop to provide 1 to 3 K subcooling (American Society of Heating, Refrigerating, and Air-Conditioning Engineers 2008).

As mentioned earlier the temperature loss per pressure loss for CO₂ is very low compared to other refrigerants, and the condenser can be designed for higher pressures drops without harm-

ing the energy efficiency of the system.

4.5 Description of the system

The investigated system is a R744 refrigeration system with an integrated R290 subcooler. It is located at the Cadio AS production facility at Heimdal. Main application of the refrigeration unit is for supermarket refrigeration. The refrigeration unit includes two systems where R744 is the primary refrigerant and R290 is the secondary refrigerant. Stated maximum refrigeration capacity of the system at 32°C ambient temperature operating with a frequency of 70 Hz, is 12kW at -10°C evaporating temperature, and 7kW at -33°C evaporating temperature (Cadio AS). Operation of the system is based on subcritical operations. At low ambient temperatures the R744 system will operate exclusively. At high ambient temperatures, the R290 system will start to operate. The R290 unit is only in operation when the primary system needs additional cooling to meet the required refrigeration capacity.

Flow chart of the prototype system is seen in figure 4.6. The system consist of three circuits. A R744 unit for main operation, a R290 unit for subcooling the R744, and an ethylene-glycol unit. The ethylene-glycol unit with the R744 evaporator is not included in the commercial available system. This circuit was added to the prototype system in order to provide heat of evaporation to the R744 during measurements in the project work.

The refrigeration system has two different operational modes. These modes depends on the temperature of the air cooling the R744 in the condenser. When the ambient temperature is low, only the R744 circuit is in operation. R744 is compressed in a semi-hermetic compressor to a condensing pressure which is correlated to the ambient temperature. Following it is condensed in an air cooled condenser, sent to a liquid receiver before it is throttled to evaporating pressure in a manual throttle valve. At last, the refrigerant is evaporated in a brazed plate heat exchanger. The evaporating pressure and temperature is determined by the area of application, namely refrigeration display counter at -10°C or frozen goods counter at -33°C.

The second operational mode is at medium to high ambient temperatures. The operation of the

Cadio system unit

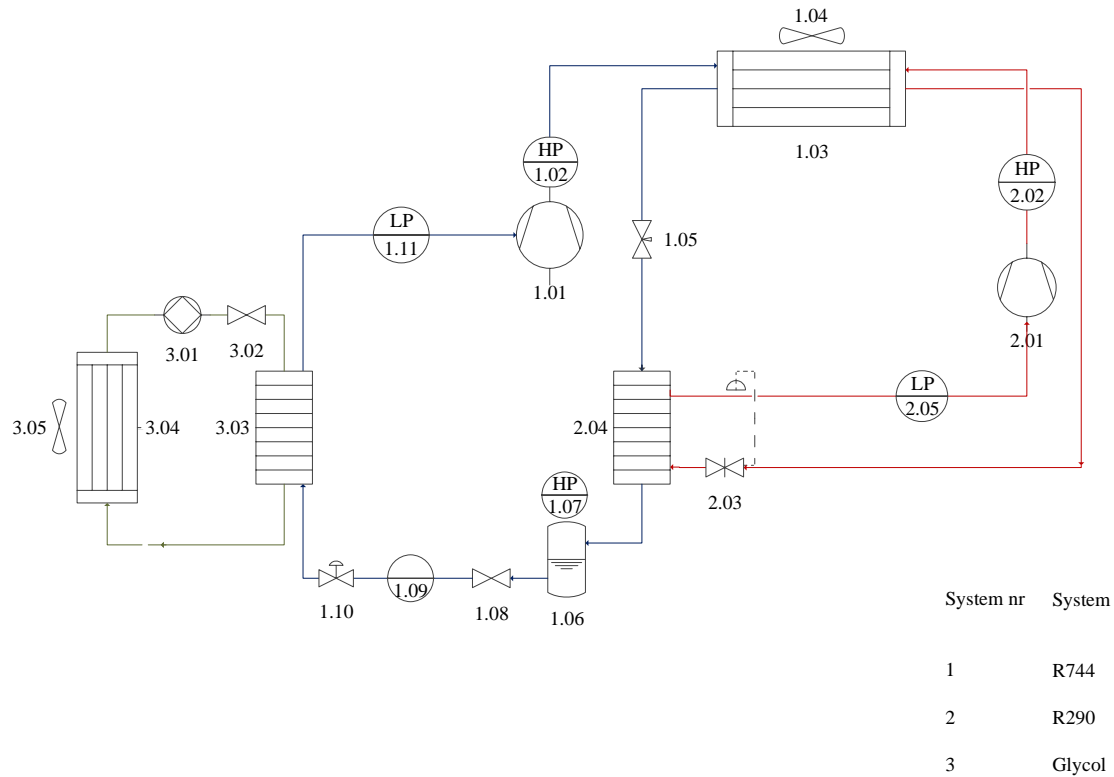


Figure 4.6: Flow chart CO₂ refrigeration system with integrated propane subcooler.

R744 circuit is almost the same as for the latter operational mode, but the R290 system will now start to operate. R290 is compressed in a scroll compressor and condensed in the integrated air cooled R744 and R290 condenser. Moreover, the R290 is throttled in a thermal expansion valve before it evaporates in a brazed plate heat exchanger. The superheat from R744 is rejected in the air cooled condenser as much as the ambient temperature grants. It then continues to the R290 evaporator where the rest of the superheat and heat of condensation from R744 is absorbed by the evaporating R290. The refrigeration capacity of the R290 system equals the heat rejected from the condensing R744, see equation 4.19. Hence if the cooling capacity of the R290 evaporator is too small, the R744 pressure will increase and the specific enthalpy of condensation is smaller.

For analysis of the prototype system some design points were provided from Cadio AS. These are summarised in the table 4.1.

Design point prototype system	
Ambient temperature	32 °C
Condensing temperature R744	25 °C
Evaporating temperature R744	−10 °C
Temperature difference R290 condenser	15 K
Approach temperature R744 gas cooler	5 K
$\Delta T_{R744,superheat}$	10 K
$\Delta T_{R290,superheat}$	7 K

Table 4.1: Data from design point (Cadio AS).

Set point for start and end of operation for the R290 system determined by Cadio AS can be seen in table 4.2. When the R744 system operates alone and the high side pressure reaches 67 bar, the R290 will start to operate. When the R290 system is in operation, the high side pressure decreases below 60 bar and the R290 system will be switched off. Practically this means that when the propane system kicks in, the high side pressure will rapidly be pulled down below 60 bar and the propane system will be switched off. This is repeated until the ambient temperature is high enough and the CO₂ condensing pressure will not fall below 60 bar.

In the project thesis the prototype system was thoroughly analysed. Instrumentation of the prototype system was performed, and thermodynamic data were measured and collected. The location of instrumentation components is seen in figure 4.7. Measurement data from the project thesis showed that the optimum set point for the propane system is at a CO₂ condensing temperature of 28 °C. The simulation model developed in the master period uses the data and settings provided by Cadio AS to further investigate the system.

$$\dot{Q}_{o,R290} = \dot{Q}_{c,R744} - \dot{Q}_{gc,R744} \quad (4.19)$$

In equation 4.19, $Q_{o,R290}$ is the heat absorbed by the evaporating R290, $Q_{c,R744}$ is the total heat rejected from the R744 and $Q_{gc,R744}$ is the heat rejected from the R744 in the gas cooler. The heat rejected from the R744 to the evaporating R290 is illustrated in the log (p)-h diagram in figure 4.8b, where the specific enthalpy difference is marked red. The enthalpy difference marked blue in figure 4.8a represents the heat rejected in the gas cooler when then ambient temperature is approximately 35 °C.

Cadio system unit with instrumentation

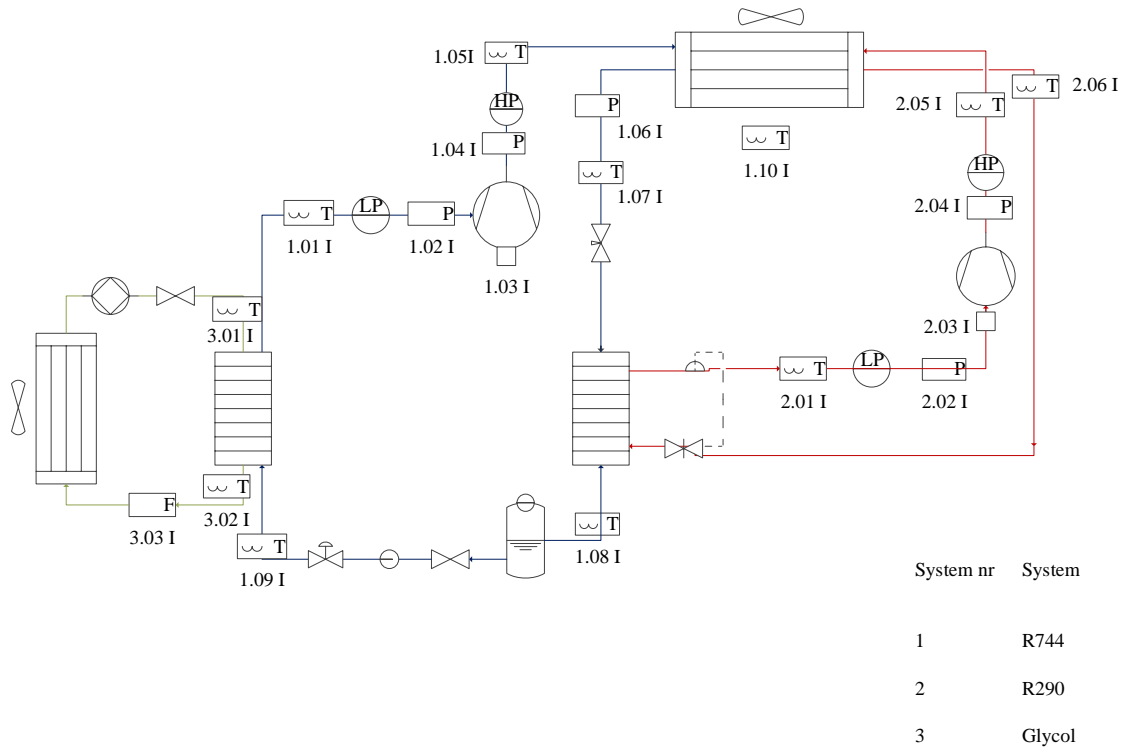
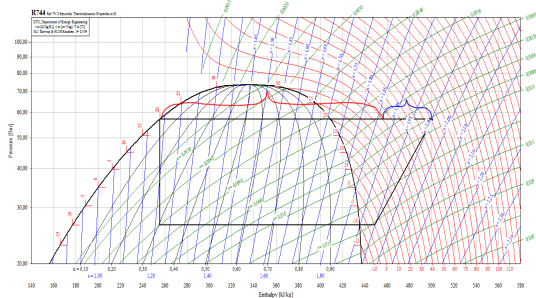
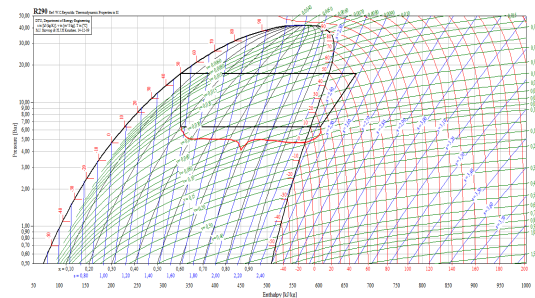


Figure 4.7: Location of instrumentation components.



(a) Heat rejected from R744.



(b) Heat absorbed R290 evaporator.

Figure 4.8: Heat exchange subcooler.

The gas cooler has been designed exclusively for this refrigeration system. It operates as a condenser for R744 at low ambient temperature, a desuperheater for R744 at high ambient temperatures and as a condenser for the R290 system at all ambient temperatures above the propane operational set point. It consists of copper pipes, aluminium fins and a galvanized plate. The

pipes for the R290 and the R744 are equally distributed over the height of the gas cooler. In figure 4.9c, the R290 represents the pipeline row which is located at the air inlet side. The two remaining pipeline rows represents the R744 pipelines. The area cooled by the ambient air, is equal for each set of pipelines. Two 230 W suction fans are installed to distribute ambient air through the gas cooler. The fan set points are described in table 4.2.

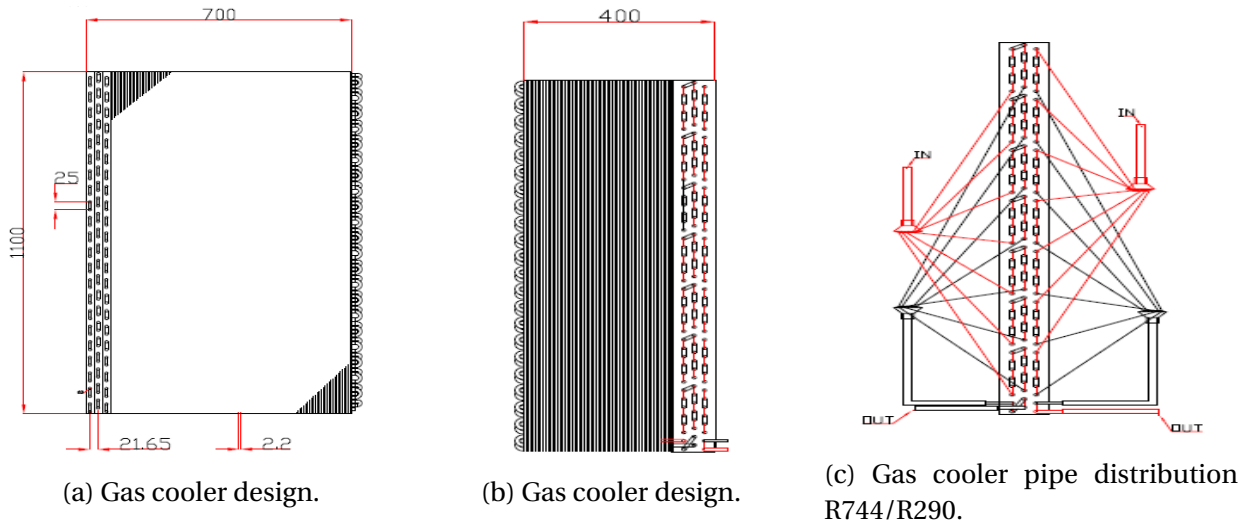


Figure 4.9: The R744/R290 gas cooler (Cadio AS).

Evaporating temperature	$T_{o,R744} = -10^{\circ}\text{C}$	$T_{o,R744} = -33^{\circ}\text{C}$
Start fan	55 bar	35 bar
Max speed fan/ Stop R290 system	60 bar	40 bar
Start R290 system	67 bar	47 bar

Table 4.2: Set point refrigeration unit described by R744 high side pressure.

The R744 evaporator is connected to a dry cooler circuit with 43 volume % ethylene-glycol. The ethylene-glycol has a freezing point of -28°C . This circuit transports heat absorbed in the dry cooler to the combined R744 evaporator and glycol chiller. A pump is installed to maintain the required flow rate in the glycol unit. The dry cooler consist of three fan units, that can be regulated by the frequency converter.

All the pipes are made of copper except the discharge pipe from the R744 compressor. This is to protect the pipe from the high discharge temperature and from harmful vibrations. The R744 and R290 pipeline diameters are 9,525 mm.

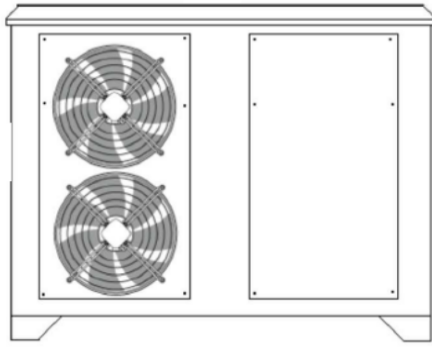
The secondary system is filled with 0,6 kg R290. Both the low and high pressure side of the R290 system are restricted to a pressure of 22 bar. The primary system is filled with approximately 5 kg R744. The components on the high pressure side are designed to withstand 150 bar, but a mechanical safety valve will lower the pressure if it exceeds 97 bar. A high side pressure controller limits the operation to 75 bar, and if the pressure exceeds this value the electricity will automatically be switched off. However the maximum allowed pressure is 80 bar on the high pressure side and 63 bar on the low pressure side. These restrictions are made due to the certification cost of systems at high pressures.

A complete overview of the components in the refrigeration unit with corresponding numbers to the flow diagram is given in table 4.3.

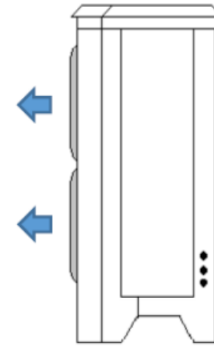
Component number	Component
1.01	R744 compressor
1.02	Pressure controller HP
1.03	Air cooled condenser/gas cooler for R290/R744
1.04	Fan
1.05	Safety valve
1.06	Liquid receiver
1.07	Pressure controller HP
1.08	Safety valve
1.09	Inspection glass
1.10	Manual throttling valve
1.11	Pressure controller LP
2.01	R290 compressor
2.02	Pressure controller HP
2.03	Thermal expansion valve R290
2.04	Evaporator R290/Subcooler R744
2.05	Pressure controller LP
3.01	Glycol pump
3.02	Glycol valve
3.03	Glycol cooler/R744 evaporator
3.04	Dry cooler glycol
3.05	Dry cooler fan

Table 4.3: Overview of the system components.

Figure 4.11 shows the CO₂ compressors application envelope. For an evaporating temperature of -10°C , the recommended range for the discharge pressure is approximately 37 to 135 bar, while for an evaporating temperature -33°C the operation is actually out of range for the rec-



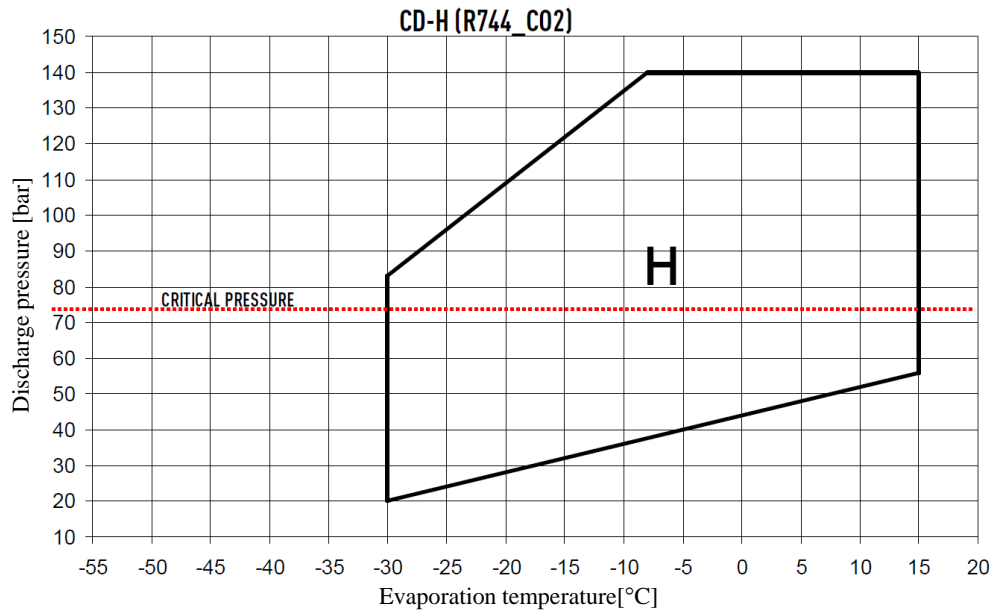
(a) Unit design seen from the front.



(b) Unit design seen from the side.

Figure 4.10: The R744/R290 unit (Cadio AS).

ommended pressures.

Figure 4.11: Application envelope for the CO₂ compressor (Dorin 2014).

The height, length and width of the system is respectively 1770 mm, 530 mm and 1270 mm, while the weight is 260 kg. The commercial system will be installed outdoors due to safety precautions. R290 is a flammable refrigerant and in case of leakage the refrigerants will leak to the atmosphere. Trained service personnel must be contacted if there is any indication of leakage.

Chapter 5

Analysis

In this chapter, the procedure for developing the simulation model using HXsim and EES has been described. Further on, the procedure for optimising both the integrated condenser/gas cooler and the overall prototype system, has been presented.

5.1 Initial plan for simulation and optimisation of the prototype system

- Thoroughly analysing measurement data and correcting possible errors.
- Simulate the integrated condenser/gas cooler in HXsim.
- Develop a simulation model in EES using correlations from HXsim.
- Compare the results from the simulation model to the measurement data.
- Run a simulation of the prototype system performance for selected European cities over a one year period.
- Optimise the condenser/gas cooler: Test different modification configurations in HXsim.
- Integrate the HXsim correlations for the condenser/gas cooler modifications in the EES simulation model and calculate the SCOP for the prototype system using the different

configurations.

- Develop simulation models for different overall system modifications.

5.2 Simulation model of prototype system

During the project thesis, the prototype system was instrumented and measured for different ambient temperatures. The data collected have been used to some extent as a foundation for assumptions when developing the simulation model. In table 5.1, an overview of the different performed tests are presented. The results from the tests are later compared to the results from the simulation model. The measurement data were corrected due to new information provided by the compressor manufacturer. The compressor measurement data showed unreasonable high values compared to calculations done with the isentropic and volumetric efficiency obtained from the compressor manufacturer. Therefore the results processed from the project thesis was recalculated by correcting the compressor discharge enthalpy and the mass flow, thus correcting the work added to the compressor.

Test conditions	Test 1	Test 2	Test 3
R744 evaporating temperature	-10°C	-10°C	$-18/ -25^{\circ}\text{C}$
System operating	R744	R744 + R290	R744 + R290
Stable temperature range	19°C to 29°C	20°C to 43°C	18°C
Frequency R744 compressor	60 Hz	60Hz	70Hz

Table 5.1: Conditions for performed tests during project thesis.

Only an evaporating temperature of -10°C have been investigated. It was not possible to stabilise the prototype system at an evaporating temperature of -33°C due to an over-sized evaporator, resulting in fluctuating boiling, evaporating temperatures and suction temperatures.

In order to simulate the performance and energy efficiency of the prototype system over a one year period, a simulation model was developed. The model was developed using the Engineering Equation Solver (EES). EES is a numerical equation-solving program with embedded thermophysical property functions. Measurements done in the project thesis showed that the

system operates fairly close to theoretical calculations with some discrepancies. Data and assumptions used in the simulation model are shown in table 5.2.

Foundation for simulation model	
Evaporating temperature R744	-10°C
Superheat R290 evaporator	7 K
Superheat R744 evaporator	10 K
Minimum temperature difference subcooler	9,9 K
Volumetric efficiency R290	0,8
Isentropic efficiency R290	0,6
Maximum volume flow air	$7000 \frac{\text{m}^3}{\text{h}}$
Heat capacity air	$1,005 \frac{\text{kJ}}{\text{kg}\cdot\text{K}}$
Density air	$1,225 \frac{\text{kg}}{\text{m}^3}$
Efficiency fan	50%
Heat loss from compressors	10%
Swept volume R290 compressor	$9,7788 \frac{\text{m}^3}{\text{h}}$
Swept volume R744 compressor	$3 \frac{\text{m}^3}{\text{h}}$

Table 5.2: Assumptions and restrictions for simulation model.

Equations for the isentropic and volumetric efficiencies of the CO₂ compressor was provided by the manufacturer after the project period. Equation 5.1 and 5.2 are valid for subcritical operation, while equation 5.3 and 5.4 for transcritical operation. π is the pressure ratio. The volumetric and isentropic efficiencies for subcritical and transcritical operation are plotted in figure 5.1. The data presented from the manufacturer are at a frequency rate of 50 Hz, but the tests were executed at a frequency rate of 60 Hz. For 60 Hz operation, the 50 Hz data obtained from the compressor manufacturer were multiplied by a factor of 1,18 (Dorin 2014). Assumptions for the volumetric and isentropic efficiencies of the propane compressor were set, as no data were available from the manufacturer.

$$\eta_{is,CO_2,sub} = -0,0832 \cdot \pi^2 + 0,3904 \cdot \pi + 0,1247 \quad (5.1)$$

$$\lambda_{CO_2,sub} = 0,0181 \cdot \pi^2 - 0,1746 \cdot \pi + 1,1078 \quad (5.2)$$

$$\eta_{is,CO_2,trans} = 0,0076 \cdot \pi^2 - 0,0438 \cdot \pi + 0,6542 \quad (5.3)$$

$$\lambda_{CO_2,trans} = 0,0207 \cdot \pi^2 - 0,2163 \cdot \pi + 1,2054 \quad (5.4)$$

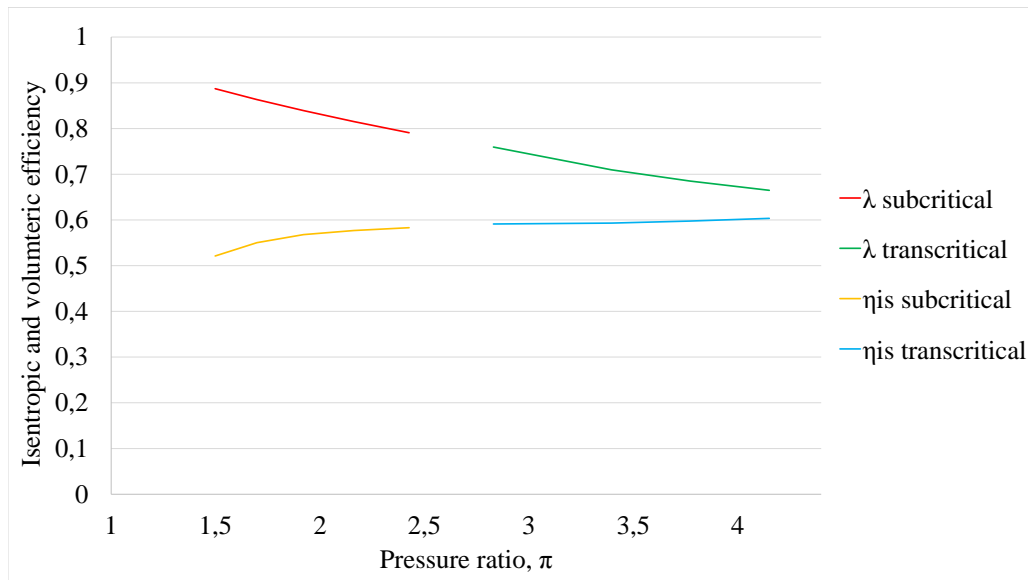


Figure 5.1: Volumetric and isentropic efficiency for the CO₂ compressor.

Measurements from the project thesis showed that the optimum point where the propane system should start to operate, is when the condensing temperature of CO₂ reaches 28°C.

5.2.1 Fundamental simulation model

Simulations of the system in EES were performed in several distinct steps. In combination with the operational data provided by Cadio AS seen in table 5.2, and information derived from the measurement data and theory, the initial script was developed. As mentioned in chapter 4.5 the refrigeration system have two operational modes, with and without the propane system in operation.

No information was available on the fan characteristics. The volume flow of air through the fan is set by the condensing pressure of CO₂, meaning an increase in condensing temperature

results in an increased volume flow. In reality, the fan is turned off when the CO₂ condensing pressure falls below of 55 bar, but since there is a constraint in HXsim that there must be an air flow for the heat balance to converge, the minimum air volume flow was set to 10% of maximum. This will represent movement in the air flow due to convection. In figure 5.2 the fan characteristics is illustrated.

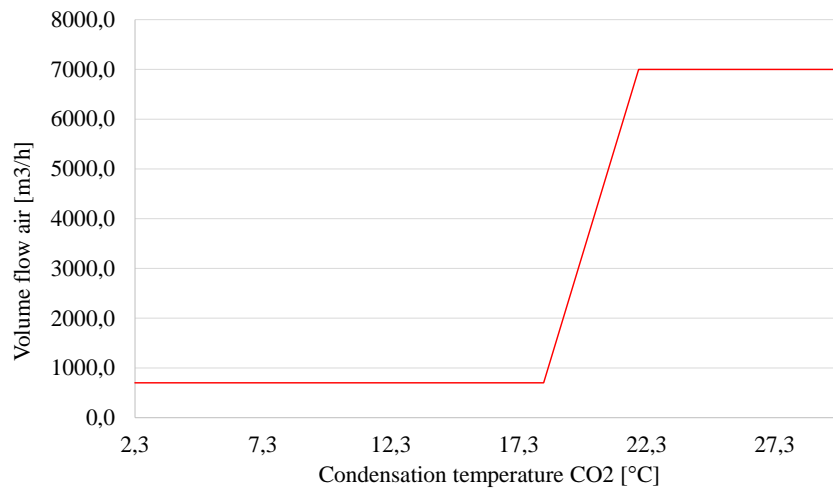


Figure 5.2: Volume flow air as a function of condensing temperature.

The CO₂ condensing temperature and propane evaporating temperature were decided by running an loop with an energy balance between the heat of evaporation and condensation. The heat removed from the CO₂ had to be equal the heat absorbed by the propane in the CO₂ sub-cooler.

The constrain for the propane evaporating temperature, T_{0p} , was developed by analysing the measurement data. T_{0p} was set to a maximum value of 9,9 K less than the CO₂ condensing temperature, T_4 , and a minimum value of 10°C. The maximum and minimum value was derived from the measurement data. The iteration started with T_4 equal to its minimum possible value, 19,9°C, also derived from the test data. Optimum operation of the system exists with as low compressor work and as high refrigeration capacity as possible, thus as low condensing temperature as possible. The maximum value of T_4 was set to 29°C, due to the restriction of subcritical operation. For each iteration of T_4 , the propane evaporating temperature was iterated between its maximum and minimum values. For every iteration the heat of condensation for CO₂ and the propane heat of evaporation was calculated. If the parameters were equal, the

loops were stopped. Further on, the thermodynamic data of the system, such as the COP and the Q_o , were calculated with the executed evaporating and condensing temperature.

The difference between the outlet refrigerant temperature of the CO₂ condenser/gas cooler and the ambient temperature, known as the temperature approach, was initially guessed to a value 5 K at ambient temperatures above 14 °C, and 12 K at ambient temperatures below 14 °C. These values were derived by analysing the data collected in the project thesis. When the ambient temperatures reaches $-4,7^{\circ}\text{C}$, the minimum saturation temperature is set to $2,3^{\circ}\text{C}$ due to compressor restrictions. The difference between the propane saturation temperature and the ambient temperature, was derived from the measurement data and set as an initial guess to 15 K. The fundamental simulation model is seen in appendix A.6 and utilised in the procedure described in figure 5.3. By initially guessing reasonable values for the approach temperatures, this procedure was less time consuming.

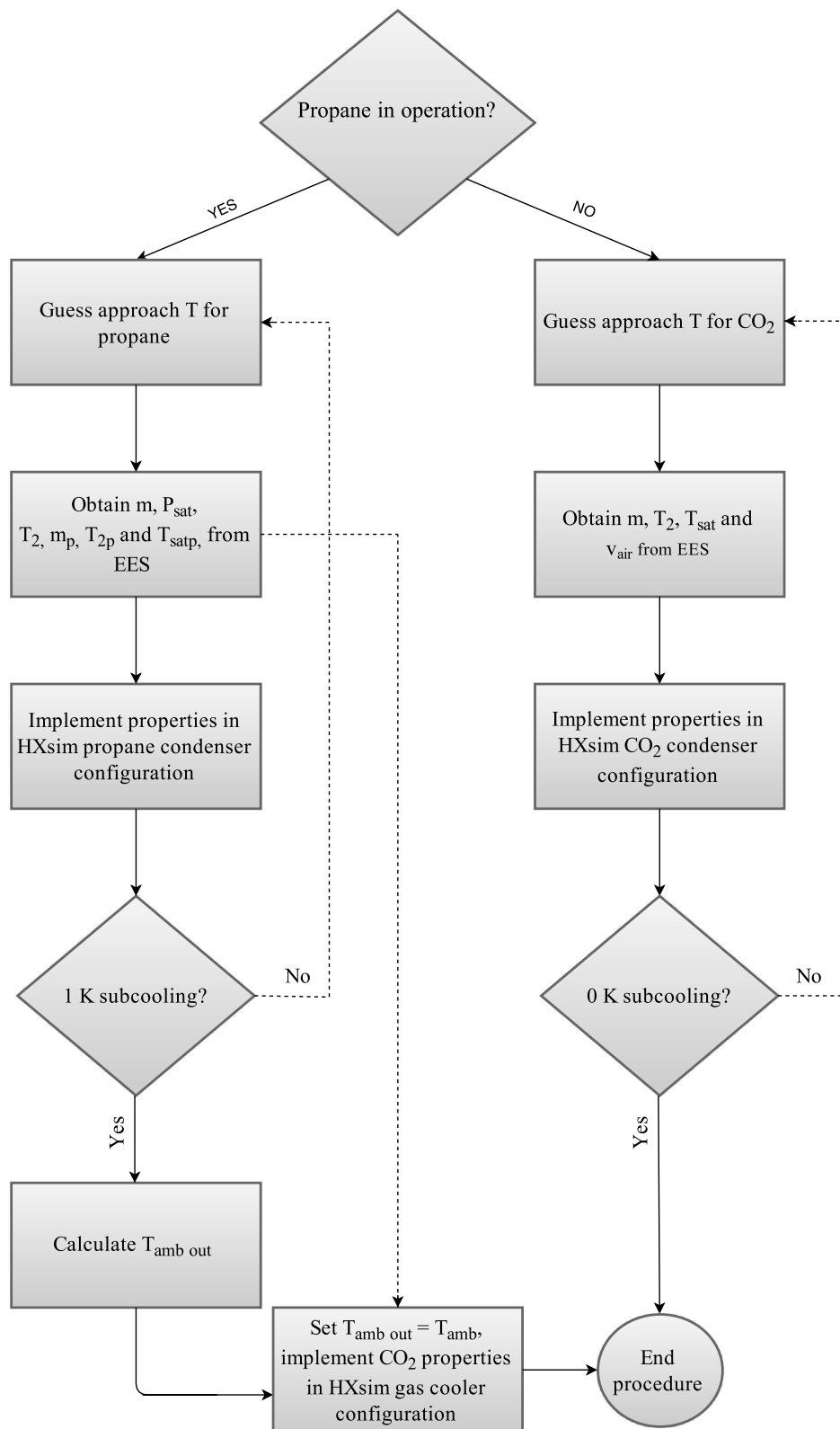


Figure 5.3: Flow chart for obtaining correlations from HXsim.

5.2.2 Simulation in EES with restrictions developed in HXsim

HXsim is a heat exchanger simulation program developed by SINTEF¹. It only simulates one heat exchanger at the time. The integrated condenser/gas cooler for CO₂ and propane was simulated separately in HXsim. The outlet air temperature from the propane simulation would be the inlet air temperature for the CO₂ gas cooler. When the CO₂ heat exchanger operates as a condenser, the propane condenser is not in operation. When the CO₂ heat exchanger operates as a gas cooler, the propane condenser is in operation.

In HXsim, the circuit design and pipe dimensions were implemented. The actual structure of the gas cooler includes a 90° bend to utilise the space of the refrigeration unit as shown in figure 5.4.

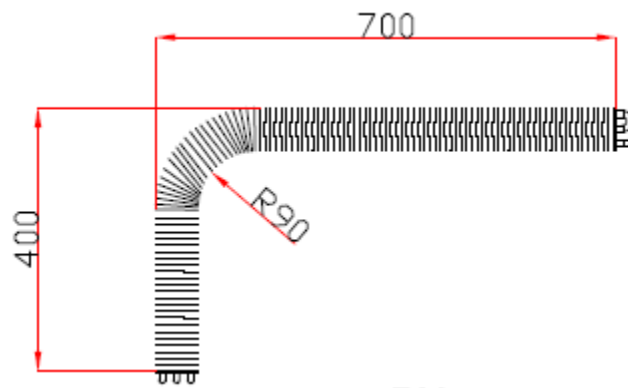


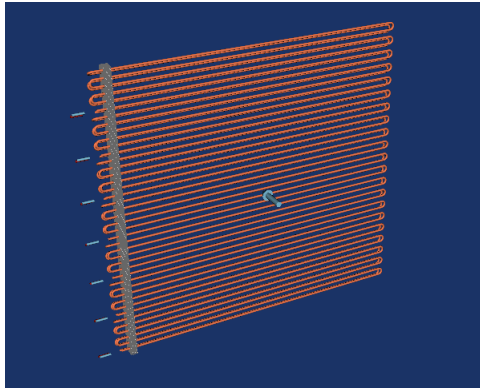
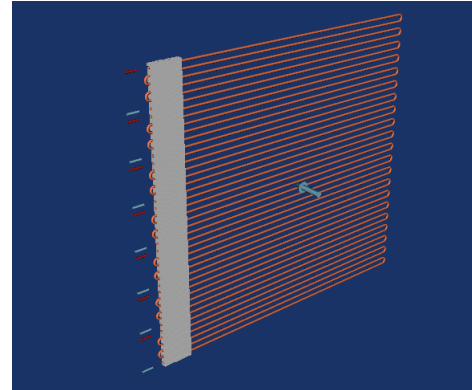
Figure 5.4: Integrated CO₂ and propane condenser seen from above.

Due to constraint in the software, the heat exchangers were calculated in HXsim without the bend as shown in figure 5.5. In the original configuration, the final pipe duplication for both the propane and the CO₂ is a manifold that collects the cooled refrigerant and is sent through the heat exchanger one last time. This feature is not possible to implement in HXsim. Input data used to simulate the heat exchanger is shown in table 5.3.

In the original CO₂ condenser design there are no subcooling, due to the liquid receiver, and the propane condenser design is assumed to have 1 K subcooling.

Simulation data from HXsim were used in order to find the actual correlations between the U-

¹SINTEF is the largest independent research company in Scandinavia, that has a close relation to NTNU.

(a) CO₂ condenser/gas cooler.

(b) Propane condenser.

Figure 5.5: Hxsim models of CO₂ condenser and propane condenser.

Condenser/Gas cooler	
Tube configuration	Tube-in-fin
Tube variant	Round
Tube material	Copper
Fin configuration	Plain
Fin material	Aluminium
Fin pitch	2,20 mm
Tube outer diameter	7,94 mm
Wall thickness pipe	0,60 mm
Vertical tube pitch	25,00 mm
Horizontal tube pitch	21,65 mm
Header outer diameter	6,00 mm
Header wall thickness	0,60 mm

Table 5.3: Specifications simulation HXsim.

values, LMTD-values and the ambient temperature. The fundamental simulation model was utilised in order to achieve operational data, such as the refrigerant mass flow and condensing pressure, with the heat balance in the subcooler as a restriction. These values were further on applied in HXsim. Initially the approach temperatures was guessed and implemented in the fundamental EES script. Further on, operational data from EES was implemented in HXsim. When the appropriate subcooling was achieved, the procedure stopped. This time consuming approach, using both EES and HXsim, is described in figure 5.3.

In HXsim a great deviation in the calculated LMTD was discovered when manually recalculating the values. The calculation of the LMTD for a crossflow heat exchanger is too advanced for HXsim. Therefore the LMTD was obtained from the performance, Q , the area and the heat trans-

fer coefficient for the air side, using equation 4.14. Manual calculations helped discover an error in the exit air temperature, hence this was calculated using equation 4.13 and not obtained from HXsim. U-value and LMTD-value correlations for the original CO₂ condenser are seen in figures 5.6 and 5.7. These correlations were implemented in the final EES script.

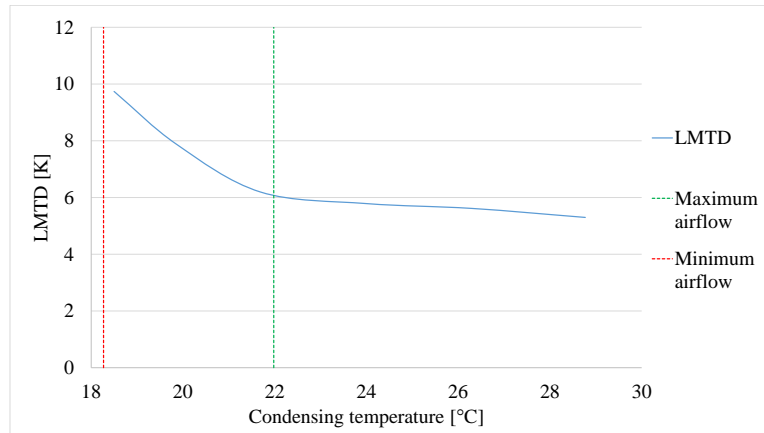


Figure 5.6: LMTD as a function of CO₂ condensing temperature.

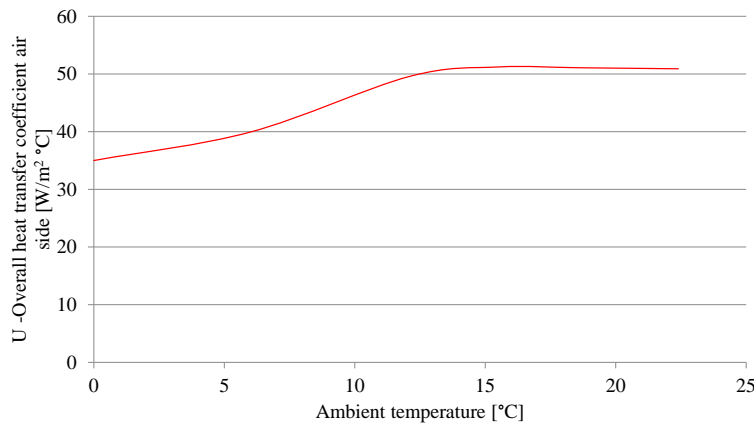


Figure 5.7: U-value for CO₂ condenser as a function of ambient temperature.

Normal simulation control demanded a heat balance error deviation of maximum 2,5 %. The fin variant was set to "plain", but due to slightly curved and splitted fins, the fin enhancement factor was set to 1,1.

Several constrains were used when simulating the system in EES. The same energy balance between the heat of evaporation and condensation was implemented, iterating between the values for the CO₂ condensing temperature and propane evaporating temperature. Further on, the energy balance between the heat absorbed by the air, the heat rejected by the two working fluids

as found in equation 4.18 was implemented. This was achieved by creating a loop for the gas cooler exit temperature, T_3 , or propane condensing temperature, T_{3p} , and the air exit temperature T_{exit} . T_3 and T_{3p} could achieve a minimum value of a few degrees higher than the ambient temperature and a maximum value of 60°C. Figure 5.8 represents the final EES script, where the correlations from HXsim were implemented. The aim was to obtain different correlations for the different condenser modifications when optimising the heat exchanger. In this manner it would be possible to map the improvements on the system for different ambient temperatures and compare the SCOP's of the prototype system for all the different heat exchanger modifications.

Only two input parameters were necessary on order to run the simulation model; The hourly ambient temperature T_{amb} , and the propane operational ON/OFF parameter, ON. ON tells if the propane system is running or not. As described in chapter 4.5, the set points for turning on and off the propane system are respectively 60 and 67 bar. Consequently, for a range of ambient temperatures, the propane system will be switched on and off sporadically.

When the propane system was switched on and off within an hour of these ambient temperatures, this temperature range was simulated by choosing one temperature set point for turning the propane system on and off. This procedure was repeated four times, with six different ambient temperatures, in order to compare these different set points.

Weather data were collected from Meteonorm 7, a comprehensive meteorological reference program, in order to simulate the performance in different European cities. Weather data were given for the chosen cities from the year of 2005, and an average mean temperature for every hour was provided.

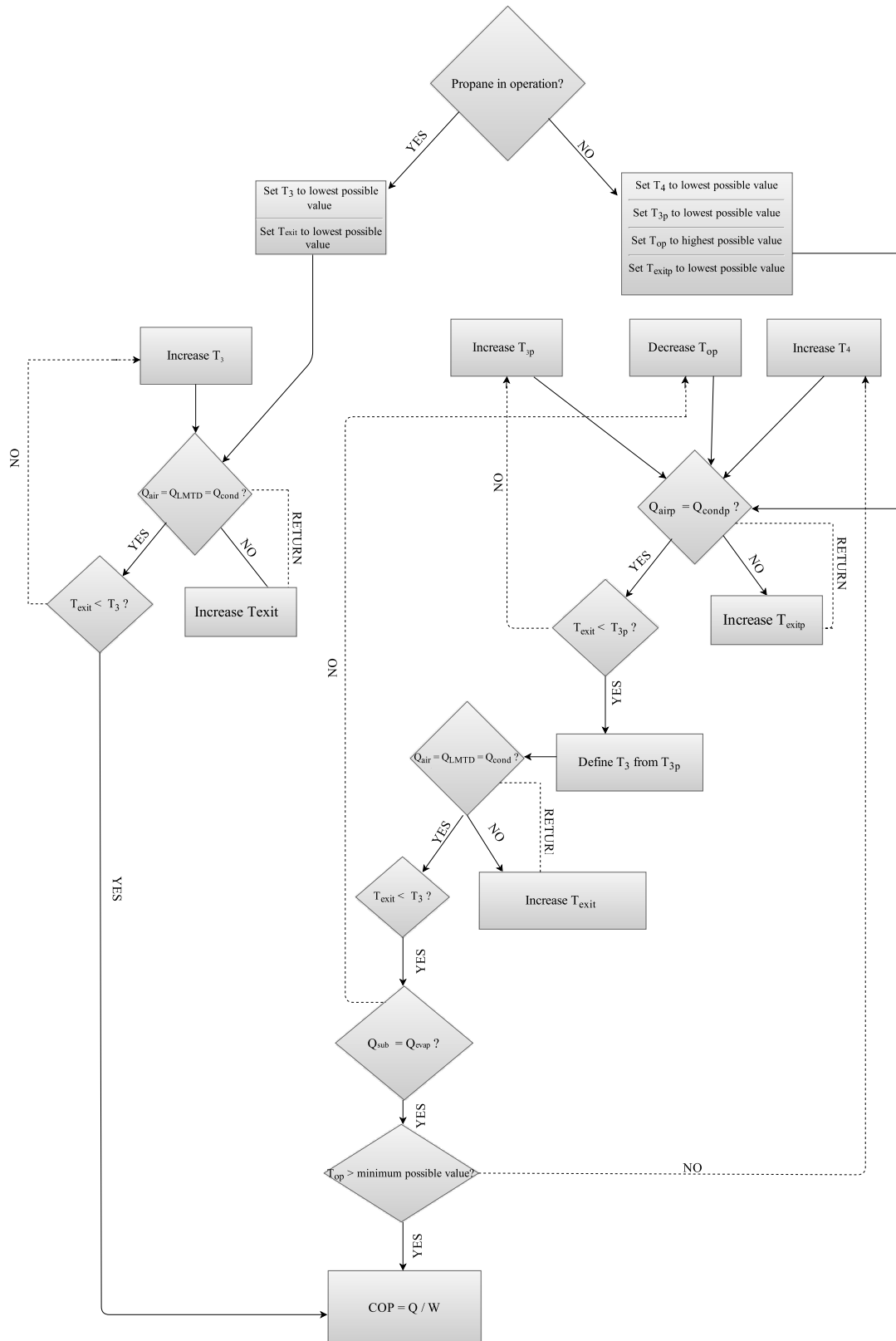


Figure 5.8: Process flow chart of simulation model in EES with input variables T_{amb} and propane operational variable ON/OFF.

5.3 Optimisation of energy efficiency

To provide recommendations to improve the energy efficiency of the system, different configurations were programmed and simulated. These modifications were later compared to the original configuration at different ambient temperatures.

5.3.1 Modifications condenser and gas cooler

Various configurations of the CO₂ gas cooler were tested in HXsim. The aim was to achieve correlations for the U-values and LMTD-values for the different modifications. Later the system would be simulated in EES using these correlations to map the systems operation with a new and more optimal gas cooler/condenser. Several configurations were tested, with both an integrated heat exchanger, as the original configuration, and with separate propane and CO₂ heat exchangers. The difference between these two distinct configurations is that with the integrated heat exchanger, the temperature of the inlet air is the outlet air temperature from the propane condenser. There were few restrictions when choosing new configurations; both cost and size restrictions could be varied, meaning that the number of pipes could be increased. The main focus was to find the best circuit design, while keeping the cost and size as low as possible.

In order to find the best heat exchanger modification, the configurations were simulated with the same saturation temperature, pressure and mass flow as the original design in HXsim. Comparing the subcooling for the different configurations with the same operational parameters, helped spot the best condenser configurations. The new correlations were further implemented in the EES script described in figure 5.8. When implementing the new HXsim correlations in the EES script, no changes were seen on the resulting performance. This was due to the heat balance restrictions set in EES, where initially the Q_{LMTD} was required to be equal to the Q_{air} and Q_{cond} . In order to run the simulation model, the heat balance was allowed a 10 % deviation for the Q_{LMTD} . With this heat balance allowance, no difference were seen when comparing the simulation model using the original and the modified condenser/gas cooler.

When the best condenser configuration modifications were found, the improvement was calcu-

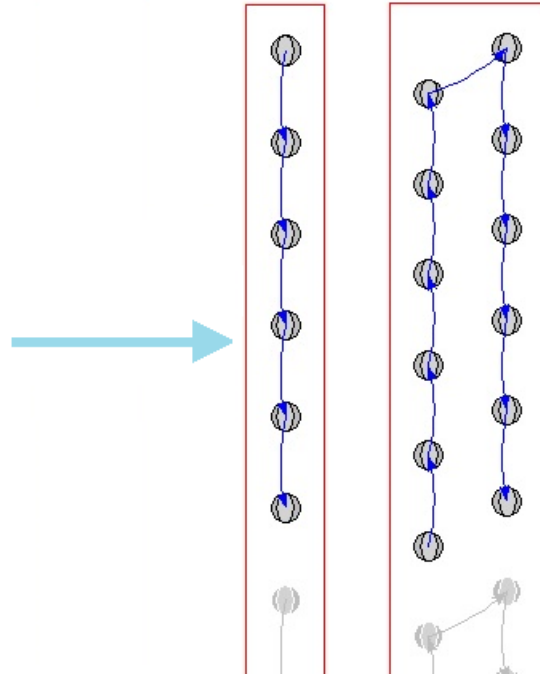


Figure 5.9: Original configuration with propane condenser (6-1-7) and CO₂ gas cooler (6-2-7). The air flow is represented by the blue arrow.

lated in two distinct ways. Either by keeping the subcooling and the high side pressure, achieving an increase in refrigeration capacity, or by decreasing the high side pressure and demanding 0 K and 1 K subcooling for the CO₂ and the propane. By demanding 0 K and 1 K subcooling, new operational parameters were obtained by again following the procedure is described in figure 5.3. New correlations could be implemented in the EES script described in figure 5.8 and the SCOP could be compared to the original configuration. To obtain the new operational parameters, a new minimum CO₂ condensing temperature of 15°C had to be set, due to the improved propane condenser.

A system for naming the different configurations has been developed. The original configuration is seen in figure 5.9. The blue arrow represents the air flow from left to right. This is the same for all the tested configurations. The original propane configuration is named 6-1-7 and the CO₂ configuration is named 6-2-7. The first digit represents the number of vertical tubes, the second digit represents the number of rows and the third represents the number of vertical duplications. Figure 5.10 explains how the different modifications have been named.

Initially a configuration with the propane located in centred the pipe row, and the CO₂ in the

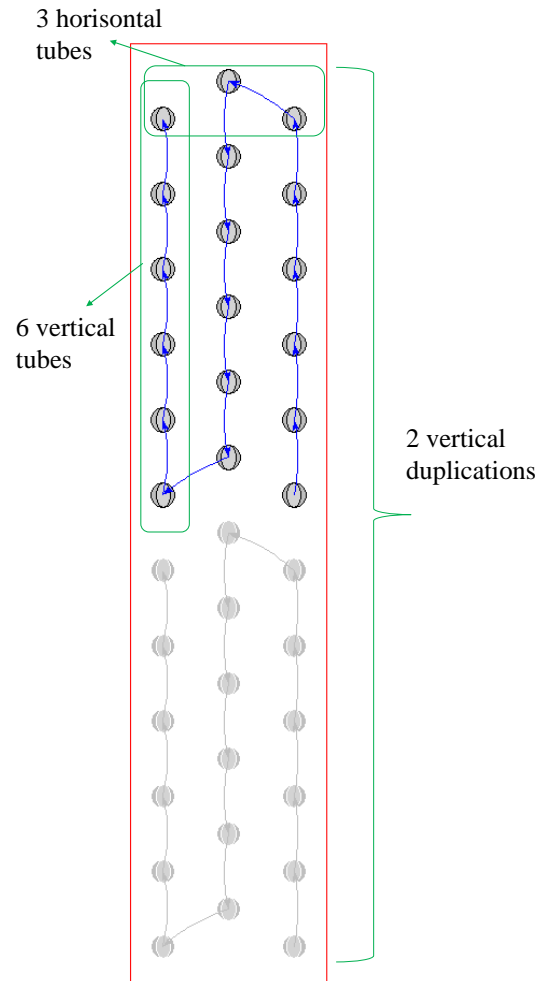


Figure 5.10: Example of a 6-3-2 condenser.

exterior pipe rows as seen in figure 5.11, was tested. The aim was to achieve a better temperature glide, where the warmest air met the warmest refrigerant and the coldest air would be heated by the cooled refrigerant. Unfortunately, this configuration was too extensive to simulate in HXsim. In order to simulate this configuration, a temperature difference over the two first pipeline rows needs to be guessed. Further the CO₂ outlet temperature from the third row is obtained, and is set as the inlet temperature in the first CO₂ pipeline row. When the first row is simulated, the outlet air temperature from this row is obtained, and then set as the inlet air temperature for the middle propane row. When this row is further simulated in HXsim, the initial guess for the temperature difference over the two first rows of pipelines is checked versus the outlet air temperature obtained when simulating the propane pipeline row.

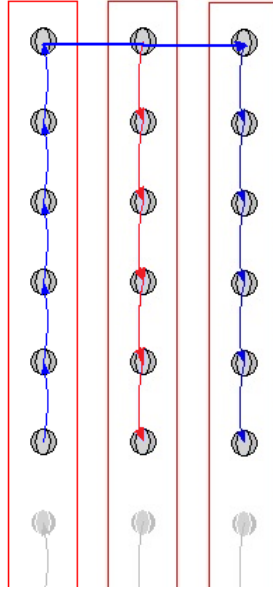


Figure 5.11: Condenser modification with propane in the middle pipeline row, and CO₂ in the two outer pipelines.

Further on, the configuration in figure 5.12 was tested. This includes one combined row for propane and CO₂, one middle row with propane and the one row with only CO₂, getting the coldest air too cool the coldest CO₂. The aim was again to achieve a good temperature glide for the air and the refrigerant and to obtain a small temperature difference between air and CO₂ at the exit. By having the inlet of both the refrigerant in the last row, the superheat would be removed with the heated air. The heat exchanger is illustrated in figure 5.12 where the blue and red arrows represent respectively the CO₂ and propane. When this configuration was tested as a CO₂ condenser, it resulted in a pressure loss of 2,7 bar and a vapour fraction of 0,25, which reflected on a poor performance compared to the original configuration.

An option of moving the propane condenser pipes to the bottom of the heat exchanger was tested. The initial idea was that the air cooling CO₂ pipes would not be heated by the propane pipes. This configuration is shown in figure 5.13. Here the CO₂ condenser/gas cooler will receive a smaller fraction of the fan air.

Further on different circuit designs were tested. The material and the fin design remained the same for all configurations. Data on available pipes with a smaller diameter was provided by SINTEF and tested for the original circuit design in HXsim.

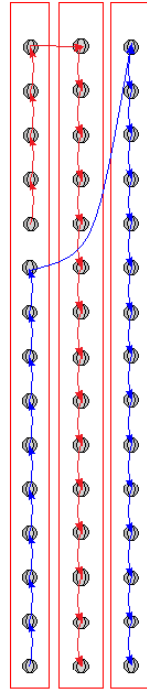


Figure 5.12: CO₂ front row, shared last row.

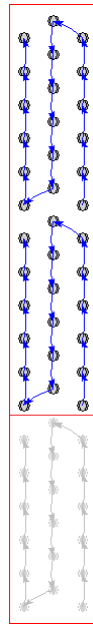


Figure 5.13: Condenser modification with propane condenser tubes at the bottom and CO₂ tubes at the top.

In appendix [A.1](#), [A.3](#) and [A.4](#), the different arrangements simulated in HXsim is presented. At higher ambient temperatures, the arrangements represented in appendix [A.3](#) was also simu-

lated as gas coolers.

Subcooling, performance divided by area and additional pipes shown in table 5.4 for the CO₂ condenser are for an ambient temperature of 18,7°C, and an ambient temperature of 40°C for the propane condenser and the CO₂ gas cooler.

Configuration Vertical tubes · Horizontal · Duplications	Performance/area [$\frac{kW}{m^2}$]	Subcooling [K]	Additional tubes [%]
<i>Original</i>			
6·2·7	0,29	0	0
<i>New pipe dimension</i>			
6·2·7	0,43	0,03 ²	0
1·4·50	0,19	0,42	138
<i>CO₂ upper part, propane lower part</i>			
6·3·4	0,30	0,24 ²	-14,3
12·3·2	0,31	0,12 ²	-14,3
9·3·3	0,29	0,06 ²	-3,57
<i>CO₂ front row, shared last row</i>			
15/10·2·1	0,83	0,25 ²	-82,14
<i>Two rows</i>			
8·2·6	0,27	2,54	14,3
9·2·5	0,29	2,48	7,14
10·2·4	0,32	2,04	-4,76
11·2·4	0,29	3,14	4,76
12·2·4	0,27	4,16	14,3
13·2·3	0,33	2,90	-7,14
14·2·3	0,32	3,69	0
15·2·3	0,29	4,35	7,14
<i>Three rows</i>			
6·3·4	0,35	2,72	-14,3
9·3·3	0,33	5,16	-3,57
12·3·2	0,37	5,41	-14,3
<i>Four rows</i>			
4·4·5	0,32	3,96	-4,76
4·4·6	0,27	4,98	14,3
3·4·7	0,30	2,66	0
3·4·8	0,27	3,53	14,3

Table 5.4: Modifications CO₂ condenser at a T_{amb} of 18,7°C.²Outlet vapour quality, hence no subcooling

Configuration Vertical tubes · Horizontal · Duplications	Performance/area [$\frac{kW}{m^2}$]	Subcooling [K]	Additional tubes [%]
<i>Original</i>			
6·1·7	0,50	1	-
10·3·3	0,26	15,90	114,3
11·2·2	0,53	14,47	4,76
6·6·3	0,43	15,27	28,6
9·2·3	0,43	10,75	28,8
4·2·6	0,46	7,96	14,3
12·2·2	0,48	10,83	14,3
8·1·6	0,47	8,05	14,3
10·1·4	0,57	8,07	-4,76
11·1·4	0,53	10,40	4,76
12·1·4	0,49	12,03	14,3
13·1·3	0,59	10,39	-7,14
14·1·3	0,56	11,81	0
15·1·3	0,52	12,87	7,14

Table 5.5: Modifications propane condenser at a T_{amb} of 40°C.

Configuration Vertical tubes · Horizontal · Duplications	Performance/area [$\frac{kW}{m^2}$]	Δh [kJ/kg]	Additional tubes [%]
<i>Original</i>			
6·2·7	0,08	63,0	-
<i>Separate CO₂ gas cooler</i>			
15·2·3	0,08	71,6	7,14
4·4·6 ³	0,08	72,3	14,3
11·2·4	0,08	72,4	4,76
6·3·4	0,10	71,5	-14,3
12·3·2 ³	0,09	66,1	-14,3
9·3·3 ³	0,09	71,8	-3,6
<i>Integrated CO₂ gas cooler</i>			
10·2·4	0,08	62,5	-4,76
11·2·4	0,07	62,2	4,76
12·2·4	0,07	62,2	14,3
13·2·3	0,08	61,8	-7,14
14·2·3	0,08	61,6	0
15·2·3 ³	0,07	61,4	7,1
4·4·6 ³	0,07	62,6	14,3

Table 5.6: Modifications CO₂ gas cooler at a T_{amb} of 40°C.³Modified enhancement factor from 1,1 to 0,4

When simulating the same CO₂ condenser configuration as a gas cooler in HXsim, several problems were met. First of all, good improvements were found when testing the condenser configurations. Testing the same configurations as gas coolers, raised several issues. A condenser improvement represents an over dimensioned gas cooler and pinch problems were experienced in several of the HXsim gas cooler modifications. In order to calibrate HXsim using the exact same simulation control parameters, a heat balance deviation of up to 17 % was experienced. In figure 5.14 the temperature plot for the original gas cooler configuration is shown. Normal simulation control has been implemented, with an enhancement factor of 1,1. In order to run some of the configurations without a heat balance deviation, the enhancement factor was modified.

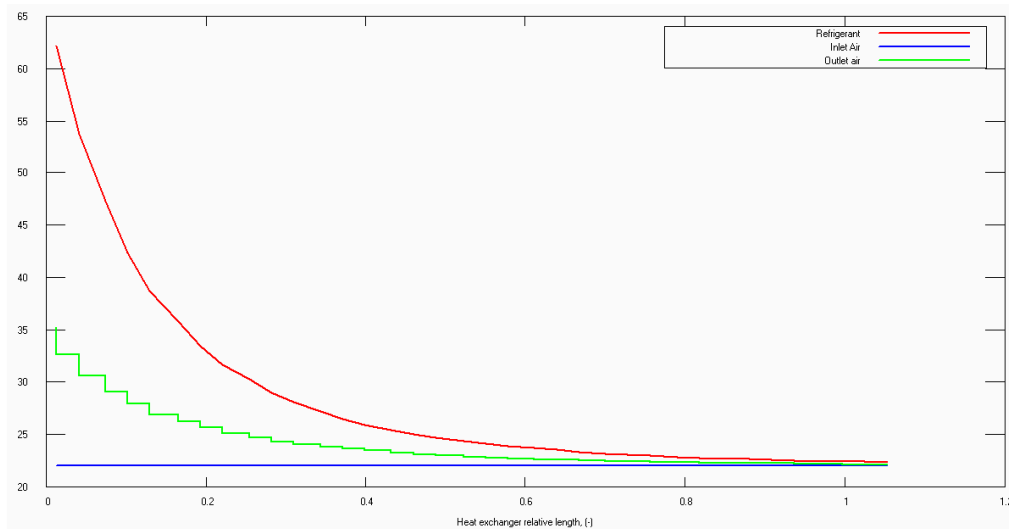


Figure 5.14: Original gas cooler configuration with an enhancement factor of 1,1 at a T_{amb} of 22°C.

In figure 5.15, the temperature profile for the original configuration is plotted with an enhancement factor of 0,7. Here the influence of adjusting the enhancement factor is clearly seen. The heat transfer from the refrigerant to the air is inhibited.

For the 15·2·3 gas cooler configuration a temperature plot can be seen in figure 5.16. This represents an integrated heat exchanger, where the propane pipes has heated the air with 5 K. This plot was achieved with a 8 % heat balance deviation. Changing the pipeline circuit to staggered down, instead of staggered up resulted in a better temperature glide. Also by changing the number of elements the tube will be divided into during simulation, the heat balance will be more accurate.

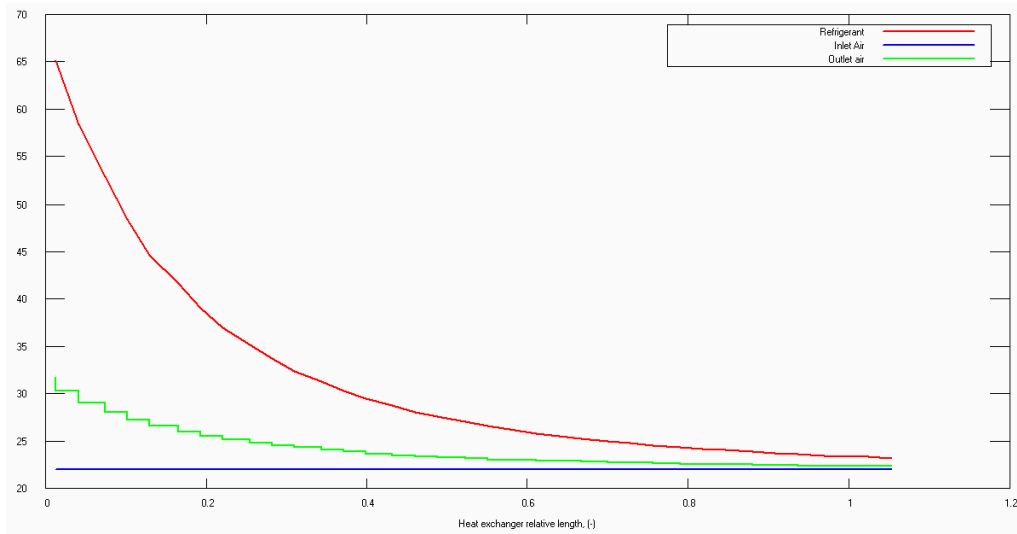


Figure 5.15: Original gas cooler configuration with an enhancement factor of 0,7 at a T_{amb} of 22°C .

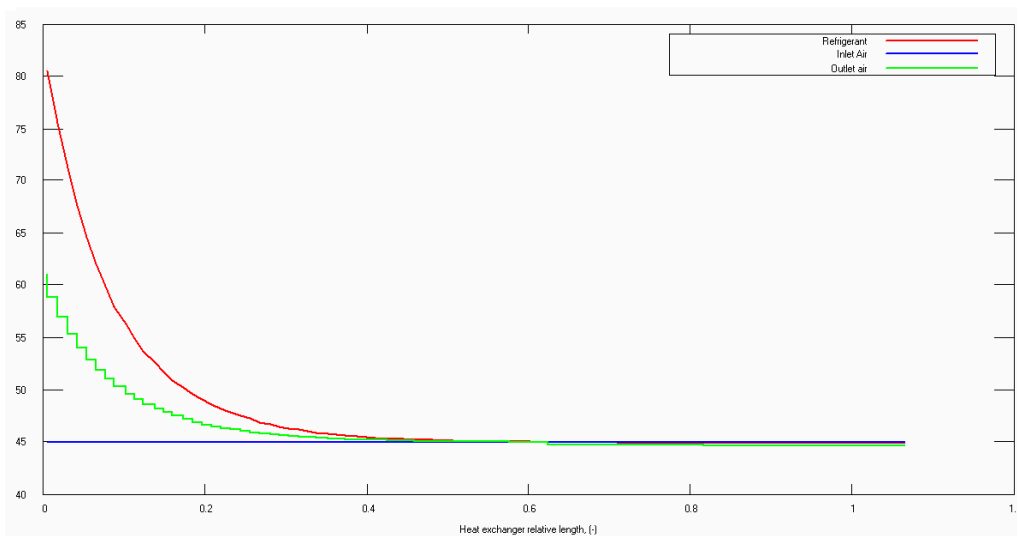


Figure 5.16: Temperature plot for the CO_2 15·2·3 gas cooler configuration with 45°C inlet air temperature. 8 % heat balance deviation.

The 15·2·3 gas cooler configuration was also simulated as a separate heat exchanger, having ambient air not heated by the propane pipeline row. The temperature plot for this configuration is seen in figure 5.17. Comparing figures 5.16 and 5.17 it is confirmed that the lower input temperature, the better temperature glide in the heat exchanger is experienced. This is represented by the outlet air temperature line that is significantly smoother for the configuration at lower inlet air temperature.

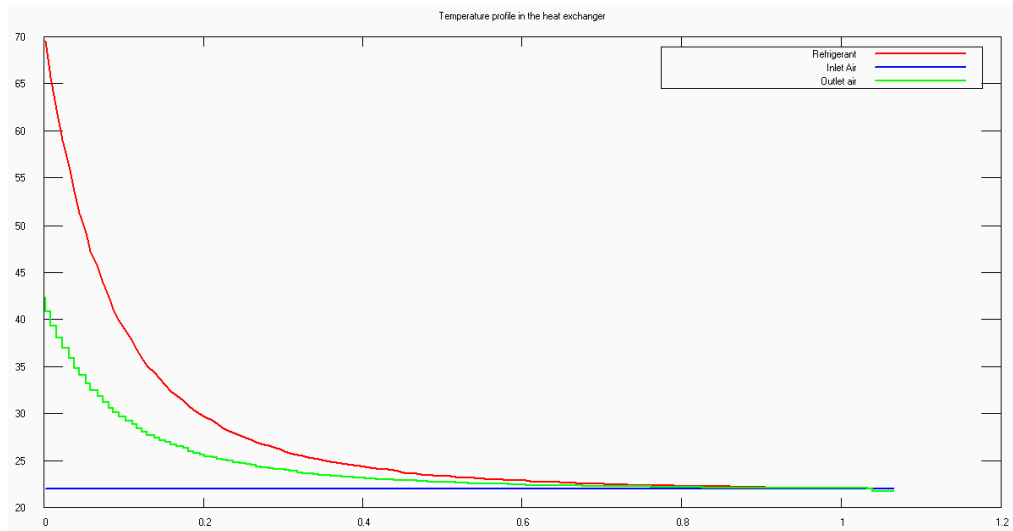


Figure 5.17: Temperature plot for the CO₂ 15·2·3 gas cooler configuration at 22°C inlet air temperature and normal simulation control.

In figures 5.18 and 5.19 the temperature plot for the 15·2·3 and 9·3·3 CO₂ condenser configurations are shown, at an ambient temperature of 6°C. It can be observed that the 9·3·3 configuration, with three rows have a temperature jump on the air side, while the 15·2·3 configuration have a more smooth air temperature glide. Figures 5.20 and 5.21 shows the temperature plot for the same configurations at a higher ambient temperature. When the condensing temperature is increasing, the fan capacity is increased as illustrated in figure 5.2. The effect of the fan can be seen as a smaller jump in air side temperature in figure 5.21.

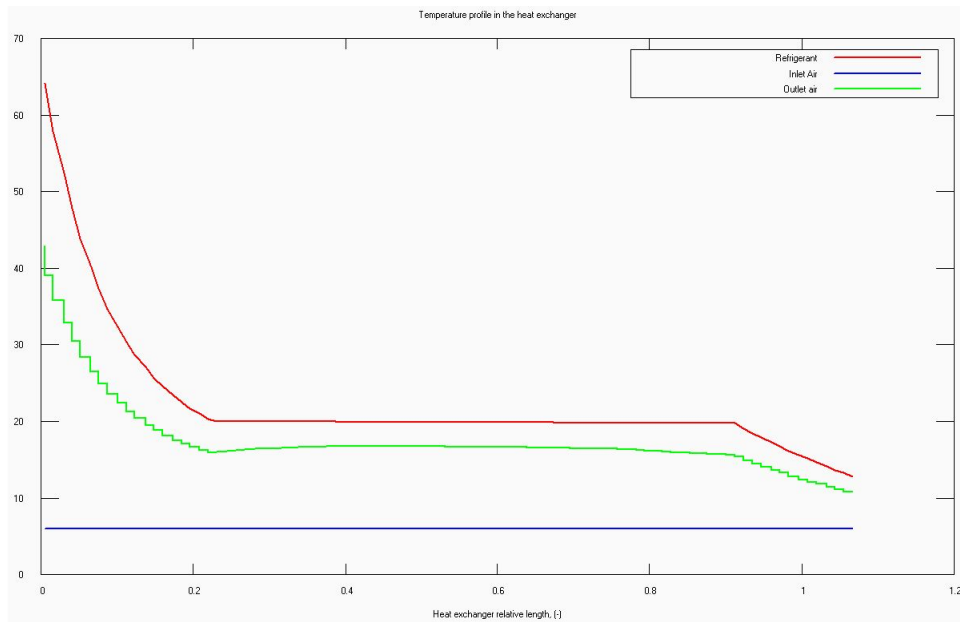


Figure 5.18: Temperature plot for the CO₂ 15.2.3 gas cooler configuration with 6°C inlet air temperature.

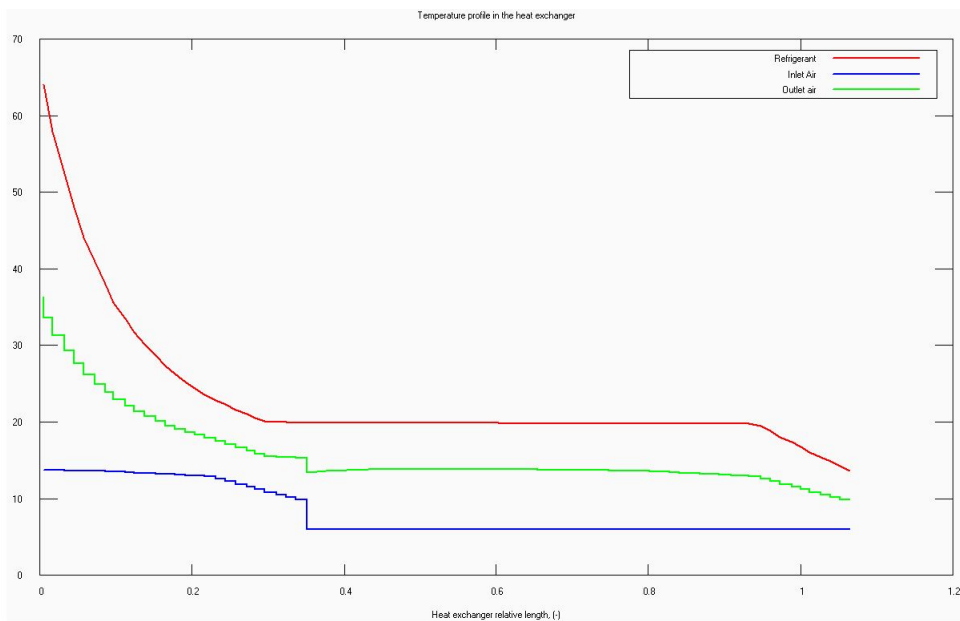


Figure 5.19: Temperature plot for the CO₂ 9.3.3 gas cooler configuration with 6°C inlet air temperature.

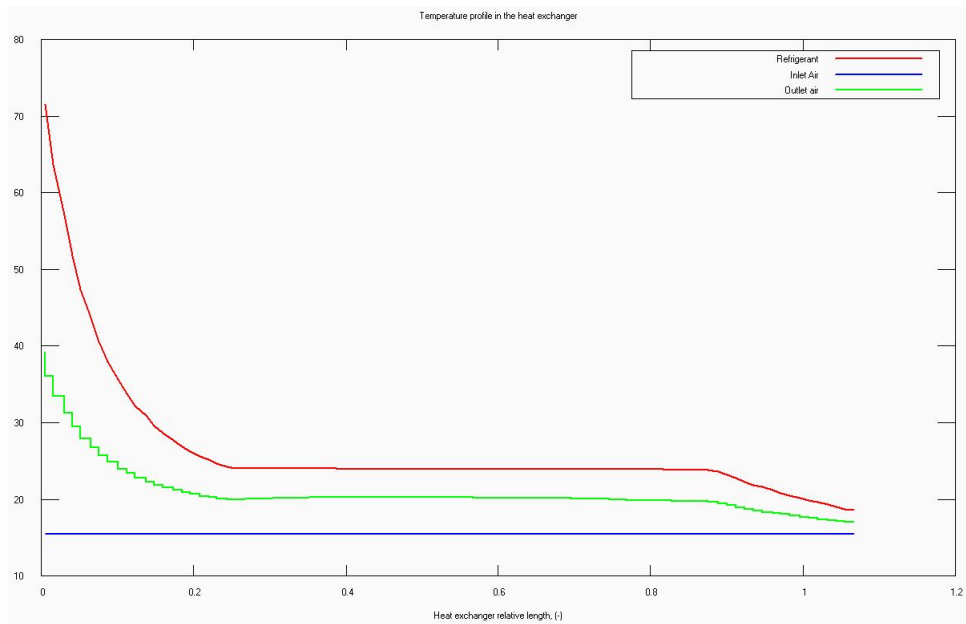


Figure 5.20: Temperature plot for the CO₂ 15·2·3 gas cooler configuration with 15,5°C inlet air temperature.

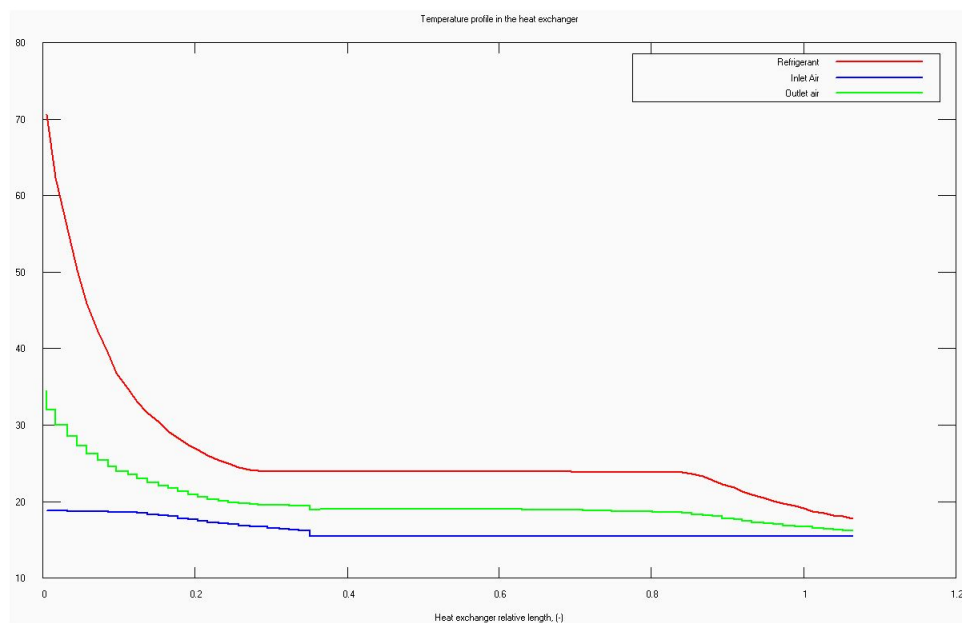


Figure 5.21: Temperature plot for the CO₂ 9·3·3 gas cooler configuration with 15,5°C inlet air temperature.

5.3.2 Modifications overall system

In addition to investigating improvements on the gas cooler, a variety of different configurations on the prototype system was simulated. Focus has been on simple solutions of well established technologies.

All of the modifications are simulated with transcritical operation above the design point. This design point corresponds to a condensing temperature of 25 °C. The subcritical operation were simulated with the same heat balance equations and correlations as the original prototype simulation model. To simplify the simulations, the approach temperature of the gas cooler was set to 5 K. All of the systems except the internal heat exchanger modification, were simulated with a superheat of 10 K. The CO₂ high side pressure was determined by performing iterations between 75 to 135 bar and selecting the pressure that maximised the COP. The iterations were performed with steps of 1 bar to minimise computational time.

Simple transcritical CO₂ refrigeration system

As discussed in the literature study, CO₂ transcritical system are commonly used at high ambient air operations. Owing to this, a simplified version of the CO₂ system was simulated with transcritical operation above the design point.

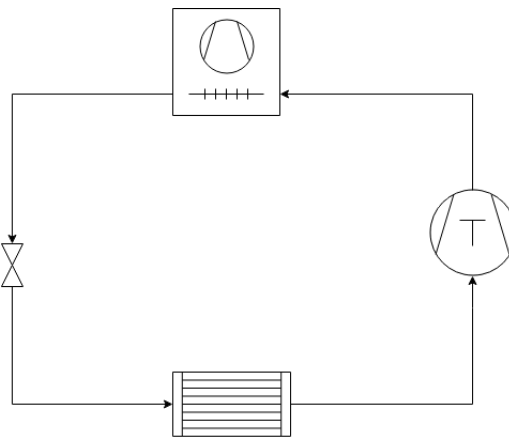


Figure 5.22: Transcritical CO₂ refrigeration system.

Transcritical CO₂ refrigeration system with internal heat exchanger

Also reviewed in the literature study, was the internal heat exchanger configuration. This is an efficient method of improving the energy efficiency for a CO₂ refrigeration system. Due to this fact, an internal heat exchanger was added to the transcritical CO₂ refrigeration system described to compare the performance. The internal heat exchanger was designed for 5% of the refrigeration capacity at the design point.

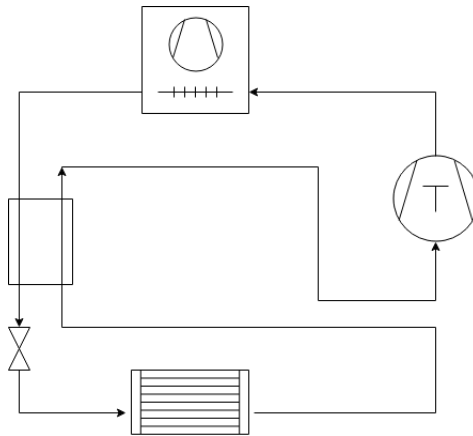


Figure 5.23: Transcritical CO₂ refrigeration unit with internal heat exchanger.

Transcritical CO₂ refrigeration system with propane subcooling

The CO₂ transcritical system was further modified by implementing a smaller mechanical subcooling unit with an external air cooled condenser. The minimum refrigeration capacity was set by the design point refrigeration capacity. When the refrigeration capacity dropped below this minimum value, the propane system was turned on. The swept volume and the volumetric efficiency of the compressor were adjusted to comply with this restriction. Further the propane system was designed to have no superheat from the evaporator, and with a 15 K exit temperature difference in the condenser. The propane evaporating pressure was determined in the same manner as the high side pressure of the CO₂. The temperature difference between the CO₂ in the subcooler and the evaporating propane was minimum 5 K.

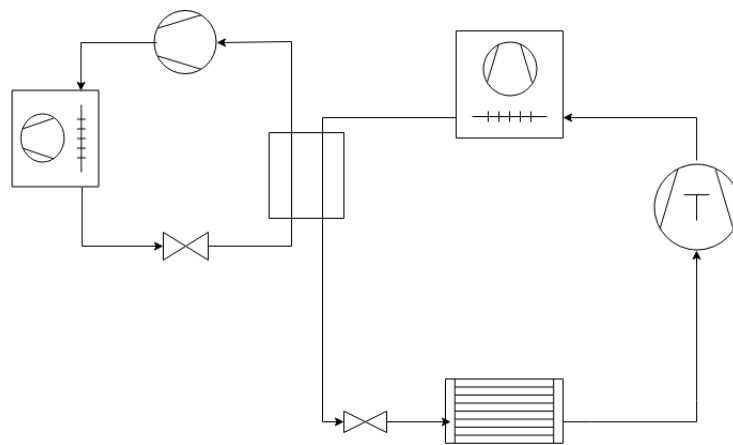


Figure 5.24: CO₂ refrigeration system with mechanical subcooling using propane.

Chapter 6

Results

In this chapter, the results from the simulation model is plotted and compared to the results from the tests performed during the project thesis. The simulation model has been used to plot the performance in different European capitals. Further on, the results from optimisation of the integrated condenser/gas cooler and the overall system is presented.

6.1 Measurements and simulation model

A simulation model has been developed using HXsim and EES, and the results has been compared to the results obtained during the projects thesis. The results calculated from the data obtained during the testing period is seen in table 6.1. As discussed in chapter 5, the compressor measurement data showed unreasonable high values compared to calculations done with the isentropic and volumetric efficiencies obtained from the compressor manufacturer. Therefore, the project thesis data results was corrected by calculating a new compressor discharge enthalpy, correcting the mass flow, thus correcting the work added to the compressor. Figures 6.1 and 6.2 shows the corrected measurements with an evaporating temperature of -10°C for the system operating with and without the propane system. The optimal ambient temperature set point where the propane system should start to operate is where the two COP lines intersects, when analysing figure 6.1. This occurred at an ambient temperature of approximately $23,5^{\circ}\text{C}$.

System in operation	T_{amb}	Q_o	$\frac{\Delta Q_o}{Q_o}$	COP	$\frac{\Delta COP}{COP}$	T_{ap}	$\frac{\Delta T_a}{T_a}$
R744	23,5°C	7,9 kW	10,5%	2,08	13,1%	5,0K	12,4%
R744 + R290	23,5°C	9,8 kW	8,7%	2,05	11,3%	3,0 K	12,8%

Table 6.1: Obtained Q_o , COP and T_a from tests performed during project thesis.

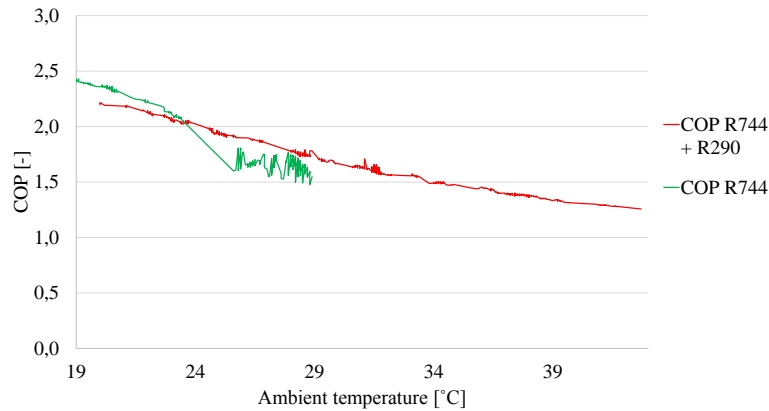


Figure 6.1: COP from measurements.

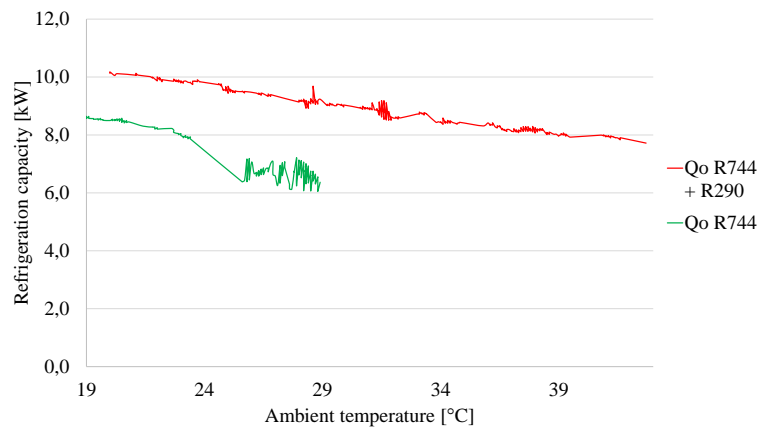


Figure 6.2: Refrigeration capacity from measurements.

Further on, the results from the simulation model was verified by comparison to the measurement data results. The differences are shown in figures 6.3 and 6.4 for the solitary CO₂ operation and in figures 6.5 and 6.6 with the propane system in operation.

When comparing the simulation and measurement results, the figures for CO₂ operation shows a slight discrepancy in slope. The maximum deviation between the to curves are 10% for the COP and 6,9% for the refrigeration capacity, both at an ambient temperature of 23,3°C.

Similar trends are observed from the figures 6.5 and 6.6, although the simulated system operates

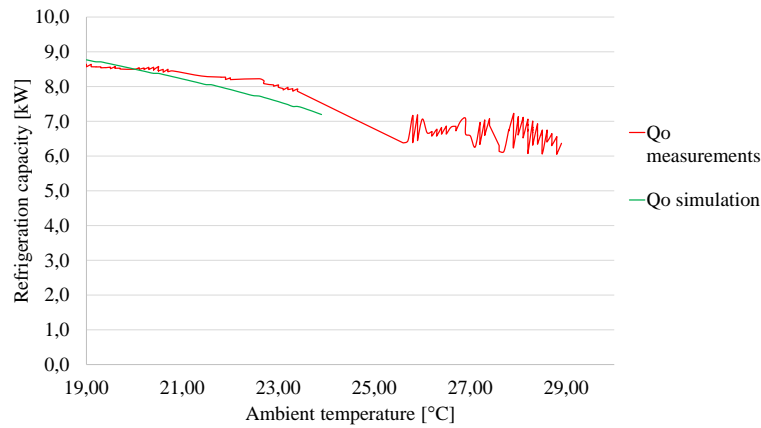


Figure 6.3: Comparison of Q_o without propane operation.

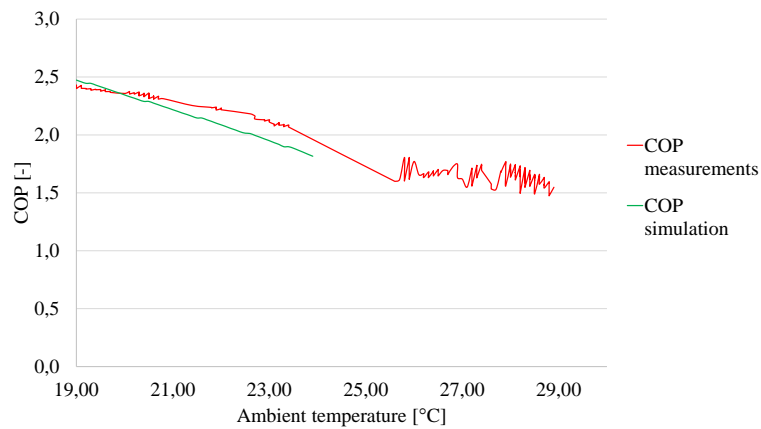


Figure 6.4: Comparison of COP without propane operation.

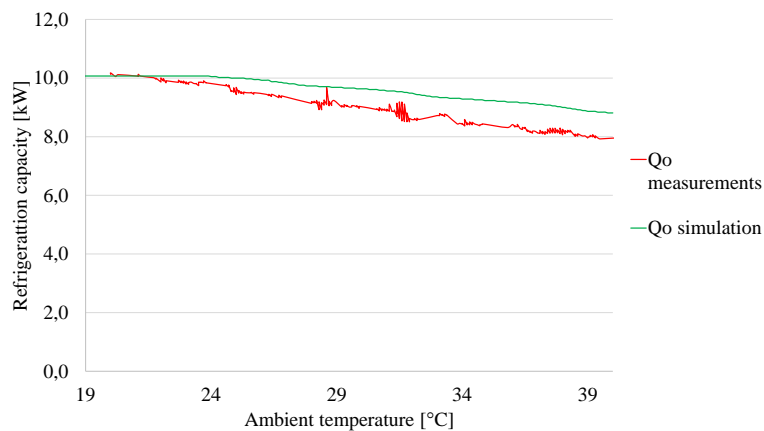


Figure 6.5: Comparison of Q_o with propane operation.

with a slightly better performance. The maximum deviation is 12% for the refrigeration capacity and 21% for the COP at an ambient temperature of approximately 37°C. The minimum devia-

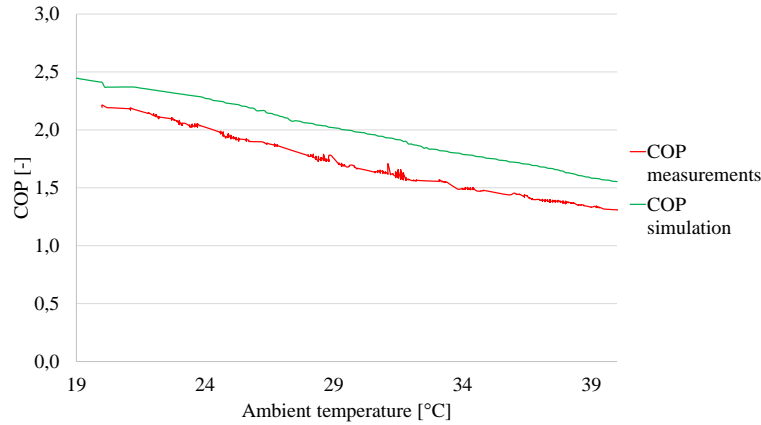


Figure 6.6: Comparison of COP with propane operation.

tion for the COP is 8% at an ambient temperature of 20°C.

The deviations from the measured values will affect the optimal point or temperature for on/off operation of the propane system. To find the optimal point based on the simulation, the refrigeration capacity and COP needs to be investigated. Figures 6.7 and 6.8 shows the results from the simulations when running the CO₂ system exclusively from -20°C to 24°C and combined CO₂ and propane operation from 18,5°C to 40°C ambient temperature.

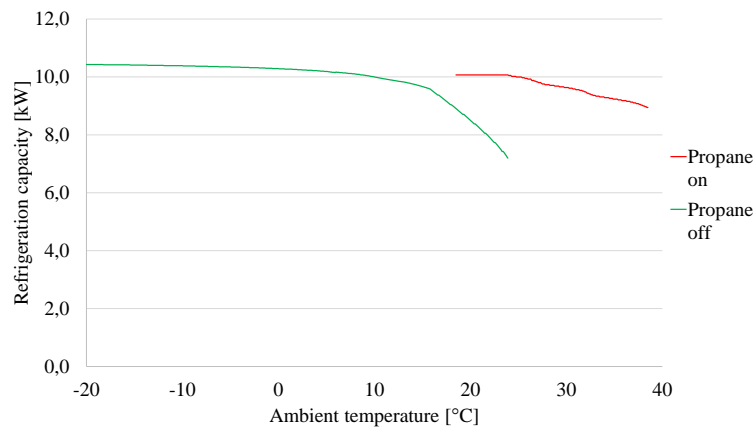


Figure 6.7: Simulated refrigeration capacity with and without propane.

Figure 6.7 and table 6.2 shows a rapid decrease in refrigeration capacity for the CO₂ operation at an ambient temperature of approximately 15°C. Further on, it can be observed that the highest refrigeration capacity would be achieved by starting propane operation before the CO₂ refrigeration capacity starts to decrease rapidly. However, from figure 6.8 it can be observed that the solely CO₂ operation have a better COP up to an ambient temperature of 19,4°C. Table 6.2

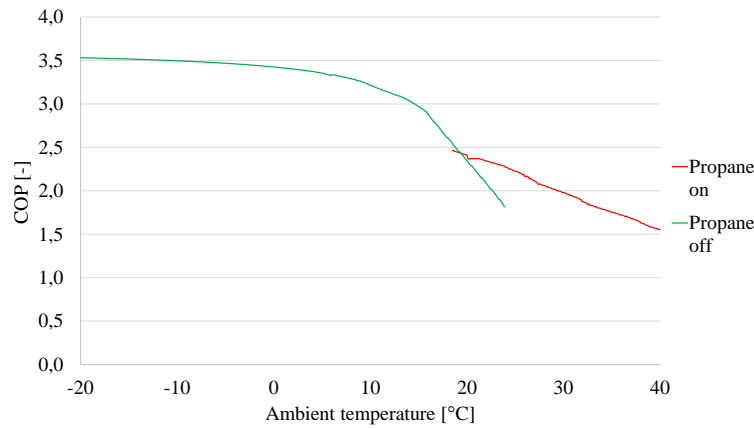


Figure 6.8: Simulated COP with and without propane.

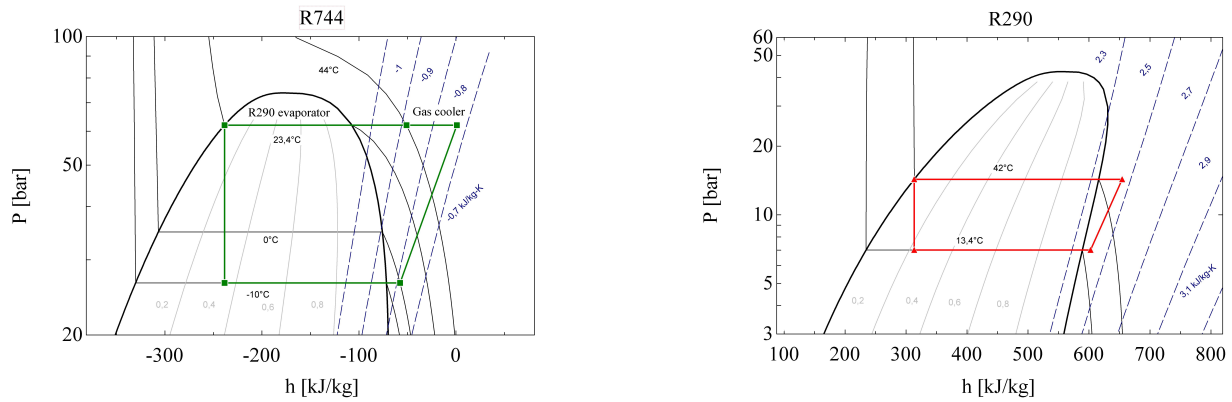
T_{amb}	R744 T_{cond}	$\Delta T_{diff,cond}$	Q_o	COP
18,4 °C	24,53 °C	6,13 K	8,94 kW	2,56
19,3 °C	25,37 °C	6,07 K	8,71 kW	2,45
20,9 °C	26,95 °C	6,05 K	8,25 kW	2,23
21,9 °C	27,90 °C	6,00 K	7,95 kW	2,10
22,9 °C	28,85 °C	5,95 K	7,61 kW	1,97
23,9 °C	29,79 °C	5,89 K	7,20 kW	1,82

Table 6.2: Set point for start of propane operation.

shows the performance of the CO₂ system at different chosen set points. It can be observed that the temperature difference in the condenser decreases with increasing ambient temperature.

An illustration of the refrigeration system is shown in the log(p)-h diagrams in figure 6.9 for an ambient temperature of 35 °C. As shown in the diagram, the gas cooler removes some of the superheat from the CO₂ while the rest of the cooling is performed in the propane evaporator.

Further results from the prototype simulation are calculated with a set point of 19,4 °C in ambient temperature.



(a) R744 log p-h diagram for the prototype.

(b) R290 log p-h diagram for the prototype.

Figure 6.9: Log p-h diagram for the prototype system at $T_{amb} = 35^\circ\text{C}$.

6.1.1 System operation in European capitals

The prototype system was simulated for five European capitals with different climates in order to investigate and compare the seasonal performance, operating hours with propane and energy consumption. The capitals were chosen in cooperation with Cadio AS. The data presented in table 6.3, figures 6.10 and 6.11 are calculated with a set point corresponding to an ambient temperature of $19,4^\circ\text{C}$.

	Oslo	London	Paris	Budapest	Madrid
Operating hours propane	461	716	1519	1975	2580
% propane operation of year	5,26	8,17	17,34	22,55	29,45
Maximum Q_o [kW]	10,43	10,35	10,36	10,39	10,34
Minimum Q_o [kW]	8,71	8,71	8,71	8,71	8,71
Seasonal performance	3,22	3,09	2,99	2,97	2,85
Yearly energy consumption [kWh]	27627	28417	29506	30058	31282

Table 6.3: System performance in different climates.

It can be seen from table 6.3 that the SCOP decreases, while the energy consumption and operational hours with propane increases in the warmer climates, and that Oslo achieves the best system performance.

Figures 6.10 and 6.11 illustrates how the refrigeration capacity and COP changes with temperature over a one year period. It can be observed that the refrigeration capacity and COP is reduced

when the ambient temperature increases. A large variation in refrigeration capacity is also observed during the months with warmer ambient temperatures.

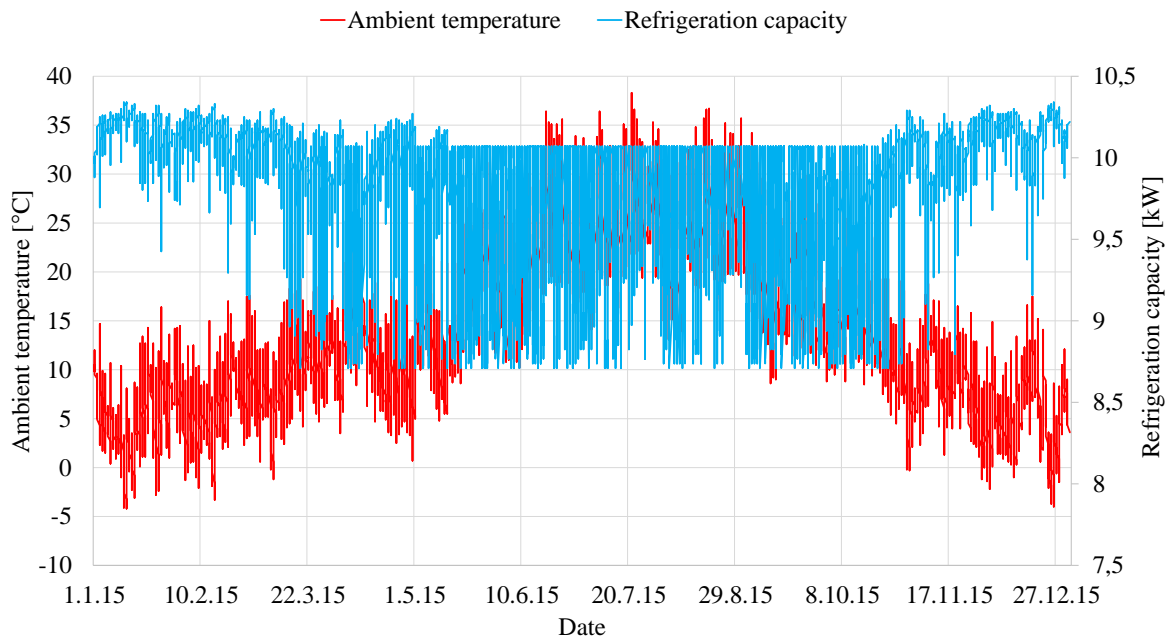


Figure 6.10: Ambient temperature versus refrigeration capacity in Madrid 2005.

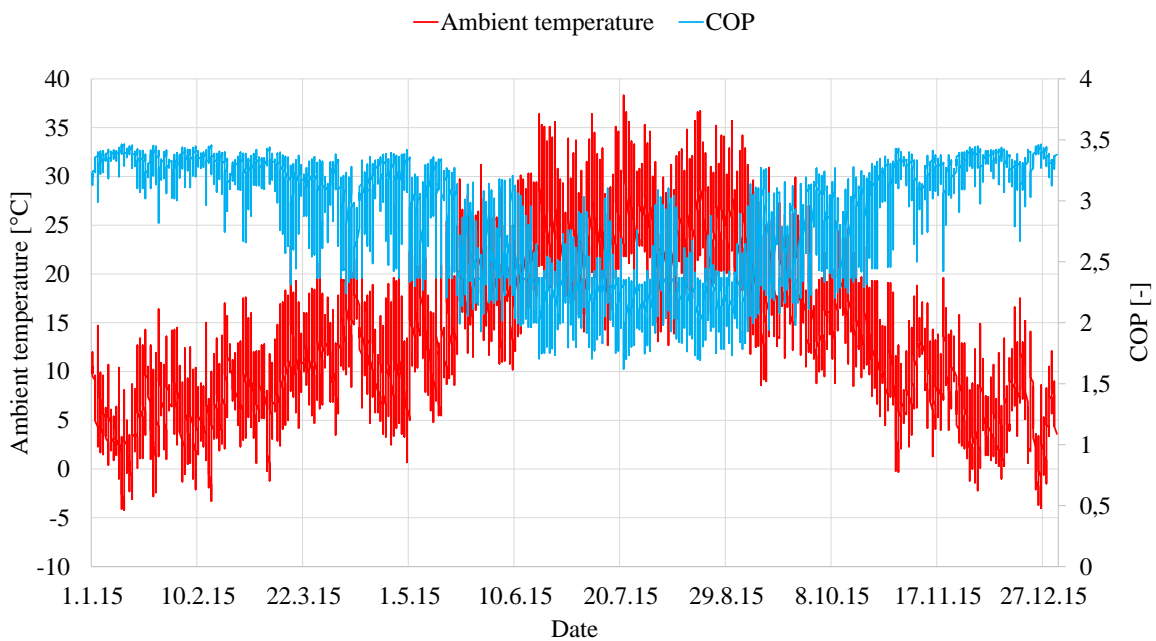


Figure 6.11: Ambient temperature versus COP in Madrid 2005.

6.2 Modification condenser and gas cooler

As presented in chapter 5, several configurations for the CO₂ condenser/gas cooler and the propane condenser, were designed and tested in HXsim. The aim was to obtain correlations for the LMTD-values and U-values and implement these in the final EES script. No differences were seen when using the new correlations from the various modifications simulated in HXsim. Thus, the SCOP for the prototype system with the new heat exchanger modification correlations could not be obtained. A theoretical approach has been utilised in order to investigate the best CO₂ and propane condensers. By calculating the subcooling for different condenser modifications in HXsim, the best configurations were spotted. In order to analyse the improvement of the condenser configurations, the Q_o and COP were calculated when maintaining the subcooling and the condensing pressure, or by a reduction in pressure and no subcooling.

6.2.1 Modification of the CO₂ condenser

In table 6.4, data on the best performing CO₂ condenser modifications are presented. An approach temperature of approximately 2 K was experienced for all the configurations at an ambient temperature of 18,7°C.

Configuration Vertical tubes · Horizontal · Duplications	Subcooling [K]	Max pressure loss [bar]	Additional tubes [%]
6·2·7 ¹	0	0,05	-
12·3·2	5,41	1,50	-14,30
9·3·3	5,16	0,53	-3,60
15·2·3	4,35	0,57	7,1
4·4·6	4,98	0,07	14,3

Table 6.4: Best CO₂ condenser configuration modifications at a T_{amb} of 18,7°C.

In figure 6.12, the subcooling is plotted for the best CO₂ condenser modifications. At a saturation temperature of 20°C, the 15·2·3 configuration achieves a subcooling of 7 K, thus the highest subcooling of all the configurations. At saturation temperatures above 21°C, the 12·3·2 configuration achieves the highest subcooling. The 15·2·3 configuration has a linear slope, compared

¹Original configuration

to the non-linear slopes of the other configurations.

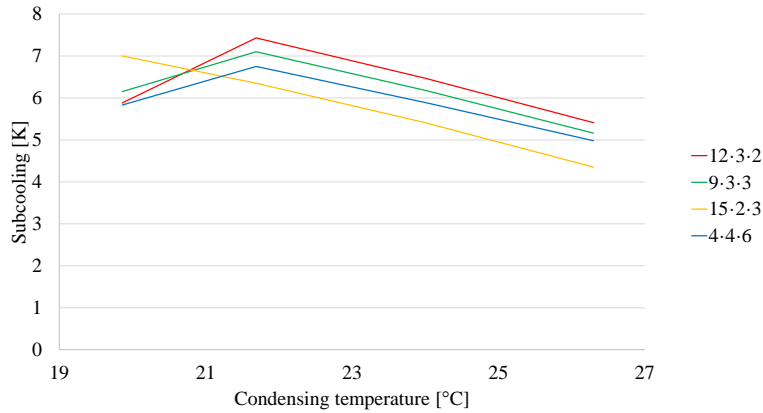
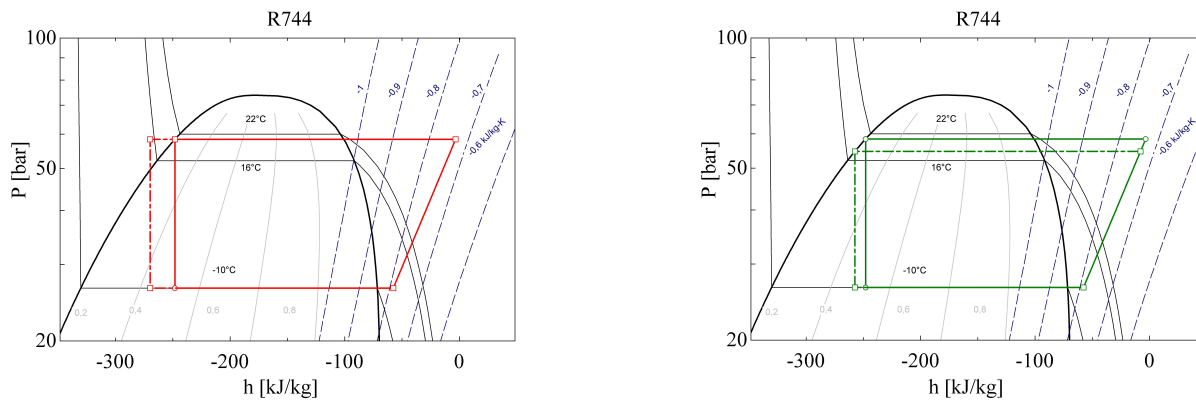


Figure 6.12: Subcooling for the best CO₂ configurations.

Subcooling has been converted into an increase in Q_o , but also as a decrease in compressor work. This procedure is illustrated in figure 6.13. It is important to note that this is a theoretical approach and in reality a subcooling to this extent will not occur.



(a) Influence of CO₂ subcooling on Q_o .

(b) Influence of reduced CO₂ pressure on Q_o .

Figure 6.13: Performance improvement for the CO₂ condenser as subcooling and reduced pressure.

The influence of the subcooling on Q_o is shown in figure 6.13a. In figure 6.14, the refrigeration capacity is plotted for the different CO₂ configurations. It can be seen that all the suggested configurations achieve a minimum of 1 kW increase in refrigeration capacity at all saturation temperatures compared to the original configuration. The 15-2-3 configuration achieves again the best operation at a saturation temperature of 20°C with a refrigeration capacity of 11,4 kW.

This represents a 12 % increase in Q_o . At temperatures above 21 °C, the 12·3·2 configuration achieves the highest Q_o .

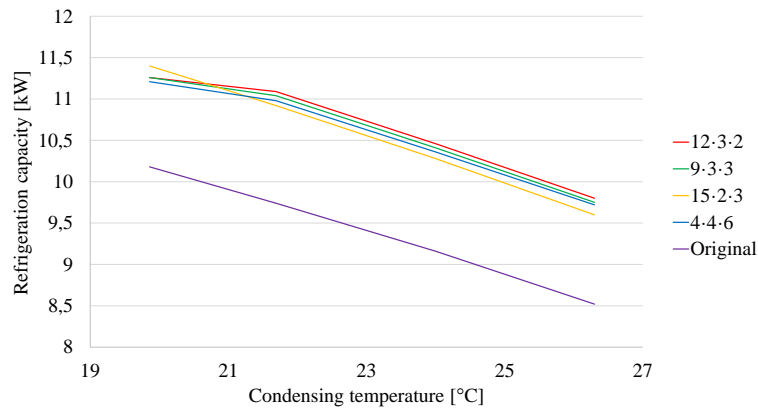


Figure 6.14: Refrigeration capacity including CO₂ subcooling.

In figure 6.15, the same trend is seen for the COP for the suggested configuration. 15·2·3 achieves a slightly higher COP at a saturation temperature of 20 °C, and 12·3·2 achieves the highest COP at saturation temperatures above 21 °C.

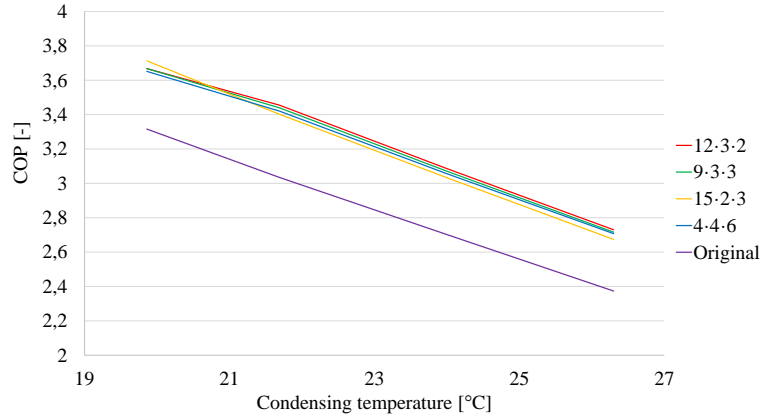


Figure 6.15: COP including CO₂ subcooling.

In table 6.5, the increase in Q_o is presented.

The other tool of analysing the effect of the subcooling obtained for the new configurations in HXsim, was a decrease in the high side as illustrated in figure 6.13b. In table 6.6, the decrease in compressor work is presented. A slight increase in Q_o is also experienced. The higher the ambient temperature, the higher the work is decreasing. For both options, the improvement in refrigeration capacity is increasing with increasing ambient temperature.

T_{amb}	T_{sat}	12·3·2	9·3·3	15·2·3	4·4·6
6,0	19,86	10,2%	10,6%	11,9%	10,1%
12,1	21,69	13,9%	13,3%	12,1%	12,7%
15,5	24	14,2%	13,7%	12,3%	13,2%
18,7	26,3	15,0%	14,5%	12,7%	14,1%

Table 6.5: Increase in Q_o and COP as a result of CO_2 subcooling.

	12·3·2		9·3·3		15·2·3		4·4·6	
T_{amb}	ΔW	ΔQ_o	ΔW	ΔQ_o	ΔW	ΔQ_o	ΔW	ΔQ_o
6,0	-0,8%	+0,7%	-0,9%	+0,8%	-1,0%	+0,9%	-0,8%	+0,8%
12,1	-1,8%	+1,9%	-1,7%	+1,8%	-1,8%	+1,9%	-1,9%	+1,9%
15,5	-3,7%	+4,3%	-3,3%	+3,8%	-3,1%	+3,6%	-3,3%	+3,8%
18,7	-3,3%	+4,3%	-3,1%	+4,2%	-2,8%	+3,7%	-3,0%	+4,0%

Table 6.6: Subcooling calculated as a decrease in work including an increase in Q_o .

The increase in COP at lower saturation temperatures is not significant when transforming the subcooling into a reduction in work. For the 12·3·2 configuration an increase in COP of 10,20 % is experienced for the subcooling option, versus 1,85 % for the reduced work option at an ambient temperature of 6 °C. The improvement in COP for the reduced work option, is seen in table 6.7.

T_{amb}	12·3·2	9·3·3	15·2·3	4·4·6
6,0	1,85%	2,03%	2,29%	1,96%
12,1	4,30%	4,05%	4,17%	4,8%
15,5	8,85%	7,92%	7,50%	7,77%
18,7	8,84%	8,48%	7,63%	8,18%

Table 6.7: Increase in COP when the work/condensing pressure is decreased.

6.2.2 Modification of the CO_2 gas cooler

In table 6.8 the CO_2 gas cooler configuration modifications are displayed. An enhancement factor of 0,7 was implemented simulating the configurations in order to have an equal basis for comparison. The 4·4·6 required an enhancement factor of 0,4 in order to run the simulation.

²Original configuration

³Enhancement factor 0,4

Configuration	Performance/area [$\frac{kW}{m^2}$]	Enthalpy difference [kJ/kg]	Additional tubes [%]	ΔP [bar]
6·2·7 ²	0,08	63,0	-	-
12·3·2	0,09	66,1	-14,30	2,81
9·3·3	0,09	71,8	-3,60	1,81
15·2·3	0,08	71,6	7,1	1,86
4·4·6 ³	0,08	72,3	14,3	0,63

Table 6.8: Best CO₂ gas cooler configurations at a T_{amb} of 40°C. Enhancement factor 0,7.

6.2.3 Modifications of the propane condenser

In table 6.9, the best propane condenser are displayed. As for the CO₂ condenser, a theoretical approach has been used when analysing the subcooling, and subcooling of this extent will not appear.

Configuration	Performance/area [$\frac{kW}{m^2}$]	Subcooling [k]	Additional tubes [%]	ΔP [bar]
6·1·7 ²	0,50	1	-	0,12
10·3·3	0,26	15,9	114	0,60
6·6·3	0,43	15,3	28,6	0,44
12·1·4	0,49	12,0	14,3	0,25
15·1·3	0,52	12,9	7,14	0,44
<i>Integrated propane condenser</i>				
12·2·2	0,48	10,8	+14,3	1,07
9·2·3	0,43	10,75	+28,6	0,5
15·1·3	0,52	12,9	+7,14	0,44
4·2·6	0,46	8,0	+14,3	0,15

Table 6.9: Best propane condenser configurations at a T_{amb} of 40°C.

In figure 6.16, the subcooling for the different propane configurations is presented. The influence of the propane subcooling on the refrigeration capacity and COP have been investigated and presented in figure 6.17, 6.18 and table 6.10. When the subcooling is translated into increased Q_o , the 10·3·3 configuration achieved the best operation an ambient temperatures above 22°C, with a minimum improvement in refrigeration capacity of 0,4 kW compared to the original configuration. For the two best configurations, 10·3·3 and 6·3·3, the exit temperature difference between the air and the subcooled propane turned out to be between 0,01 K to 0,66 K. It can be observed that the improvement in COP and refrigeration capacity increases

with increasing ambient temperature when maintaining the condensing pressure of the original propane configurations.

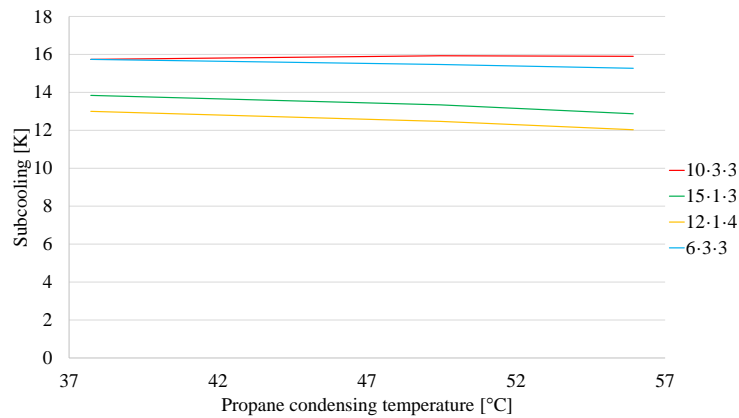


Figure 6.16: Subcooling for the best propane configurations.

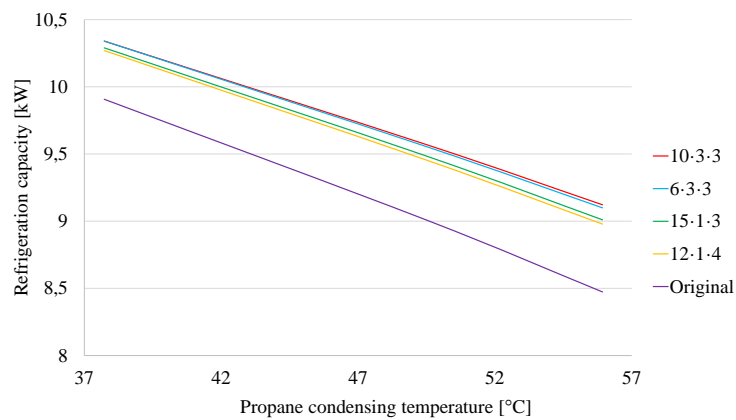


Figure 6.17: Refrigeration capacity when including propane subcooling.

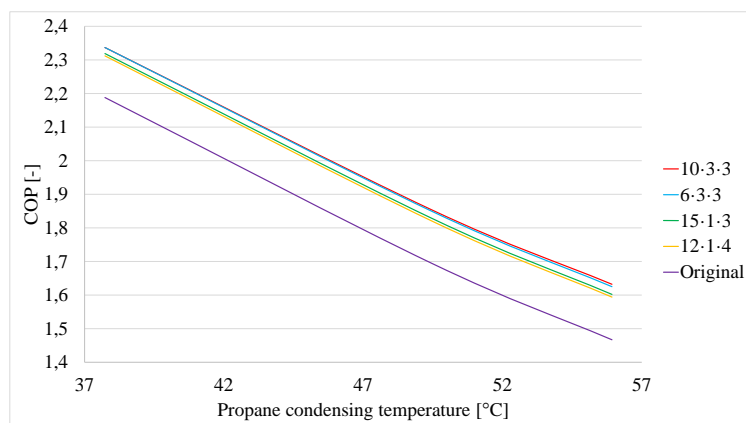


Figure 6.18: COP when including propane subcooling.

		10·3·3		6·3·3		15·1·3		12·1·4	
T_{amb}	T_{sat}	ΔQ_o	ΔCOP	ΔQ_o	ΔCOP	ΔQ_o	ΔCOP	ΔQ_o	ΔCOP
22	37,73	3,9%	6,1%	3,9%	6,1%	3,4%	5,3%	3,2%	5,0%
33,5	49,45	5,7%	8,5%	5,5%	8,3%	4,7%	7,1%	4,4%	6,6%
40	55,93	6,9%	10,2%	6,7%	9,7%	5,6%	8,2%	5,3%	7,6%

Table 6.10: Propane subcooling calculated as an increase in Q_o and an increase in COP for the overall system.

The effect of a reduced propane condensing pressure was also investigated. An approach temperature of 5 K was demanded in the gas cooler and a 1 K propane subcooling. The propane configurations effect on the overall system refrigeration capacity, total compressor work and COP are presented in tables 6.11 and 6.12. It can be seen that the 10·3·3 configuration gave the best overall improvement. However, the 10·3·3 also had the largest pressure loss in the condenser of 1,22 bar at an ambient temperature of 22°C, constituting in a temperature loss of 4,63 K. The pressure losses of the different configurations was included in the calculations.

		10·3·3		6·3·3		15·1·3		12·1·4	
T_{amb}	ΔW	ΔQ_o	ΔW	ΔQ_o	ΔW	ΔQ_o	ΔW	ΔQ_o	
22	-12,1%	+3,9%	-8,3%	+2,5%	-5,9%	+1,7%	-4,8%	+1,2%	
33,5	-10,3%	+4,7%	-7,0%	+3,1%	-4,9%	+2,2%	-4,2%	+1,7%	
40	-9,3%	+5,3%	-6,3%	+3,5%	-4,4%	+2,5%	-3,5%	+1,9%	

Table 6.11: Propane subcooling calculated as a decrease in work including an increase in Q_o for the overall system.

T_{amb}	10·3·3	6·3·3	15·1·3	12·1·4
22	18,2%	11,8%	8,0%	6,4%
33,5	16,6%	10,8%	7,4%	6,1%
40	16,2%	10,5%	7,2%	5,7%

Table 6.12: Increase in the overall systems COP when work is decreased as a result of improved propane condenser.

In figure 6.19, propane condensers are presented as suggestions for integrated CO₂/propane heat exchangers. These were developed after investigating the best CO₂ condensers. The integrated heat exchangers are summed up in table 6.13. Performance of the propane condensers are summed up in table 6.9. Note that the pressure drop for the 12·2·2 configuration is significantly higher than the other configurations. This represents an increase of 0,16 kW, or 11,4 %, for the propane compressor. Thus, the COP is decreased by almost 5%.

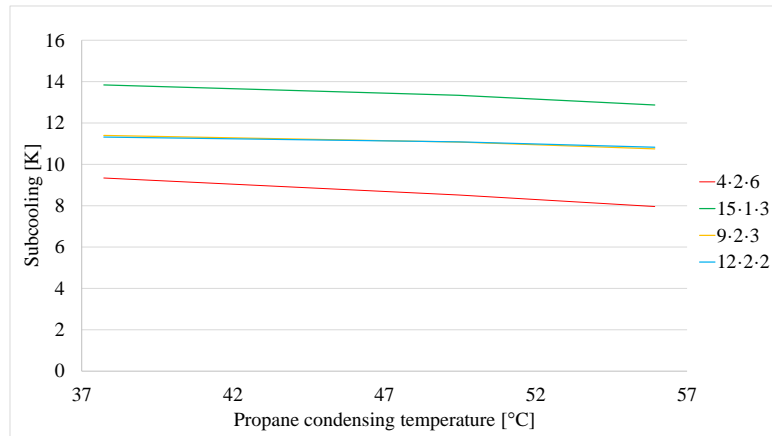


Figure 6.19: Subcooling for integrated propane condenser options.

CO ₂ Configuration	R290 Configuration	Total additional tubes
12·3·2	12·2·2	-4,76
9·3·3	9·2·3	+7,14
15·2·3	15·1·3	+7,14
4·4·6	4·2·6	+14,3

Table 6.13: The best CO₂ condenser configurations with suggested integrated propane condensers.

6.2.4 Fan modifications

The 12·3·2 configuration was also tested with different fan set points. In this procedure the actual fan characteristics was used. The fan characteristics are dependent on the saturation temperature, as seen in figure 5.2. When translating the subcooling into reduced work, the saturation temperature is lowered. This correlation was taken into consideration when testing the different modifications, in order to have a proper base for comparison. When demanding zero subcooling, fan modifications has been tested with the fan speed corresponding to the ambient temperature, instead of the saturation temperature. In figure 6.20 the 12·3·2 configuration is compared with the original and the new set points for the curve.

With the new fan set points, the zero subcooling options changes the improvement in COP from 1,85% to 4,3 % with the new fan at an ambient temperature of 6. °C. At an ambient temperature 12 °C, the COP increase changes from 4,3 % to 6,6 %.

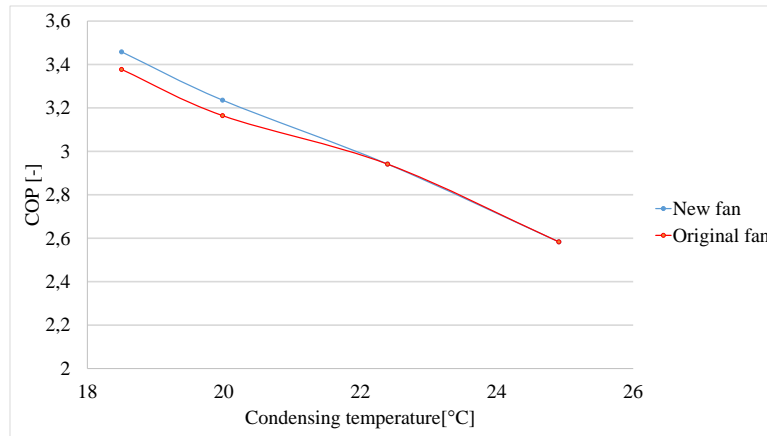


Figure 6.20: New fan set points for the 12·3·2 configuration with zero subcooling.

Figure 6.21 shows the effect on the COP when the fan speed is doubled for the original configuration, thus the scenario if a new fan were implemented. At an ambient temperature of 19°C an increase in COP of 15 % is experienced. It can be observed that the difference between the two options is greater at lower ambient temperatures.

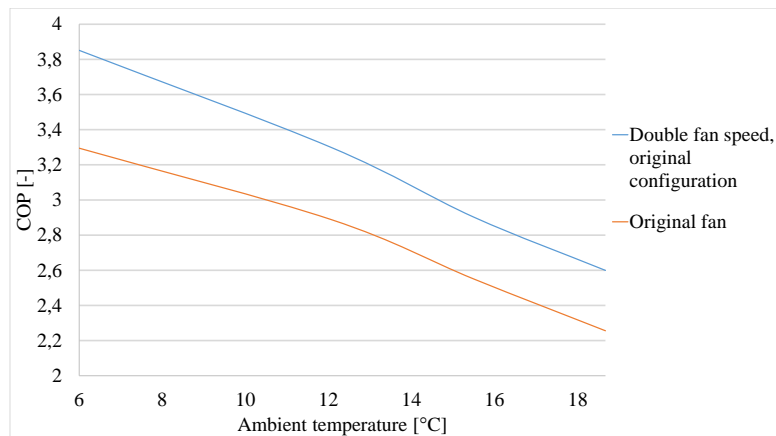


Figure 6.21: Effect on COP for original CO₂ condenser when fan speed is doubled.

6.3 Modifications overall system

As explained in section 5.3.2, all the proposals for improvements starts operating transcritically at the design point with a condensing temperature of 25°C. Figures 6.22 and 6.23 shows the COP and refrigeration capacity obtained for the different configuration compared to the original prototype system.

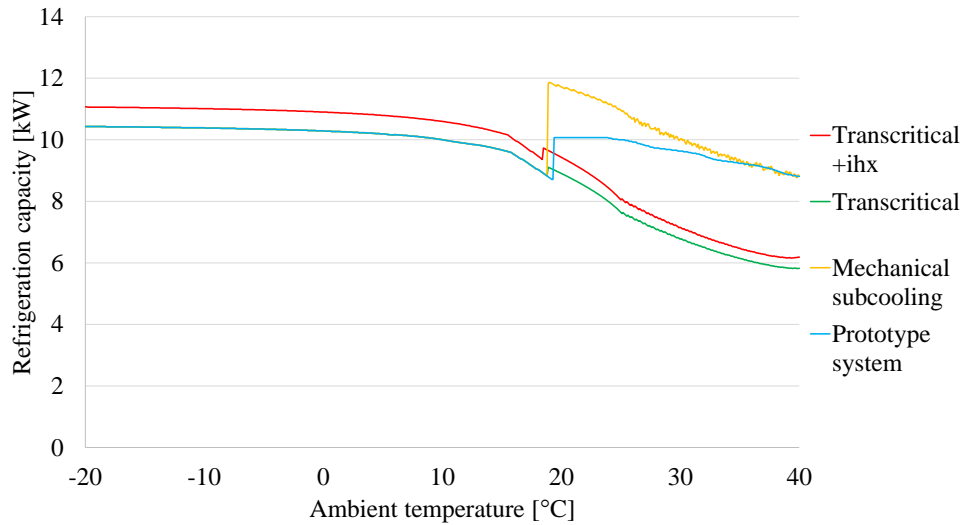


Figure 6.22: Comparison of refrigeration capacity for the modifications.

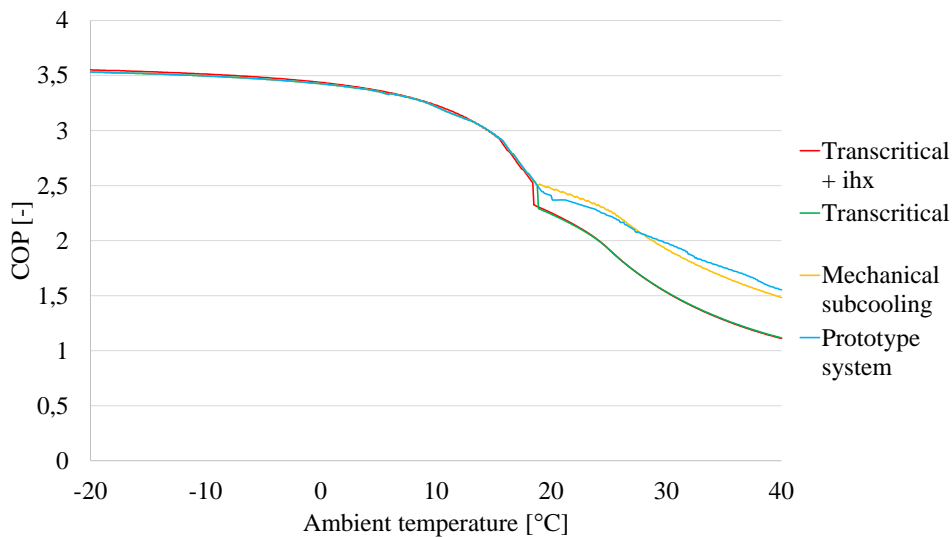


Figure 6.23: Comparison of COP for the modifications.

Since all of the modifications except the one including an internal heat exchanger was programmed to have the same behaviour in subcritical operation, they display the same refrigeration capacity and COP. However when the ambient temperature exceeds $18,8^{\circ}\text{C}$, the behaviour of the different systems are unequal. The modifications displaying the overall best refrigeration capacity at high ambient temperature is mechanical subcooling. To meet the demanded refrigeration capacity at an ambient temperature of 40°C , the propane compressor in the mechanical subcooling unit was designed to have a swept volume of $6 \frac{\text{m}^3}{\text{h}}$, a volumetric efficiency of 0,60 and

an isentropic efficiency of 0,60. Mechanical subcooling also have the best COP of the modifications, but at an ambient air temperature of approximately 28°C, the COP of the prototype system surpass mechanical subcooling. The mechanical subcooling system also delivers the best refrigeration capacity from an ambient temperature of 18,8°C to 37°C, and approximately the same as the prototype system up to 40°C.

It can be observed that when including an internal heat exchanger to the transcritical configuration, the refrigeration capacity is higher at all simulated temperatures, while the COP is slightly higher at low ambient temperatures. Operation with an internal heat exchanger represents an improved refrigeration capacity of 5-6% for subcritical and transcritical operation. However, when ambient temperatures exceeds 18,8°C the COP drops and the configuration with internal heat exchanger shows a small reduction in the COP compared to the transcritical configuration.

Table 6.14, shows the seasonal performance of the various modifications for the different climates compared to the original prototype system. It can be observed that mechanical subcooling gives the best seasonal performance of the three modifications. For the cities with warmer climates, namely Paris, Budapest and Madrid, the mechanical subcooling system also provides a slightly better seasonal performance than the prototype system.

		Oslo	London	Paris	Budapest	Madrid
Transcritical	SCOP	3,20	3,07	2,95	2,91	2,76
	E [kWh] ⁴	27521	28264	29040	29374	30325
Transcritical + IHX	SCOP	3,21	3,07	2,95	2,91	2,76
	E [kWh]	29094	29907	30725	31077	32073
Mechanical subcooling	SCOP	3,22	3,09	3,00	2,98	2,86
	E [kWh]	27953	28933	30343	31057	32488
Prototype system	SCOP	3,22	3,09	2,99	2,97	2,85
	E [kWh]	27627	28417	29506	30058	31282

Table 6.14: Seasonal performance and yearly energy consumption for modifications.

Figures 6.24, 6.25 and 6.26, illustrates the process of the three modifications in log(p)-h diagrams at $T_{amb} = 35^\circ\text{C}$. It can be seen that transcritical system has an outlet temperature from the gas cooler of 40°C, achieving the smallest enthalpy difference in the evaporator. The modification with the internal heat exchanger has less superheat, thus a smaller discharge enthalpy

⁴Yearly energy consumption

and temperature. The temperature before the throttling valve is 38°C , lower than the simple transcritical system, giving an enhanced heat of evaporation. In figure 6.26a, the CO_2 part of the mechanical subcooling system is illustrated. The temperature before the throttling is reduced to 18°C , thus increasing the enthalpy difference in the evaporator. The process needed to provide the mechanical subcooling is shown in figure 6.26b.

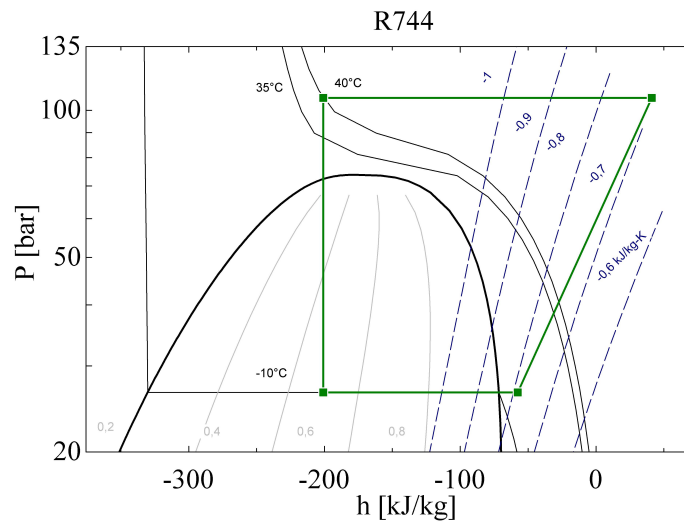


Figure 6.24: R744 log(p)-h diagram for the transcritical system at $T_{amb} = 35^\circ\text{C}$.

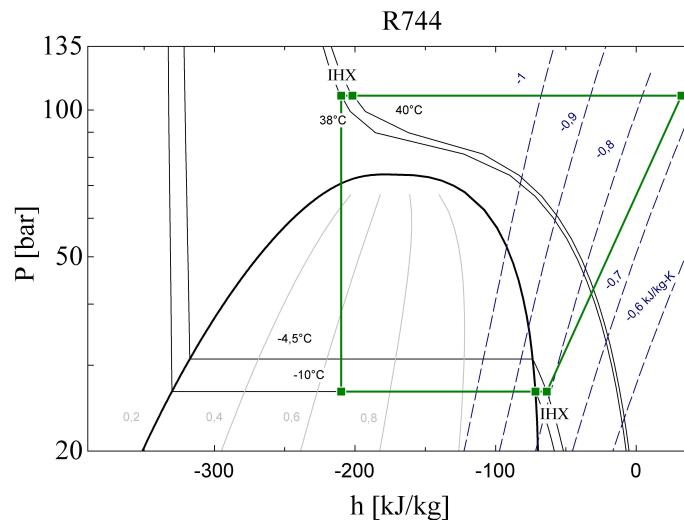
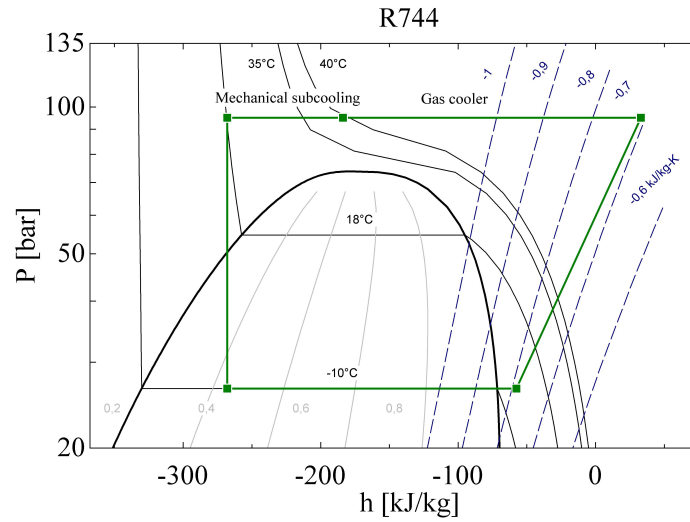
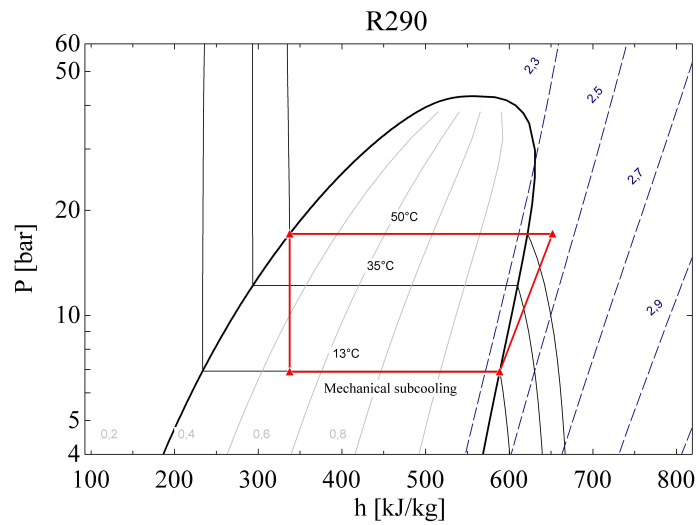


Figure 6.25: R744 log(p)-h diagram for the transcritical system with internal heat exchanger at $T_{amb} = 35^\circ\text{C}$.



(a) R744 log(p)-h diagram for mechanical subcooling.



(b) R290 log(p)-h diagram for mechanical subcooling.

Figure 6.26: Log(p)-h diagram for the mechanical subcooling system at $T_{amb} = 35^\circ\text{C}$.

Chapter 7

Discussion

In this chapter the results presented in chapter 6 are further discussed.

7.1 Measurements and simulation model

In figure 7.1 the corrected measurement data are presented. A higher refrigeration capacity was observed with both systems operating, compared to when the CO₂ system operates exclusively. This is due to fact that the propane system reduces the high side pressure of the CO₂ system, thereby decreasing the condensing temperature and increasing the refrigeration capacity. However, the increased refrigeration capacity of both systems operating is penalised by a decreased COP, as a result of the increased work for operation of the propane system. As seen in figure 7.1b, exclusive operation of CO₂ gives a superior COP until an ambient temperature of approximately 23,5°C. From an energy efficient perspective, the propane system should start to operate at this ambient temperature. An ambient temperature of 23,5°C corresponds to a condensing temperature of approximately 28,5°C. At condensing temperatures above 28,5°C, but below the critical temperature, the COP drops excessively due to a rapid reduction in heat of condensation. The results coincide with theory of the upper practical condensation limit for CO₂ being 28°C.

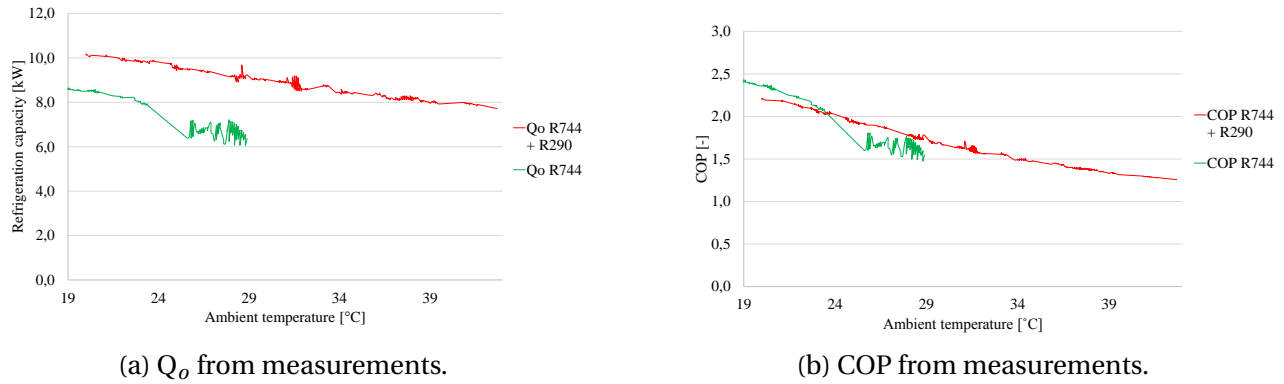


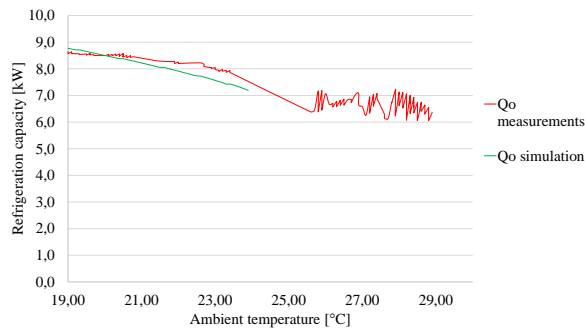
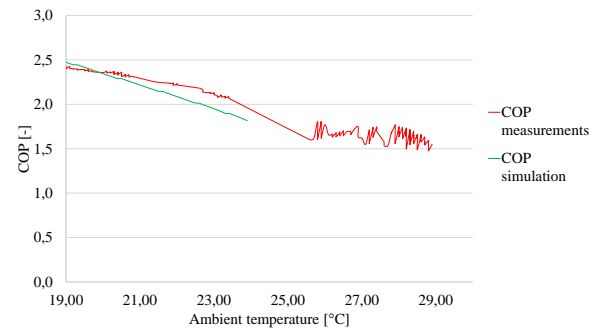
Figure 7.1: Comparison of Q_o and COP from measurements.

7.1.1 Comparison of measurements and simulation

Figures 7.2a and 7.2b illustrates the deviation between simulations and measurement data for CO₂ operation. There are several reasons for these deviations. In the ambient temperature range from 19°C to 23,4°C, the suction temperatures from the measurement data are relatively stable, but some discrepancies occurs. The suction temperature is kept in the range from -1,3°C to 4°C in the measurement data, compared to the simulation where it is kept constant at 0°C. This will affect the enthalpy difference in the evaporator, specific volume at the inlet of the compressor, which affects the mass flow, thus the compressor work. Another reason for the deviations is the difference in the measured and simulated condensing temperatures. As the ambient temperature is increasing, the difference in the condensing temperature is also increasing, due to the results obtained from the simulations done in HXsim. The simulated condensing temperature was observed to be lower than the measured condensing temperature, up to an ambient temperature of approximately 20,5°C. This can be observed by the point of intersection in figures 7.2a and 7.2b. The largest difference of 0,91 K in condensing temperature was observed at an ambient temperature of 23,4°C, constituting in a 4% change in enthalpy difference in the evaporator between the measurement data and the simulation. Together with the reduced compressor work due to a reduced pressure, this resulted in lower refrigeration capacity and COP for the simulations above an ambient temperature 20,5°C.

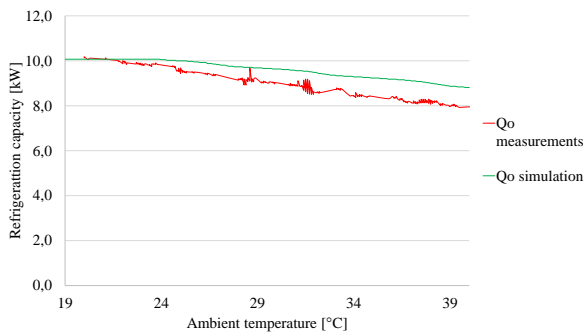
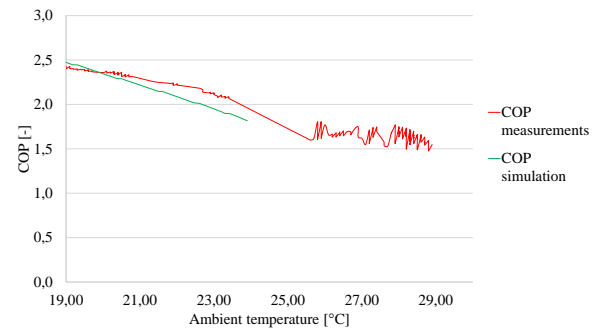
For system operation with propane, the simulations and measurements follows a more similar trend, but shows a larger deviation between the measured and simulated COP and refrigeration

capacity. When the propane is in operation, there are more factors influencing the deviations. As for the CO₂ operation without propane, variation in suction temperature was observed in the measurement data. The suction temperatures varies from $-7,5^{\circ}\text{C}$ to 12°C , thus changing the operational conditions. This is represented by the fluctuations in the measurement data shown in figure 7.3a. There was also observed a difference in the CO₂ condensing temperature between measurement data and simulation. However, when the propane system is operating, the CO₂ condensing temperature from the measurement data are higher than the simulated condensing temperature. The differences ranges from 0,2 K at 20°C ambient temperature up to 3,5 K at an ambient temperature of 40°C . This explains the different slopes for the refrigeration capacity illustrated in figure 7.3a. As observed in figure 7.3b, the COP from the simulations follow a similar slope to the measurements, in contrast to the refrigeration capacity. The reason for this could be that the simulated condensing temperature for propane was observed to be lower than the measured temperature up to an ambient temperature of approximately 32°C , while increasing at higher temperatures. This means that pressure ratio would be reduced if the propane evaporating pressure is constant, resulting in less compressor work, thus a higher COP. However, there are more factors affecting the compressor work for the propane system. When the CO₂ condensing pressure is reduced, a larger cooling capacity is required for the propane evaporator in order to remove the heat of condensation from the CO₂ system. If the propane condensing pressure is kept constant, the propane evaporation pressure needs to be increased to meet the needed cooling demand. By increasing the propane evaporating pressure, the enthalpy of evaporation increases as well as the mass flow, since the specific volume decreases with increasing pressure. The propane condensation pressure also influence the propane cooling capacity. This is due to the gentle slope of the propane dew point line. A small change in propane condensing temperature will have a large effect on the enthalpy difference in the propane evaporator. When all of the factors mentioned above changes simultaneously, the outcome will be variations in the refrigeration capacity and COP.

(a) Comparison of Q_o .

(b) Comparison of COP.

Figure 7.2: Comparison of Q_o and COP from measurements and simulations without propane operation.

(a) Comparison of Q_o .

(b) Comparison of COP.

Figure 7.3: Comparison of Q_o and COP from measurements and simulations with propane operation.

7.1.2 Prototype simulation

Different set points for start of propane operation were investigated and presented in figures 6.7 and 6.8. Table 6.2 summarises data for the CO_2 operation without propane for further discussion of the set point.

As can be seen in the table 6.2, the refrigeration capacity and the COP drops rapidly in the range presented. When the ambient temperature increases, the CO_2 high side pressure must increase to be able to condense the CO_2 completely. This affects the enthalpy difference in the evaporator, decreasing the refrigeration capacity while increasing the compressor work due to higher pressure ratio. It can also be observed that the exit temperature difference in the condenser decreases with increasing temperatures. When the condensing temperature increases, the heat of condensation is reduced while the same area of the heat exchanger is available, thus reducing

the exit temperature difference.

From an energy efficiency perspective, the propane system should start to operate at an ambient temperature of $19,4^{\circ}\text{C}$. As seen in figure 6.8, the COP is lower for the system operating without propane at ambient temperatures higher than $19,4^{\circ}\text{C}$. However, the refrigeration capacity drops rapidly for CO_2 from an ambient temperature of 15°C . Hence, with focus on maintaining a certain level of refrigeration capacity, the propane system should start to operate just before the capacity starts to drop. On the other hand, the optimal point where the propane system should start to operate needs to be weighted between the refrigeration capacity and the COP. The system was not simulated for lower set points than $18,5^{\circ}\text{C}$, but there is reason to believe that the COP would be notably lower than with CO_2 operation alone, as seen from the measurement data.

Today the propane system starts to operate at a CO_2 condensation pressure of 67 bar and stops when the CO_2 condensation pressure decrease below 60 bar. This corresponds to CO_2 condensing temperatures of respectively $26,75^{\circ}\text{C}$ and $21,98^{\circ}\text{C}$. If these operational set points had been implemented in the EES script, the minimum refrigeration capacity for the system would have been even lower than 8,71 kW due to the higher CO_2 condensing temperature before start of propane operation. If the simulation had operated with these on/off set points, the propane system would have started at an ambient temperature of $26,75^{\circ}\text{C}$. Then the propane system would have decreased the CO_2 condensation pressure below 60 bar, turned off the propane system, and the condensation pressure would have been increased again up to 67 bar. This operation would have been repeated until the ambient temperature surpassed $30,70^{\circ}\text{C}$, where the condensation pressure of CO_2 always is kept above 60 bar. An operational setting like this, switching the propane system on and off at a wide temperature range, will cause wear on the electrical components and result in large variations in the refrigeration capacity and COP.

Compared to the result obtained from the measurements, the ambient temperature and CO_2 condensing temperature for optimal start of propane differ respectively 4,1 K and 3,1 K, where the measurements obtain the highest temperatures. This is expected since the measurements and simulation deviates as discussed earlier.

	Measurements	Simulation
CO ₂ condensing temperature	28,5 °C	25,4 °C
Ambient temperature	23,5 °C	19,4 °C

Table 7.1: Comparison of optimal start of propane operation for the best COP.

7.1.3 System operation in some selected European capital cities

Weather data for simulations of the system in European capitals were collected from Meteonorm. Meteonorm provides an hourly average of the ambient temperature, so if any peak temperatures occur during an hour these peaks will be shaved off. Temperature data for five different capitals with an hourly time step were concluded to be sufficient.

In figures 6.10 and 6.11, the effect of the ambient temperature on the refrigeration capacity and COP is clearly illustrated. As the ambient temperature is increasing, both the refrigeration capacity and COP decreases, coinciding with theory. Large variation can be observed in the refrigeration capacity seen in figure 6.10. The ambient temperature often shifts between the set point for with and without the propane operation, giving large variation in the refrigeration capacity.

The great variation in the refrigeration capacity and the COP during the summer months is explained by the large variation in ambient temperature from night to day.

	Oslo	London	Paris	Budapest	Madrid
Operating hours propane	461	716	1519	1975	2580
% propane operation of year	5,26	8,17	17,34	22,55	29,45
Maximum Q_o [kW]	10,43	10,35	10,36	10,39	10,34
Minimum Q_o [kW]	8,71	8,71	8,71	8,71	8,71
Seasonal performance	3,22	3,09	2,99	2,97	2,85
Yearly energy consumption [kWh]	27627	28417	29506	30058	31282

Table 7.2: System performance in different climates.

As shown in table 7.2, there are great variations in the operating hours with propane between the different capitals. The difference in operating hours with propane between Oslo and Madrid equals nearly three months. The energy consumption in Madrid is also 13% higher than in Oslo due to the high ambient air temperatures in Madrid. The lowest refrigeration capacity for all the capitals was calculated to be 8,71 kW. The reason for this, despite the large variations in ambient air temperatures, is that the refrigeration capacity drops significantly before the propane system

starts to operate. The lowest capacity is achieved at an ambient temperature of $19,3^{\circ}\text{C}$, corresponding to a condensing temperature of $25,4^{\circ}\text{C}$, while the refrigeration capacity increase to $10,05\text{ kW}$ when the propane system start to operate at an ambient temperature of $19,4^{\circ}\text{C}$. Figure 6.10 shows the importance of choosing an optimal propane set point and how it influences the refrigeration capacity in warmer climates.

7.2 Modification of the condenser and gas cooler

When optimising a heat exchanger, the options are infinite when few restrictions are set. The aim is to achieve as high heat transfer from the refrigerant to the air as possible, within the allowable pressure drop. A low approach temperature and pinch at the refrigerant outlet, also characterises a good heat exchanger design.

The heat exchanger simulated in HXsim differs from the actual heat exchanger in several ways. Hence, the performance of the heat exchangers simulated in HXsim will deviate from the actual performance. The condenser/gas cooler is angled 90° , where in HXsim the heat exchanger is not angled. In the original configuration, the final pipe duplication for both the propane and the CO_2 is a manifold that collects the cooled refrigerant and is sent through the heat exchanger one last time. This design feature is probably implemented in order to ensure some pressure drop, but was not possible to design in HXsim. Thus, it was not included for any of the HXsim models. From the data measurements it is seen that there are no measurable pressure drop in the CO_2 condenser/gas cooler. Longer pipes will be a more efficient solutions in order to obtain the desirable pressure drop for the CO_2 . When investigating the different condenser/gas cooler modifications, the results were compared to the original configuration in HXSim.

7.2.1 Modification of the CO_2 condenser

A good heat exchanger design can help the operation of the system in two distinct ways; it can reduce the high side pressure, thus the compressor work, or it can increase the refrigeration capacity by subcooling. In both alternatives, the COP increases. A theoretical approach was

utilised when analysing the effect of the subcooling. The best configurations tested in HXsim were the 12·3·2, 9·3·3, 15·2·3 and 4·4·6 configurations, as shown on page 52. For all the configurations, except 9·3·3, the area was increased. An increase in area equals an increase in heat transfer. However, the percentage increase of tubes are not extensive for any of the configurations and an increase in heat transfer was achieved for the 9·3·3 without increasing the heat transfer area.

It can be observed from figure 7.4 that all the configurations with more than two pipe rows achieved a subcooling of approximately 6 K at a condensing temperature of 20°C, while increasing linearly up to a condensing temperature of 22°C. The reason for this is that the volume flow of air increases linearly, as seen in figure 5.2, thereby boosting the cooling provided by the air. The configuration with two rows experienced more subcooling at the lower saturation temperatures and a different trend than the configurations with more tube rows. This is due to the fact that the both of the two first pipelines will meet fresh air. An optional third row will be cooled by air that is heated by the first rows. The air is less heated by the first row when increasing the condensation temperature, thus the volume air flow. When the air volume flow is increasing, this feature will have less effect on the third row. This feature is illustrated in the temperature plots in chapter 5. The temperature plot for 9·3·3 in figures 5.19 and 5.21, shows the transition to a better temperature glide due to an increase in ambient temperature.

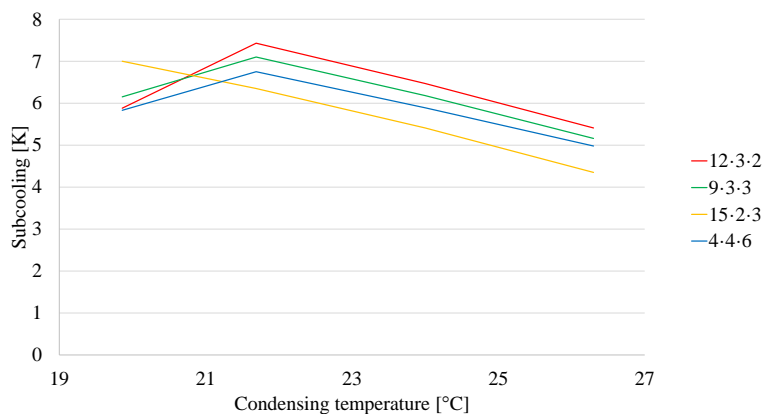


Figure 7.4: Subcooling for the best CO₂ configurations.

Since the two-phase area decreases when approaching the critical point, a reduction in condensing pressure at high ambient temperatures, thus at high condensing pressures, will give a

larger percentage improvement in enthalpy difference in the evaporator compared to at lower condensing pressures. Also, when reducing the CO₂ condensing pressure, a lower pressure ratio is obtained and the volumetric efficiency of the compressor is improved as seen in figure 5.1. This will result in a slightly larger CO₂ mass flow and an increase in the refrigeration capacity. If the modifications were implemented directly to the prototype system, a reduction in pressure will occur due to the liquid receiver.

Comparing tables 6.5 and 6.7, it is clearly seen that keeping the subcooling results in the highest COP. This is mainly due to the larger temperature required in the condenser when the fan capacity is decreased at lower condensing temperatures. This can also be explained by the reduction in LMTD when the pressure is decreased. The U-value and area remains constant, thus the CO₂ will be less cooled by the air. As mentioned, this is a theoretical approach and subcoolings of this extent will not occur in reality. The reduction in pressure depends on the friction and height drop of the refrigerant from the condenser outlet to the liquid receiver. As seen in theory, a subcooling of 1 to 3 K is common for CO₂ condensers. Therefore, when implementing these configurations, both a reduction in pressure and some subcooling is attainable. The improvement on the system when implementing the new configurations will be in the range of the results presented for both analytic approaches. Therefore, the 12·3·2 configuration represents a minimum COP increase of 8,8 %, corresponding to the reduced pressure option.

The 12·3·2 configuration experiences the highest pressure drop of all tested configuration, but also the overall best performance. This was expected due to the great length of the pipes. Nonetheless, a maximum pressure drop of 1,5 bar is in the allowable range when considering the CO₂ condenser for the prototype system. The 12·3·2 configuration also has the highest reduction in tubes, thus a good option for a new CO₂ condenser design.

7.2.2 Modification of the CO₂ gas cooler

In table 6.8, it was confirmed that the CO₂ gas coolers with 12·3·2 and 9·3·3 configuration have the highest performance/area value, due to the few tubes. The enhancement factor for the fins was set to 0,7 in order to have an equal basis for comparison. A decrease in enhancement fac-

tor equals a decrease in heat transferred from the refrigerant to the air, thus a lower performance/area value. In this matter, the gas cooler simulation results was only used in order to compare the different configurations, not to map the actual performance of the gas coolers. The reason for this is that the gas cooler only operates as a desuperheater and only rejects a small amount of heat compared to when it operates as a condenser. Thus, it will be over-dimensioned when operating as a gas cooler. The heat rejected when operating as a condenser is up to four times larger than when operating as a desuperheater. This was also proved by the simulations, where a very small approach temperature was obtained.

7.2.3 Modification of the propane condenser

Propane condenser configurations were also tested in HXsim. The best propane condensers were the 10·3·3 and the 6·3·3 configurations. The 10·3·3 experienced a slightly higher subcooling at higher ambient temperatures as seen in figure 7.5, due to a larger heat exchanger area. A larger area will result in a larger investment cost. As presented in table 6.9, the 10·3·3 configuration has a much lower performance/area value. This is due to the high increase in number of pipes compared to the original configuration. The 15·1·3 configuration experiences the highest performance/area value due to its few additional tubes. Again, the theoretical approach was used when analysing the effect of the propane subcooling. When keeping the same operating pressures in the propane unit, the effect of the subcooling was investigated on the systems refrigeration capacity and COP. The percentage increase in COP will differ from the percentage increase in refrigeration capacity since the propane subcooling will lead to larger enthalpy difference in the propane evaporator, hence a reduction in CO₂ condensing pressure and compressor work. As mentioned in chapter 6 the exit temperature difference between the subcooled propane and the ambient air was observed to be from 0,01 K to 0,66 K for the 10·3·3 and 6·3·3 configurations. The reason for this is that the condenser is over-dimensioned and that the fin enhancement factor was set to 1,1. This enhancement factor was also used for the original configuration, so the percentage improvement might represent a more realistic performance improvement despite the low approach temperatures.

By demanding 1 K subcooling the enthalpy difference in the propane evaporator increases, thus

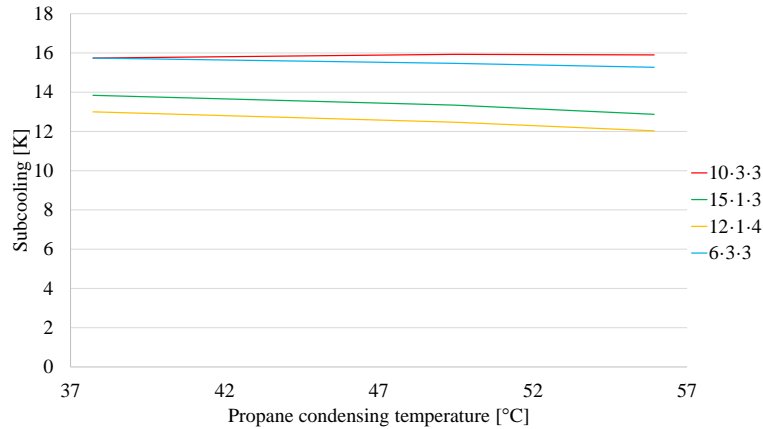


Figure 7.5: Subcooling for the best propane configurations.

both the propane and CO₂ compressor work decreases and the CO₂ refrigeration capacity increases. This will clearly lead to an increase in the COP. Table 6.11 showed the influence of the reduced propane condensing pressure on the total compressor work and refrigeration capacity compared to the original propane condenser. When the ambient temperature increases, the improvement in work is reduced. The reason for this is that the temperature difference required in the condenser increases at higher ambient air temperatures, as well as a rise in condensing pressure. Due to the gentle slope of the saturation curve for propane, an increased pressure leads to a smaller enthalpy difference in the propane evaporator. This means that less heat can be removed in the CO₂ condenser and that the CO₂ condensing pressure will not be reduced in the same extent as when the ambient temperature is lower. When considering the refrigeration capacity, as the ambient temperature increases the improvement in refrigeration capacity is also increasing. The reason for this, is the same as explained for the CO₂ condenser.

When summing up the improvements in work and refrigeration capacity, the COP improvement is obtained and shown in table 6.12. The improvement in COP decreases at increasing temperatures as a result of the compressor work. The 10-3-3 condenser experienced an improvement of 18,4% at an ambient temperature of 22°C, but with a pressure drop of 1,22 bar. This pressure loss, corresponding to a temperature loss of 4,63 K, reduces the effective temperature difference for heat transfer between the refrigerant and the pipe wall. Similarly, a higher condensing pressure is needed and an increased compressor work, compared to a smaller pressure loss. The pressure loss was observed to be smaller at higher propane condensing pressures, while also

constituting a lower temperature loss due to the shape of the temperature loss per pressure loss curve of propane shown in 4.1.

Suggestions for integrated heat exchangers are presented in table 6.13. The advantage with having an integrated heat exchanger is the need for only one fan to cool both refrigerants, including a reduction of space occupied. The 12·2·2 propane condenser configuration experienced a 1,07 bar pressure drop. This represents a 11,4 % increase in propane compressor work. This minimises the COP by 4 % compared to no pressure loss. However, this configuration is better than the original, where the significant increase in subcooling might be transformed into reduction in high side pressure for the propane and increase in refrigerating capacity. Subcooling also provides a larger enthalpy difference in the evaporator, which means that a smaller compressor can be implemented to provide the same refrigeration capacity, thus reducing the investment costs.

7.2.4 Fan modifications

In literature, it is seen that increasing the fan velocity, the refrigeration capacity and the COP increases. This is also seen in figure 6.20, where operation of the 12·3·2 configuration is plotted for different fan set points. Here it is confirmed that the COP increases when increasing the fan speed, despite the increase in fan work. If the new set points are implemented for the 12·3·2 configuration, the compressor work can be decreased with 4,0 % and the Q_o can be increased with 4,1 %. At an ambient temperature of 15 °C the fan has reached its maximum air flow value. This is illustrated in the graph, where both options follows the same trend after this temperature. Investigating the possibility to buy a better fan, might increase the refrigeration capacity, thus the COP, significantly. Figure 7.6 shows the effect on the COP when the fan speed is doubled, thus the scenario if a new fan were implemented using the original configuration. The difference in COP is greatest at low ambient temperatures, and this difference stabilises at approximately 12,5 °C. This is the point where the original fan reaches its maximum value, and therefore the discrepancy will stabilise after this value. At an ambient temperature of 19 °C an increase in COP of 15 % is experienced for the original configuration.

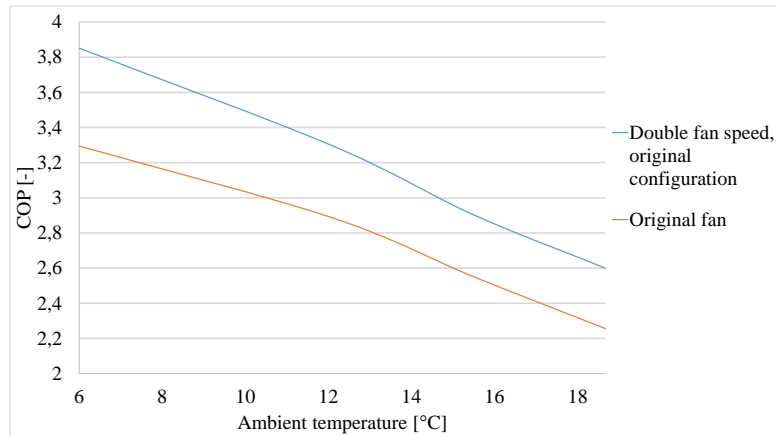


Figure 7.6: Effect on COP for original CO₂ condenser when fan speed is doubled.

7.3 Modifications overall system

Table 7.3 shows the seasonal performance and yearly energy consumption for the modifications in different climates. Only small variations were shown in the performance and energy consumptions between the modifications. Since all of the subcritical operations have approximately the same restrictions, the main influence on the refrigeration capacity and COP is the transcritical operation. This is clearly illustrated in table 7.3, where the largest difference in SCOP between the modifications are shown for the cities with the warmest climates. Madrid is the city that experiences the highest ambient temperatures, thus the city where high air temperature operation has the biggest influence. Consequently, the largest variations in SCOP are shown for Madrid, where the mechanical subcooling system achieves the best SCOP. The main difference separating the mechanical subcooling system and the prototype system is the yearly energy consumption, where the mechanical subcooling system has a higher energy consumption. The reason for this, as can be seen in figure 6.22, is different system refrigeration capacities, where the mechanical subcooling system delivers the highest refrigeration capacity up to an ambient temperature of 37°C. Although the prototype system achieves a slightly higher COP at ambient temperatures between 28°C to 40°C, the mechanical subcooling system achieves a higher SCOP. The reason for this is that the days with ambient temperatures above 28°C only constitutes a small part of the year, therefore the performance of the system below 28°C have the greatest influence on the SCOP. The prototype system have the best COP at high ambient temperature due to a lower pressure ratio in the CO₂ system, resulting in lower compressor work. Hence, the

ratio of refrigeration capacity and compressor work for the prototype system surpass the COP of the mechanical subcooling system.

		Oslo	London	Paris	Budapest	Madrid
Transcritical	SCOP	3,20	3,07	2,95	2,91	2,76
	E [kWh]	27521	28264	29040	29374	30325
Transcritical + IHX	SCOP	3,21	3,07	2,95	2,91	2,76
	E [kWh]	29094	29907	30725	31077	32073
Mechanical subcooling	SCOP	3,22	3,09	3,00	2,98	2,86
	E [kWh]	27953	28933	30343	31057	32488
Prototype system	SCOP	3,22	3,09	2,99	2,97	2,85
	E [kWh]	27627	28417	29506	30058	31282

Table 7.3: Seasonal performance and yearly energy consumption for modifications.

As mentioned in the results, the transcritical system including an internal heat exchanger have an improved refrigeration capacity compared to the ordinary transcritical system. The internal heat exchanger utilises the superheat to subcool the condensed or air-cooled CO₂ exiting the condenser or gas cooler. However, this also influence the COP of the system. When operating at the same pressure, and at high ambient temperatures, the reduced COP is due to a lower specific volume at the inlet, resulting in an higher mass flow. Even though this leads to a higher refrigeration capacity, the increased compressor work exceeds the benefit of the higher refrigeration capacity, resulting in an approximately same COP as the simple transcritical system. The sudden drop in COP is explained by the change in operational conditions from subcritical to transcritical. The pressure is rapidly increased, giving an increased compressor work, resulting in a decrease in the COP.

The mayor difference between the mechanical subcooling system and the prototype system is the integrated condenser/gas cooler for propane and CO₂, and the operational conditions. While the prototype system always operate subcritically, the mechanical subcooling system starts to operate transcritically at high ambient temperatures, and when further cooling by the propane system is required. In terms of size, the mechanical subcooling system designed is smaller due to the reduced size of the compressor and propane condenser.

A disadvantage of having propane in the system, is the risk of leakage in the heat exchanger between the two refrigerants. When comparing a transcritical system to a subcritical system, the

main difference is cost. A transcritical system need more extensive dimensioning, in addition to pressure testing and certification of all components exposed to supercritical pressures. The systems also need service and maintenance, and the knowledge on transcritical systems between refrigeration technicians is still under development.

Only one condensing temperature for start of transcritical operation was investigated, making it difficult to evaluate the best performance of the modified systems. Simulation was also based on simplified system without a proper energy balance for transcritical operation. System performance could have been improved if the set point for transcritical operation was optimised. Considerations regarding cost, necessary refrigeration capacity and energy efficiency have to be taken into account when further evaluating the different options.

Chapter 8

Conclusion

In this chapter, the discussion done in chapter 7 is summarised and a conclusion is provided.

The optimal point for start of propane operation is a question of conflicting interests, due to the improved refrigeration capacity with the propane system in operation. Measurement data collected in the project period have been corrected and the optimal propane set point providing the best COP was found at an ambient temperature of 23,5 °C. Simulations showed that the set point for propane operation giving a maximised COP was at an ambient temperature of 19,4 °C. However, when the propane system is not in operation, the refrigeration capacity starts to drop significantly at an increasing ambient temperature from 15 °C.

Minor inequalities were observed when analysing the prototype system in the different capitals, compared to the significant inequalities in the climatic conditions. The seasonal performance in Madrid was found to be 2,85 in comparison to 3,22 in Oslo. The propane system also have almost three more months of operation in Madrid than Oslo, which clarifies the importance of the set point and efficient high temperature operations.

A theoretical approach has been utilised in order to investigate the best CO₂ and propane condensers. By calculating the subcooling for different condenser modifications in HXsim, the best configurations were spotted. In order to analyse the improvement of the condenser configurations, the Q_o and COP were calculated when maintaining the subcooling and the condensing pressure, or by a reduction in pressure and no subcooling. The subcooling used in these calcu-

lations is not attainable, but a subcooling of approximately 2 K is prevalent for CO₂ condensers. The improvement on the system when implementing the new configurations will be in the range of the results presented for both analytic approaches. At an ambient temperature of 18,7 °C, the 12·3·2 CO₂ condenser configuration gave an increased Q_o and COP of 15% when keeping the subcooling, and a increase in Q_o and COP of respectively 4,3% and 8,8% by transforming the subcooling into a reduced condensing pressure. Thus, a minimum COP improvement of 8,8 % is achieved. In regards of the gas cooler, the 12·3·2 and 9·3·3 gave the best performance/area of 0,09 $\frac{kW}{m^2}$ due to few tubes. The condenser only operates as a gas cooler when the propane system is in operation. The gas cooler is over-dimensioned because it only operates as a desuperheater as a result of the subcritical operation.

The 10·3·3 and 6·3·3 propane condenser configuration showed to have the best subcooling of respectively 15,9 K and 15,3 K at an ambient temperature of 40 °C. When translating the subcooling into a reduction in condensing pressure, the 10·3·3 experienced an increase in COP of 18,2 % and 16,2 % at ambient temperatures of 22 °C and 40 °C. This is a feasible option providing a great improvement in the COP of the overall system. When the subcooling was kept, the 10·3·3 experienced an increase in COP of 6,1 % and 10,2 % at ambient temperatures of 22 °C and 40 °C.

The energy efficiency of the system was also significantly improved by changing the set point of the fan, i.e. increasing the volume flow of air for lower saturation temperatures. The fan speed was also doubled, staging the scenario if a new fan was implemented. At an ambient temperature of 19 °C an increase in COP of 15 % was experienced for the original configuration.

The modified system that gave the best SCOP for the capitals with the warmest climates proved to be the mechanical subcooling system, even though the prototype system gave the best COP from an ambient temperature 28 °C. The mechanical subcooling system also provided the best refrigeration capacity up to an ambient temperature of 37 °C, where the prototype system can compete when it comes to refrigeration capacity. The transcritical system with an internal heat exchanger had an improved refrigeration capacity of 5-6% at high temperature operation compared to the simple transcritical system, indicating a simple and cost-effective method of improving the refrigeration capacity of the system.

Chapter 9

Proposal for further work

Perform extensive measurement on the integrated condenser/gas cooler for detailed investigation. This would help provide accurate correlations for implementation in the simulation model. In this matter, the script can be even more accurate and the SCOP for operation with the different heat exchangers can be calculated. In this matter a cost analysis can be performed for operation with the different heat exchangers.

Perform simulation in a dynamic simulation program to test the actual set points for start and stop of propane system. This will give more accurate results to how the prototype system operates today.

Improve HXsim for more detailed and accurate simulation. Currently, the program has a restricted numbers of fin configurations and provides an incorrect calculation of the log mean temperature difference when simulating a cross flow heat exchanger. By further developing the program, the accuracy of the simulation might be improved and provide more feasible results.

Performing a simulation on the heat exchanger configuration with a centred propane tube row. This time consuming iterative procedure might be simplified by performed in a dynamic simulation program.

Build a prototype of the best configurations of the gas cooler/condenser, connect to existing CO₂ refrigeration systems and perform extensive measurements. Implement a higher fan speed and

a smaller propane compressor. This will allow investigation of the performance of the system at different operating conditions.

Bibliography

- American Society of Heating, Refrigerating, and Air-Conditioning Engineers (2008). *ASHRAE Handbook - HVAC Systems and Equipment (SI)*. American Society of Heating Refrigerating and Air-Conditioning Engineers.
- ATMOsphere, Europe 2015 (2015). “Summare Report International Workshop”. In:
- Banasiak, K. et al. (2014). “A CFD-based investigation of the energy performance of two-phase R744 ejectors to recover the expansion work in refrigeration systems: An irreversibility analysis”. In: *Proceeding of the 11th IIR Gustav Lorentzen Conference on Natural Refrigerants, Hangzhou, China*.
- Comission, The European (2014). “The 2020 Climate and Energy Package”. In: Accessed 25.11.2014. URL: http://ec.europa.eu/clima/policies/package/index_en.htm.
- Dincer, I. (2003). *Refrigeration systems and application*. Department of Mechanical Engineering, KFUPM, Saudi Arabia.
- Dorin (2014). “Dorin Innovation”. In: Accessed 03.02.2015. URL: <http://www.dorin.com/en/catalogo/SE/CD/CD200/CD%20380H/>.
- Eikevik, T.M. (2015). *Compendium in TEP4255 - Heat Pumping Processes and Systems*. NTNU. Chap. 7 - CO₂ as a working fluid.
- Elbel, S.W. and P.S. Hrnjak (2008). “Experimental validation and design study of transcritical CO₂ prototype ejector system”. In: *International Journal of Refrigeration* 31, pp. 411–422.
- Fornasieri, E., S. Girotto, and S. Minetto (2008). “Refrigeration systems for hot climates using CO₂ as the working fluid”. In: *Proceeding of the 8th IIR Gustav Lorentzen Conference on Natural Working Fluids, Copenhagen, Denmark*.

- Fornasieri, E., C. Zilio, et al. (2009). *Natural Refrigerant CO₂*. Leonardo Da Vinci project. University of Padova, pp. 17–38.
- Ge, Y.T. et al. (2015). “Design optimisation of CO₂ gas cooler/condenser in a refrigeration system”. In: *Applied Energy*.
- Hafner, A., S. Forsterling, and K. Banasiak (2014). “Multi-ejector concept for R-744 supermarket refrigeration”. In: *Proceeding of the 43th International Journal of Refrigeration*, pp. 1–13.
- Hafner, A., A.K. Hemmingsen, and P. Neksa (2014). “System configurations for supermarkets in warm climates applying R744 refrigeration technologies. A case studies of selected Chinese cities”. In: *Proceeding of the 11th IIR Gustav Lorentzen Conference on Natural Refrigerants, Hangzhou, China*.
- Hafner, A., A.K. Hemmingsen, and A. Van de Ven (2014). “R744 Refrigeration system configurations for supermarkets in warm climates”. In: *Proceedings of the 3rd IIR International Conference on Sustainability and the Cold Chain, London, UK*.
- Hafner, A., J. Schonenberger, et al. (2014). “R744 EJECTOR SUPPORTED PARALLEL VAPOUR COMPRESSION SYSTEM”. In: *Proceeding of the 3rd IIR International Conference on Sustainability and the Cold Chain, London, UK*.
- Haukaas, H.T. (2005). “Kulde- og varmepumpende prosesser med CO₂ som kuldemedium”. In: pp. 1–13.
- Kadam, A.D., A.S. Padalkar, and V.U. Walekar (2013). “Comparative Study of Transcritical CO₂ Cycle with and Without Suction Line Heat Exchanger at High Ambient temperature”. In: *International Journal Of Computational Engineering Research Vol. 3 Issue. 3*.
- Kima, M-H., J. Pettersen, and C. W. Bullard (2004). “Fundamental process and system design issues in CO₂ vapor compression systems”. In: *Progress in Energy and Combustion Science* 30.2, pp. 119–174.
- Lorentzen, G. (1993). “Revival of carbon dioxide as a refrigerant”. In: *NTH-SINTEF Refrigeration Engineering*.
- Lorentzen, G. and J. Pettersen (31 July 1992). “A new, efficient and environmentally benign system for car air-conditioning”. In: *NTH-SINTEF Refrigeration Engineering, N-7034 Trondheim*.
- Maa, Y., Z. Liu, and H. Tian (2013). “A review of transcritical carbon dioxide heat pump and refrigeration cycles”. In: *Energy*, pp. 156–172.

- Minetto, S. et al. (2015). "Experience with ejector work recovery and auxiliary compressors in CO₂ refrigeration systems. Technological aspects and application perspectives". In: *6th IIR Conference, Ammonia and CO₂ Refrigeration Technologies*.
- Nickl, J. et al. (2005). "Integration of a three-stage expander into a CO₂ refrigeration system". In: *International journal of refrigeration 28*.
- Penarrocha, I. et al. (2014). "A new approach to optimize the energy efficiency of CO₂ transcritical refrigeration plants". In: *Applied Thermal Engineering*.
- Petrak, M. (2013). "Efficiency improvements of CO₂ transcritical refrigeration systems by machine-made subcooling". In: *Proceeding of the 8th International Conference on Compressors and Coolants, Castá Papiernicka, Slovakia*.
- Riha, J., H. Quack, and J. Nickl (2006). "Sub-Critical Operation of the CO₂ Expander/Compressor". In: *International Compressor Engineering Conference, paper 1765*.
- Sharma, V., B. Fricke, and P. Bansal (2014). "CO₂ SUPERMARKET REFRIGERATION SYSTEMS FOR SOUTHEAST ASIA AND THE USA". In: *Proceeding of the 11th IIR Gustav Lorentzen Conference on Natural Refrigerants, Hangzhou, China*.
- shecco (2014). "Guide 2014: Natural refrigerants continued growth and innovation in Europe". In:
- Thevenot, R. (1979). *A history of Refrigeration Throughout the World*. Paris International Institute of Refrigeration.
- Torella, E. et al. (2011). "Energetic evaluation of an internal heat exchanger in a CO₂ transcritical refrigeration plant using experimental data". In: *International journal of refrigeration 34th*.

Appendix A

Additional Information

A.1 Files on flash drive

Folder	Description
Cadio	Technical data List of component Flow chart system Brochure of system Technical specifications R290 evaporator Technical specifications R744/R290 condenser Data sheet R744 compressor
Excel calculations	Calculation sheet condenser/gas cooler Dorin compressor data Measurement data SCOP calculations Subcooling calculations
Papers	All papers used in report
Raw data	All raw data collected during project period
Summary	In English and Norwegian
Full report	pdf-file
EES	EES documents of all simulations
HXsim	HX-file of all condensers and gas coolers
Metenorm	Temperature data from all capitals
Scientific paper	Scientific paper word-file Scientific paper pdf-file All figures and graphs used in the scientific paper
	Powerpoint presentation thesis

A.2 Scientific paper

Optimisation of a CO₂ refrigeration system with propane subcooling

SYNNE BERTELSEN, STINE HAUGSDAL AND TRYGVE M. EIKEVIK

Cadio AS has developed a CO₂ system with a secondary propane cycle for operation at higher ambient air temperatures. The system has a CO₂ gas cooler with integrated propane condenser and a propane subcooler that condenses the CO₂. This allows subcritical operation at all ambient temperatures. A prototype unit was instrumented and tested, where the optimal point for start of propane operation was found at an ambient temperature of 23,5 °C. Further, these measurement data have been compared to results from a simulation model developed using the Heat Exchanger simulation program (HXsim) and the Engineering Equation Solver (EES). Simulations showed that a set point for start of propane operation corresponding to an ambient temperature of 19,4 °C provided the best Coefficient of Performance. By implementing a new suggested propane condenser, the systems Coefficient of Performance experienced an increase of 16,2 % at an ambient temperature of 40 °C. The best CO₂ condenser experienced an increase in the Coefficient of Performance of minimum 9 %. By rising the fan speed, the performance of the system can be increased even further. When implementing the improved propane condenser, a smaller propane compressor can be applied. Performance of the system was tested for different European capitals. The seasonal performance in Madrid was found to be 2,85 in comparison to 3,22 in Oslo, where the propane system operates almost three more months in Madrid.

1. INTRODUCTION

The development of CO₂ as a refrigerant has been intriguing. From being discovered as a natural working fluid at the 19th century, nearly abandoned during the second world war to later be rediscovered at the end of the 20th century. This ideal refrigerant as described by Gustav Lorentzen is environmentally benign with zero Global Warming Potential (GWP) and zero Ozone Depletion Potential (ODP), safe, cheap and compatible with normal machine construction. The prevalence of R744 refrigeration is experiencing a steady increase. This trend is especially seen in northern climates, due to the reduced efficiency of the basic CO₂ cycle in warmer climates when compared to other synthetic refrigerants.

When the ambient temperature is increasing, the basic CO₂ cycle experience a decrease in the refrigeration capacity (Q_o), thus the Coefficient of Performance (COP). The challenge is to keep both the gas cooler outlet enthalpy and the power consumption as low as possible. Today, an array of technology solutions are available that improve the system efficiency in higher ambient temperatures, including but not limited to economisers, mechanical subcoolers, ejectors, expanders, CO₂ integrated systems, parallel compression and auxiliary compressors for flash vapour compression and evaporator overfeed.

In a study of Chinese cities presented in (Hafner, Hemmingsen, and Neksa 2014), a R404A system was used as a reference compared to three R744 systems using the standard booster architecture, the ejector

system and R290 mechanical subcooling. The R744 ejector supported units with parallel compression had the highest energy efficiency values (25 % saving) compared to a R404A unit. 16 % saving was achieved by the standard booster system equipped with an external mechanical subcooling system. Due to the high ambient temperatures in southern China, energy savings of 5-10 % was be obtained when replacing R404A units with a standard R744 booster system. Their conclusion was that these innovative R744 architectures soon will outperform all HFC refrigeration systems in the future.

Cadio AS approach to the problem is a CO₂ system with integrated propane subcooler for high air temperatures operations. This subcooler is only in operation above a certain temperature, due to the extra compressor work of the propane cycle. Instrumentation and testing of Cadio's prototype has been performed. Following, the performance of the prototype system has been identified using simulation programs HXsim and EES. The integrated CO₂ and propane condenser has been simulated in HXsim, and compared to other configurations in order to optimise the heat exchanger.

2. SYSTEM DESCRIPTION

Flow chart of the prototype system with instrumentation is seen in figure 1. The system consist of three circuits. A R744 unit for main operation, a R290 unit for subcooling the R744, and an ethylene-glycol unit. The ethylene-glycol unit with the R744 evaporator is not included in the commercial available system. This circuit

Nomenclature and Abbreviations	
A	Heat transfer area, m^2
c_p	Specific heat capacity, $\frac{J}{kg \cdot K}$
h	enthalpy, $\frac{kJ}{kg}$
\dot{m}	mass flow rate, $\frac{kg}{s}$
P	Pressure, bar
\dot{Q}	Heat transfer rate, kW
Q_o	Refrigeration capacity, kW
T	Temperature, $^{\circ}C$
ΔT	Temperature difference, K
ΔT_{LMTD}	Log mean temperature difference, K
U	Heat transfer coefficient, $\frac{W}{m^2 K}$
V_s	Swept volume, $\frac{m^3}{s}$
v	Specific volume, $\frac{m^3}{kg}$
\dot{W}	Work, kW
η_{is}	isentropic efficiency, -
π	Pressure ratio, -
λ	Volumetric efficiency, -
COP	Coefficient Of Performance
EES	Engineering equation solver
GWP	Global Warming Potential
ODP	Ozone Depletion Potential
R290	Propane
R744	Carbon dioxide
SCOP	Seasonal Coefficient of Performance

was added to the prototype system in order to provide heat of evaporation to the R744 during measurements.

The refrigeration system has two different operational modes. These modes depends on the temperature of the air cooling the R744 in the condenser. When the ambient temperature is low, only the R744 circuit is in operation. R744 is compressed in a semi-hermetic compressor to a condensing pressure which is correlated to the ambient temperature. Following it is condensed in an air cooled condenser, sent to a liquid receiver before it is throttled to evaporating pressure in a manual throttle valve. At last, the refrigerant is evaporated in a brazed plate heat exchanger. The evaporating pressure and temperature is determined by the area of application, namely refrigeration display counter at $-10^{\circ}C$ or frozen goods counter at $-33^{\circ}C$.

The second operational mode is at medium to high ambient temperatures. The operation of the R744 circuit is almost the same as for the latter operational mode, but the R290 system will now start to operate. R290 is compressed in a scroll compressor and condensed in the integrated air cooled R744 and R290 condenser. Moreover, the R290 is throttled in a thermal expansion valve before it evaporates in a brazed plate heat exchanger. The superheat from R744 is rejected in the air cooled condenser as much as the ambient temperature grants. It then continues to the R290 evaporator where the rest of the superheat and heat of condensation from R744 is absorbed by the evaporating R290. The refrigeration capacity of the R290 system equals the heat rejected from the condensing R744, see equation 5. Hence if the cooling capacity of the R290

TABLE 1: Set point refrigeration unit described by R744 high side pressure.

Evaporating temperature	$-10^{\circ}C$
Start fan	55 bar
Max speed fan/ Stop R290 system	60 bar
Start R290 system	67 bar

TABLE 2: Assumptions and restrictions for simulation model.

Foundation for simulation model	
Evaporating temperature R744	$-10^{\circ}C$
Superheat R290 evaporator	7 K
Superheat R744 evaporator	10 K
ΔT_{min} subcooler	9,9 K
Volumetric efficiency R290	0,8
Isentropic efficiency R290	0,6
Maximum volume flow air	$7000 \frac{m^3}{h}$
Heat capacity air	$1,005 \frac{kJ}{kg \cdot K}$
Density air	$1,225 \frac{kg}{m^3}$
Efficiency fan	50%
Heat loss from compressors	10%
Swept volume R290 compressor	$9,7788 \frac{m^3}{h}$
Swept volume R744 compressor	$3 \frac{m^3}{h}$

evaporator is too small, the R744 pressure will increase and the specific enthalpy of condensation is smaller. The setpoints for start and stop of the propane system and fan is seen in table 1.

3. METHOD

Instrumentation and measurements on the prototype system was performed. The location of the instrument components is seen in figure 1. The results from these measurements was later compared to the results from the simulation model. The simulation model was developed using the Engineering Equation solver (EES) and the heat exchanger simulation program (HXsim). In combination with the operational data provided by Cadio AS seen in table 2, and information derived from the measurement data and theory, the initial script was developed.

The CO_2 condensing temperature and propane evaporating temperature were decided by running a loop with an energy balance between the heat of evaporation and condensation. The heat removed from the CO_2 and the heat absorbed by the propane in the CO_2 subcooler, was calculated using equation 1 and demanded to be equal. Optimum operation of the system exists with as low compressor work and as high refrigeration capacity as possible, thus as low condensing temperature as possible. The maximum value of the CO_2 condensing temperature was set to $29^{\circ}C$, due to the restriction of subcritical operation. For each iteration of the CO_2 condensing temperature, the propane evaporating temperature was iterated

Cadio system unit with instrumentation

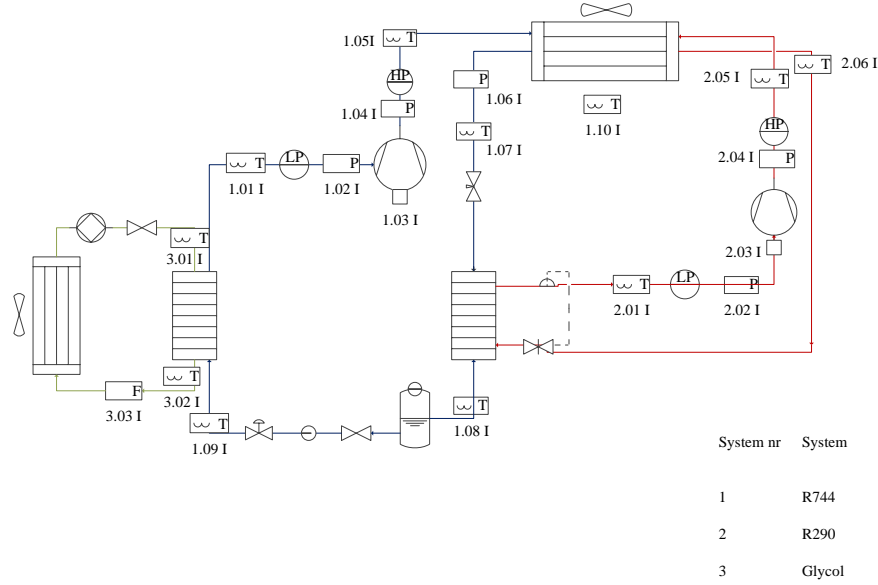


FIGURE 1: Location of instrumentation components.

between its maximum and minimum values.

$$\dot{Q} = \dot{m} \cdot \Delta h \quad (1)$$

$$\dot{Q} = \dot{m} \cdot c_p \cdot \Delta T \quad (2)$$

$$\dot{Q} = U \cdot A \cdot \Delta T_{LMTD} \quad (3)$$

$$COP = \frac{Q_o}{W} \quad (4)$$

$$\dot{Q}_{o,R290} = \dot{Q}_{c,R744} - \dot{Q}_{gc,R744} \quad (5)$$

Energy balance in the condensers is required in the EES script. This means that the heat absorbed or rejected by the heat source or sink must be equal to the heat rejected or absorbed by the refrigerant and the temperature difference in the heat exchanger. By combining equation 1, 2 and 3, equation 6 is obtained. Equation 7 represents the equation for the fan work.

$$\dot{Q} = \dot{m} \cdot \Delta h = \dot{m} \cdot c_p \cdot \Delta T = U \cdot A \cdot \Delta T_{LMTD} \quad (6)$$

$$W_{fan} = \frac{\dot{V} \cdot \Delta P_{tot}}{\eta_{fan}} \quad (7)$$

Equations for the isentropic and volumetric efficiencies of the CO₂ compressor was provided by the manufacturer. Equation 8 and 9 are valid for subcritical

operation where π is the pressure ratio. The CO₂ mass flow was calculated with equation 10 and multiplied by a factor of 1,18 for 60 Hz operation (Dorin 2014).

$$\eta_{is,CO_2} = -0,0832 \cdot \pi^2 + 0,3904 \cdot \pi + 0,1247 \quad (8)$$

$$\lambda_{CO_2} = 0,0181 \cdot \pi^2 - 0,1746 \cdot \pi + 1,1078 \quad (9)$$

$$\dot{m} = \frac{V_s \cdot \lambda}{v_1} \quad (10)$$

It was observed from the measurement that there was no subcooling in the CO₂ system, while no data were available on the propane outlet state from the condenser, so a subcooling of 1 K was assumed. Simulation data from HXsim were used in order to find the actual correlations between the U-values, LMTD-values and the ambient temperature. EES was utilised in order to achieve operational data, such as the refrigerant mass flow and condensing pressure, with the heat balance in the subcooler as a restriction. These operational data were further on applied in HXsim. Initially the approach temperatures were guessed and implemented in the fundamental EES script. Following, operational data from EES were implemented in HXsim. When the appropriate subcooling was achieved, the procedure stopped. In

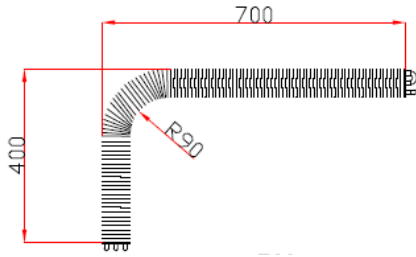


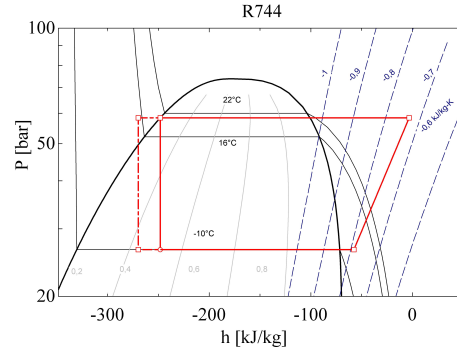
FIGURE 2: Integrated CO₂ and propane condenser seen from above.

figure 2 the integrated CO₂ and propane condenser is shown.

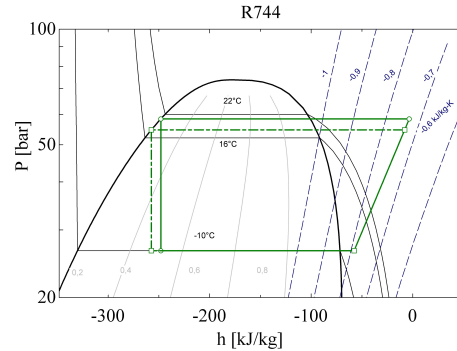
When operating as a condenser, it is important to ensure that the liquid is fully condensed at the inlet of the evaporator for proper operation. As the refrigerant flows through the condenser there is a phase change where a drop in velocity occurs (American Society of Heating, Refrigerating, and Air-Conditioning Engineers 2008). A decrease in velocity will lead to an increase in the laminar boundary layer against the pipe wall and a larger temperature difference over the boundary layer. By allowing a pressure drop when designing the condenser, the velocity is increased through the pipe, hence a thinner boundary layer is obtained and providing a more effective heat transport. However, a pressure loss through the condenser leads to a loss in temperature, which can result in flashing in the liquid line and a decrease in system efficiency. A large pressure loss will result in a higher pressure ratio, thus increased compressor work. By subcooling the liquid sufficiently, flashing in the liquid line can be prevented. Subcooling is also an efficient way to increase the refrigeration capacity and or decreasing the compressor size. The normal procedure when designing an air-cooled condenser is to provide a heat transfer area and pressure drop to provide 1 to 3 K subcooling (American Society of Heating, Refrigerating, and Air-Conditioning Engineers 2008).

(Ge et al. 2015) discovered that that variation of air flow rate is the most effective way to control and minimise the approach temperature. If the air flow rate is highly increased, a great effect on the refrigerant temperature was discovered. It was shown that the COP was not penalised as much by the extra fan work compared to the significant increase in refrigeration capacity.

Different condenser circuit designs has been tested in HXsim. Subcooling was used as a tool to spot the best condenser configurations. A theoretical approach has been utilised in order to investigate the best CO₂ and propane condensers. By analysing the subcooling for different condenser modifications in HXsim, the best configurations were spotted. A configurations with subcooling at the same operational parameters



(a) Influence of CO₂ subcooling on Q_o .



(b) Influence of reduced CO₂ pressure on Q_o .

FIGURE 3: Performance improvement for the CO₂ condenser as subcooling and reduced pressure.

as the original configuration, was seen as an improved configuration. In order to analyse the improvement of the condenser configurations, the Q_o and COP were calculated when maintaining the subcooling and the condensing pressure, or by a reduction in pressure where the CO₂ had no subcooling and the propane had a subcooling of 1 K. This feature is visualised in figure 3.

A system for naming the different configurations has been developed. The original propane configuration is named 6-1-7 and the CO₂ configuration is named 6-2-7. The first digit represents the number of vertical tubes, the second digit represents the number of rows and the third represents the number of vertical duplications. Figure 4 explains how the different modifications have been named.

4. RESULTS

4.1. Measurements and simulation model

Figure 5a and 5b shows the refrigeration capacity and COP from the measurements when the system is operating with and without the propane system. The best overall COP of the system is obtained when the propane system starts to operate at an ambient temperature of 23,5 °C. This is observed in figure 5b

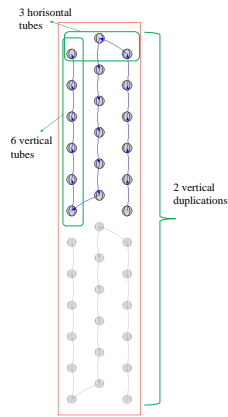
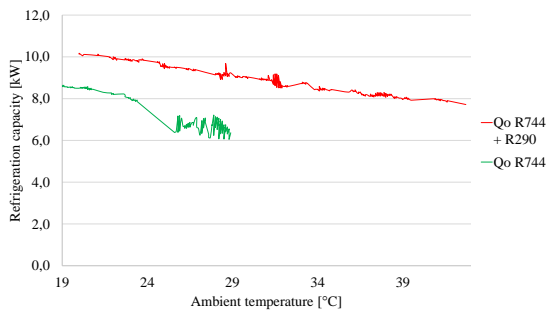
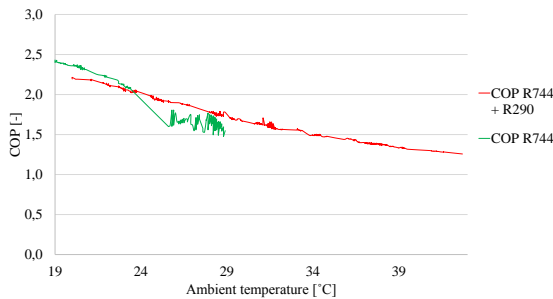


FIGURE 4: Example of a 6-3-2 condenser.

where the two lines intersects.



(a) Refrigeration capacity from measurements.



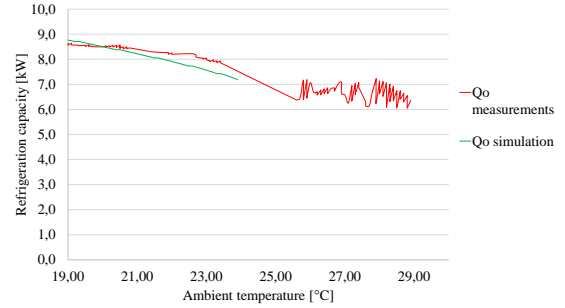
(b) COP from measurements.

FIGURE 5: Q_o and COP from measurements

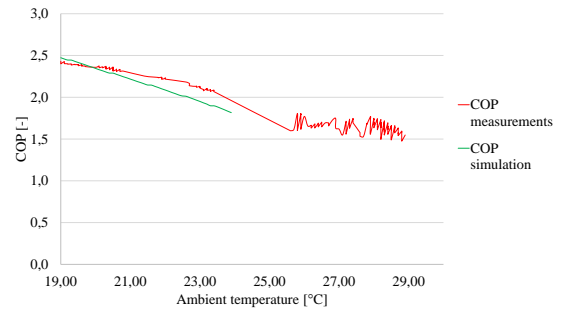
Further on, the results from the simulation model was verified by comparison to the measurement data results. The differences are shown in figures 6a and 6b for the solitary CO₂ operation and in figures 7a and 7b with the propane system in operation.

When comparing the simulation and measurement results, the figures for CO₂ operation shows a slight discrepancy in slope. The maximum deviation between the to curves are 10% for the COP and 6,9% for the refrigeration capacity, both at an ambient temperature of 23,3 °C.

Similar trends are observed in figures 7a and 7b,

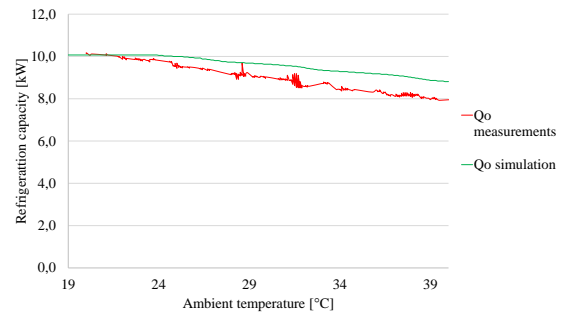


(a) Comparison of Q_o without propane operation.

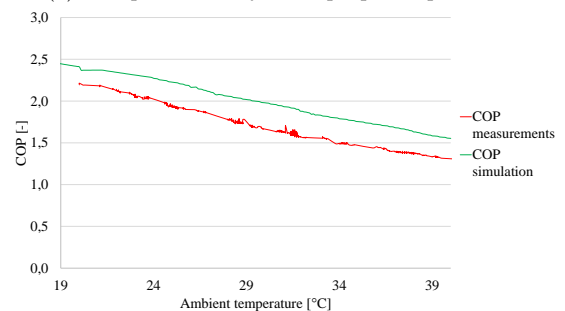


(b) Comparison of COP without propane operation.

FIGURE 6: Comparison of Q_o and COP from measurements and simulations without propane operation.



(a) Comparison of Q_o with propane operation.



(b) Comparison of COP with propane operation.

FIGURE 7: Comparison of Q_o and COP from measurements and simulations with propane operation.

although the simulated system operates with a slightly better performance. The maximum deviation is 12%

for the refrigeration capacity and 21% for the COP at an ambient temperature of approximately 37°C. The minimum deviation for the COP is 8% at an ambient temperature of 20°C.

4.2. System operation in European capitals

The prototype system was simulated for five European capitals with different climates in order to investigate and compare the seasonal performance, operating hours with propane and energy consumption. The data presented in table 3, figures 8 and 9 are calculated with a set point corresponding to an ambient temperature of 19,4°C. It can be observed from table 3 that the operating hours with propane and the yearly energy consumption increases in the warmer climates. Further it can be seen that the minimum refrigeration capacity is the same for all the capitals.

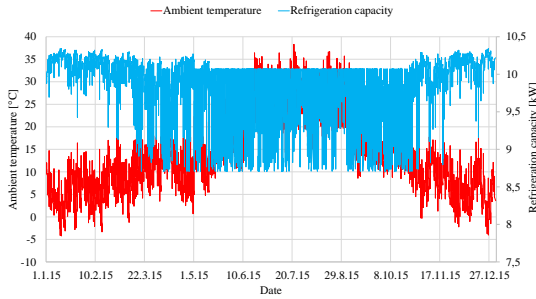


FIGURE 8: Ambient temperature versus refrigeration capacity in Madrid 2005.

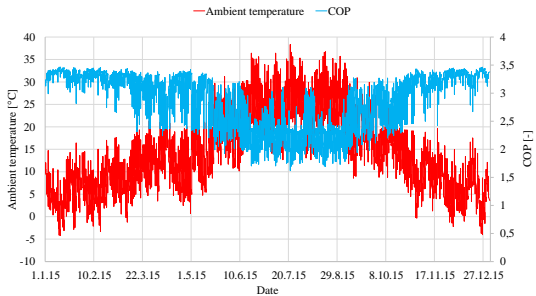


FIGURE 9: Ambient temperature versus COP in Madrid 2005.

TABLE 3: System performance in different climates.

	Oslo	London	Paris	Budapest	Madrid
Operating hours propane	461	716	1519	1975	2580
% propane operation of year	5,26	8,17	17,34	22,55	29,45
Maximum Q_o [kW]	10,43	10,35	10,36	10,39	10,34
Minimum Q_o [kW]	8,71	8,71	8,71	8,71	8,71
Seasonal performance	3,22	3,09	2,99	2,97	2,85
Yearly energy consumption [kWh]	27627	28417	29506	30058	31282

TABLE 4: Increase in Q_o and COP as a result of CO₂ subcooling.

T_{amb}	T_{sat}	12-3-2	9-3-3	15-2-3	4-4-6
6,0	19,86	10,2%	10,6%	11,9%	10,1%
12,1	21,69	13,9%	13,3%	12,1%	12,7%
15,5	24	14,2%	13,7%	12,3%	13,2%
18,7	26,3	15,0%	14,5%	12,7%	14,1%

4.3. Optimisation of CO₂ condenser

In figure 10, the subcooling is plotted for the best CO₂ condenser modifications. Here the 15-2-3 configuration has a linear slope, compared to the non-linear slopes of the other configurations. It can be observed from figure 10 that the configuration with two rows experienced more subcooling at the lower saturation temperatures and a different trend than the configurations with more tube rows. The reason for this is that the both of the two first pipelines will meet fresh air. An optional third row will be cooled by air that is heated by the first rows.

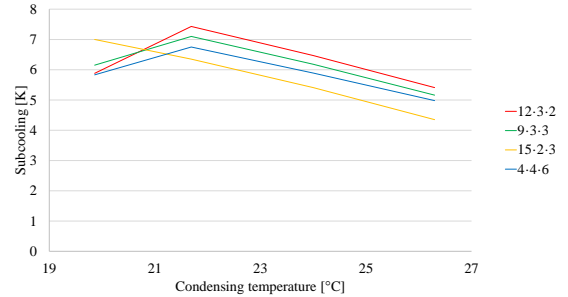


FIGURE 10: Subcooling for best CO₂ configurations.

Table 4 sums up the increase in Q_o when the the condensing pressure and the subcooling is maintained. A theoretical approach has been utilised and in reality a subcooling to this extent will not exist.

Table 5 represents the subcooling when it is transformed into a reduction in condensing pressure. This leads to an increase in Q_o and a decrease in compressor work. In figure 11, the fan speed is doubled for the original CO₂ condenser.

TABLE 5: Subcooling calculated as a decrease in work including an increase in Q_o .

T_{amb}	12-3-2			9-3-3			15-2-3			4-4-6		
	ΔW	ΔQ_o	ΔCOP	ΔW	ΔQ_o	ΔCOP	ΔW	ΔQ_o	ΔCOP	ΔW	ΔQ_o	ΔCOP
6,0	-0,8%	+0,7%	1,9%	-0,9%	+0,8%	2,0 %	-1,0%	+0,9%	2,3%	-0,8%	+0,8%	2,0%
12,1	-1,8%	+1,9%	4,3%	-1,7%	+1,8%	4,1 %	-1,8%	+1,9%	4,2%	-1,9%	+1,9%	4,8%
15,5	-3,7%	+4,3%	8,9%	-3,3%	+3,8%	7,9%	-3,1%	+3,6%	7,5%	-3,3%	+3,8%	7,8%
18,7	-3,3%	+4,3%	8,8%	-3,1%	+4,2%	8,5%	-2,8%	+3,7%	7,6%	-3,0%	+4,0%	8,2%

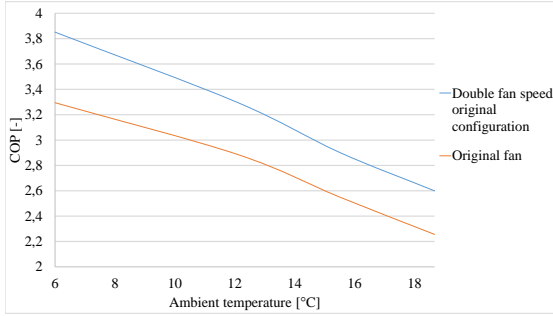
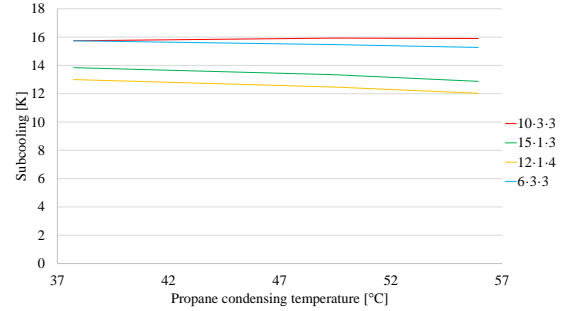
FIGURE 11: Effect on COP for original CO₂ condenser when fan speed is doubled.

FIGURE 12: Subcooling for the best propane configurations.

4.4. Optimisation of propane condenser

The same theoretical approach was utilised when analysing the propane condensers. In figure 12 the subcooling for the propane condensers is shown. Table 6 represents the increase in the overall systems COP and Q_o when the condensing pressure is maintained. Table 7 represents the increase in the overall systems Q_o and a decrease in the overall systems work, when the propane subcooling is translated into a decrease in pressure.

TABLE 6: Propane subcooling calculated as an increase in Q_o and an increase in COP.

T_{amb}	10-3-3		6-3-3		15-1-3		12-1-4		
	T_{sat}	ΔQ_o	ΔCOP	ΔQ_o	ΔCOP	ΔQ_o	ΔCOP	ΔQ_o	ΔCOP
22	37,73	3,9%	6,1%	3,9%	6,1%	3,4%	5,3%	3,2%	5,0%
33,5	49,45	5,7%	8,5%	5,5%	8,3%	4,7%	7,1%	4,4%	6,6%
40	55,93	6,9%	10,2%	6,7%	9,7%	5,6%	8,2%	5,3%	7,6%

TABLE 7: Propane subcooling calculated as a decrease in work including an increase in Q_o and COP for the overall system.

T_{amb}	10-3-3			6-3-3			15-1-3			12-1-4		
	ΔW	ΔQ_o	ΔCOP	ΔW	ΔQ_o	ΔCOP	ΔW	ΔQ_o	ΔCOP	ΔW	ΔQ_o	ΔCOP
22	-12,1%	+3,9%	18,2%	-8,3%	+2,5%	11,8%	-5,9%	+1,7%	8,0%	-4,8%	+1,2%	6,4%
33,5	-10,3%	+4,7%	16,6%	-7,0%	+3,1%	10,8%	-4,9%	+2,2%	7,4%	-4,2%	+1,7%	6,1%
40	-9,3%	+5,3%	16,2%	-6,3%	+3,5%	10,5%	-4,4%	+2,5%	7,2%	-3,5%	+1,9%	5,7%

5. DISCUSSION AND CONCLUSION

5.1. Measurements and simulation model

In figure 5a the corrected measurement data is presented. The optimal point for start of the propane operation is a question of conflicting interests, due to the improved refrigeration capacity with the propane system in operation. Measurements shows that the optimal point for start of propane operation was found at an ambient temperature of 23,5 °C, when aiming to maximise the COP. In comparison, simulations provided a propane set point corresponding to an ambient temperature of 19,4 °C. However, when the propane system is not in operation, the refrigeration capacity start to drop significantly from an ambient

temperature of 15 °C.

Figures 6a and 6b illustrates the deviation between simulations and measurement data for CO₂ operation. There are several reasons for these deviations. Differences between the suction and condensing temperatures in the measurement and simulation data was observed. The suction temperature is kept in the range from -1,3 °C to 4 °C in the measurement data, compared to the simulation where the suction temperature is kept constant at 0 °C. The condensing temperature in the simulation was observed to be lower than the measurements up to an ambient temperature of approximately 20,5 °C. This can be observed by the point of intersection in figures 6a and 6b. When the propane is in operation there are more factors influencing the deviations. The suction temperatures varies from -7,5 °C to 12 °C, thus changing the operational conditions. However, when the propane system is operating, the CO₂ condensing temperature from the measurement data are higher than the simulated condensing temperature. The differences ranges from 0,2 K at 20 °C ambient temperature up to 3,5 K at an ambient temperature of 40 °C. This explains the different slopes for the refrigeration capacity illustrated in figure 7a.

5.2. System operations in European capitals

In figures 8 and 9, the effect of the ambient temperature on the refrigeration capacity and COP is clearly illustrated. As the ambient temperature is increasing, both the refrigeration capacity and COP decreases, coinciding with theory. Large variation can be observed in the refrigeration capacity in figure 8. This is because the ambient temperature often shifts between the propane set points, giving large variations in the refrigeration capacity.

The great range in refrigeration capacity and COP during the summer months is explained by the large variation in ambient temperature from night to day.

As shown in table 3, there are great variations in the operating hours with propane between the different capitals. The difference in operating hours with propane between Oslo and Madrid equals nearly three months. The energy consumption in Madrid is also 13% higher than in Oslo due to the high ambient air temperatures in Madrid. The lowest refrigeration capacity for all the capitals was calculated to be 8,71 kW. The reason for this, despite the large variations in ambient air temperatures, is that the refrigeration capacity drops significantly before the propane system starts to operate. The lowest capacity is achieved at an ambient temperature of 19,3 °C, corresponding to a condensing temperature of 25,4 °C, while the refrigeration capacity increase to 10,05 kW when the propane system start to operate at an ambient temperature of 19,4 °C. Figure 8 show the importance of choosing the optimal temperature for start of propane

operation and how it influence the refrigeration capacity in warmer climates.

5.3. Optimisation of the CO₂ condenser

A theoretical approach was utilised when analysing the effect of the subcooling. Comparing tables 4 and 5, it is clearly seen that keeping the subcooling results in the highest COP. This is mainly due to the larger temperature required in the condenser when the fan capacity is decreased at lower condensing temperatures. This can also be explained by the reduction in LMTD when the pressure is decreased. The U-value and area remains constant, thus the CO₂ will be less cooled by the air. As mentioned, this is a theoretical approach and subcoolings of this extent will not occur in reality. A subcooling of approximately 2 K is prevalent for CO₂ condensers. Therefor, when implementing these configurations, both a reduction in pressure and some subcooling is achievable. The improvement on the system when implementing the new configurations will be in the range of the results presented for both analytic approaches. Therefor, the 12·3·2 configuration represents a minimum COP increase of 8,8 %, corresponding to the reduced pressure option.

The energy efficiency of the system was also significantly improved by changing the set point of the fan, i.e increasing the volume flow of air for lower saturation temperatures. When the fan speed is doubled, thus the scenario if a new fan were implemented using the original configuration. At an ambient temperature of 19 °C an increase in COP of 15 % was experienced for the original configuration.

5.4. Optimisation of the propane condenser

Propane condenser configurations were also tested in HXsim. The percentage increase in COP will differ from the percentage increase in refrigeration capacity since the propane subcooling will lead to larger enthalpy difference in the propane evaporator, hence a reduction in CO₂ condensing pressure and compressor work. The exit temperature difference between the subcooled propane and the ambient air was observed to be from 0,01 K to 0,66 K for the 10·3·3 and 6·3·3 configuration. The reason for this is that the condenser is overdimensioned. The 10·3·3 condenser experienced an improvement of 18,4% at an ambient temperature of 22 °C.

ACKNOWLEDGEMENTS

We would like to thank Professor Trygve Magne Eikevik for great guidance and for his dedication to the project and Armin Hafner for helpful advice for improvements. We would also use this opportunity to thank Trond Andresen for helpful assistance with HXsim and Inge Hvard Rekstad for advantageous consultations.

We would like to acknowledge the help from Sigmund Jenssen at Cadio AS for good academic discussions and guidance. Last but not least, we thank Roger Tellefsen for useful help with the prototype system.

REFERENCES

- American Society of Heating, Refrigerating, and Air-Conditioning Engineers (2008). *ASHRAE Handbook - HVAC Systems and Equipment (SI)*. American Society of Heating Refrigerating and Air-Conditioning Engineers.
- Dorin (2014). “Dorin Innovation”. In: Accessed 03.02.2015. URL: <http://www.dorin.com/en/catalogo/SE/CD/CD200/CD%20380H/>.
- Ge, Y.T. et al. (2015). “Design optimisation of CO₂ gas cooler/condenser in a refrigeration system”. In: *Applied Energy*.
- Hafner, A., A.K. Hemmingsen, and P. Neksa (2014). “System configurations for supermarkets in warm climates applying R744 refrigeration technologies. A case studies of selected Chinese cities”. In: *Proceeding of the 11th IIR Gustav Lorentzen Conference on Natural Refrigerants, Hangzhou, China*.

A.3 List of instrumentation components

Component number	Type of component
1.01 I	Thermocouple R744 evaporator outlet
1.02 I	Pressure transmitter R744 evaporator outlet
1.03 I	Wattmeter R744 compressor
1.04 I	Pressure transmitter R744 gas cooler inlet
1.05 I	Thermocouple R744 gas cooler inlet
1.06 I	Pressure transmitter R744 gas cooler outlet
1.07 I	Thermocouple R744 gas cooler outlet
1.08 I	Thermocouple R744 subcooler outlet
1.09 I	Thermocouple R744 evaporator inlet
1.10 I	Thermocouple ambient air
2.01 I	Thermocouple R290 evaporator outlet
2.02 I	Pressure transmitter R290 compressor inlet
2.03 I	Wattmeter R290 compressor
2.04 I	Pressure transmitter R290 compressor outlet
2.05 I	Thermocouple R290 condenser inlet
2.06 I	Thermocouple R290 condenser outlet
3.01 I	Thermocouple glycol inlet chiller
3.02 I	Thermocouple glycol inlet chiller
3.03 I	Flow measurer glycol

Table A.1: Overview of instrumentation component

A.4 Modifications condenser and gas cooler

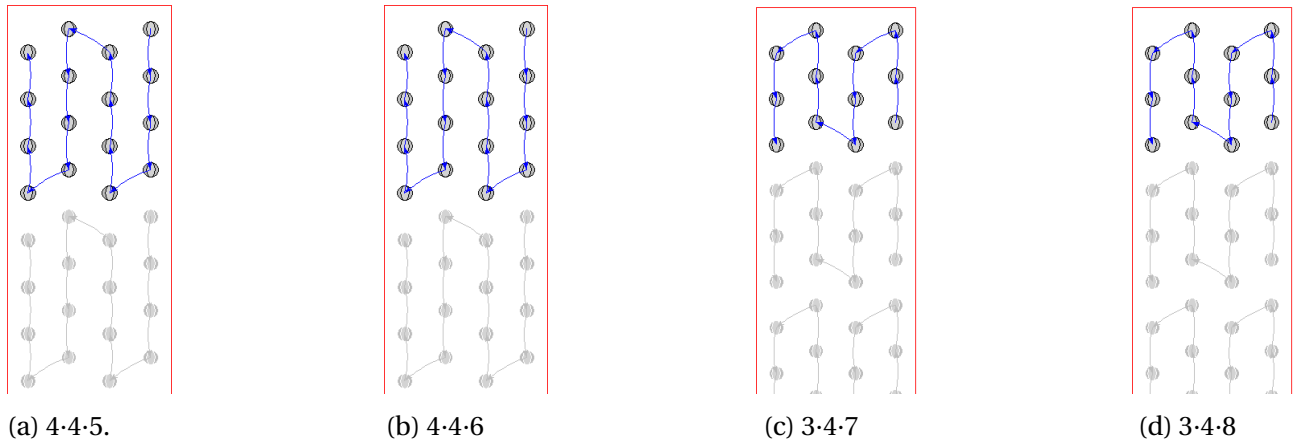
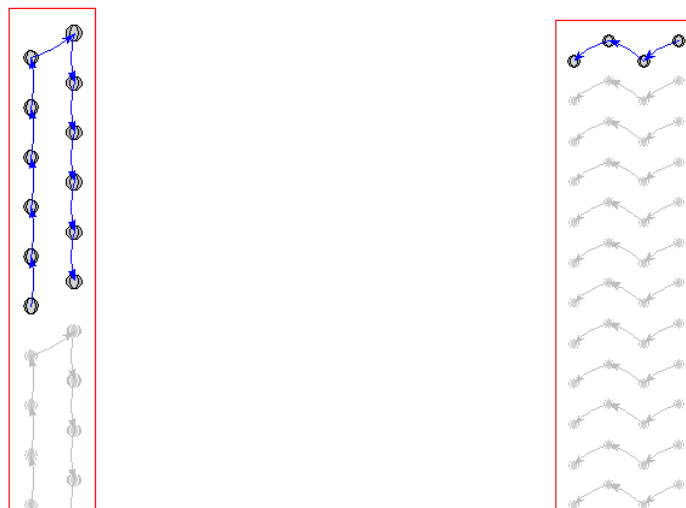


Figure A.1: CO₂ condenser configurations with four rows and different vertical duplications.



(a) New pipe dimension 6·2·7

(b) New pipe dimension 1·4·50

Figure A.2: CO₂ condenser configurations with new pipe dimension.

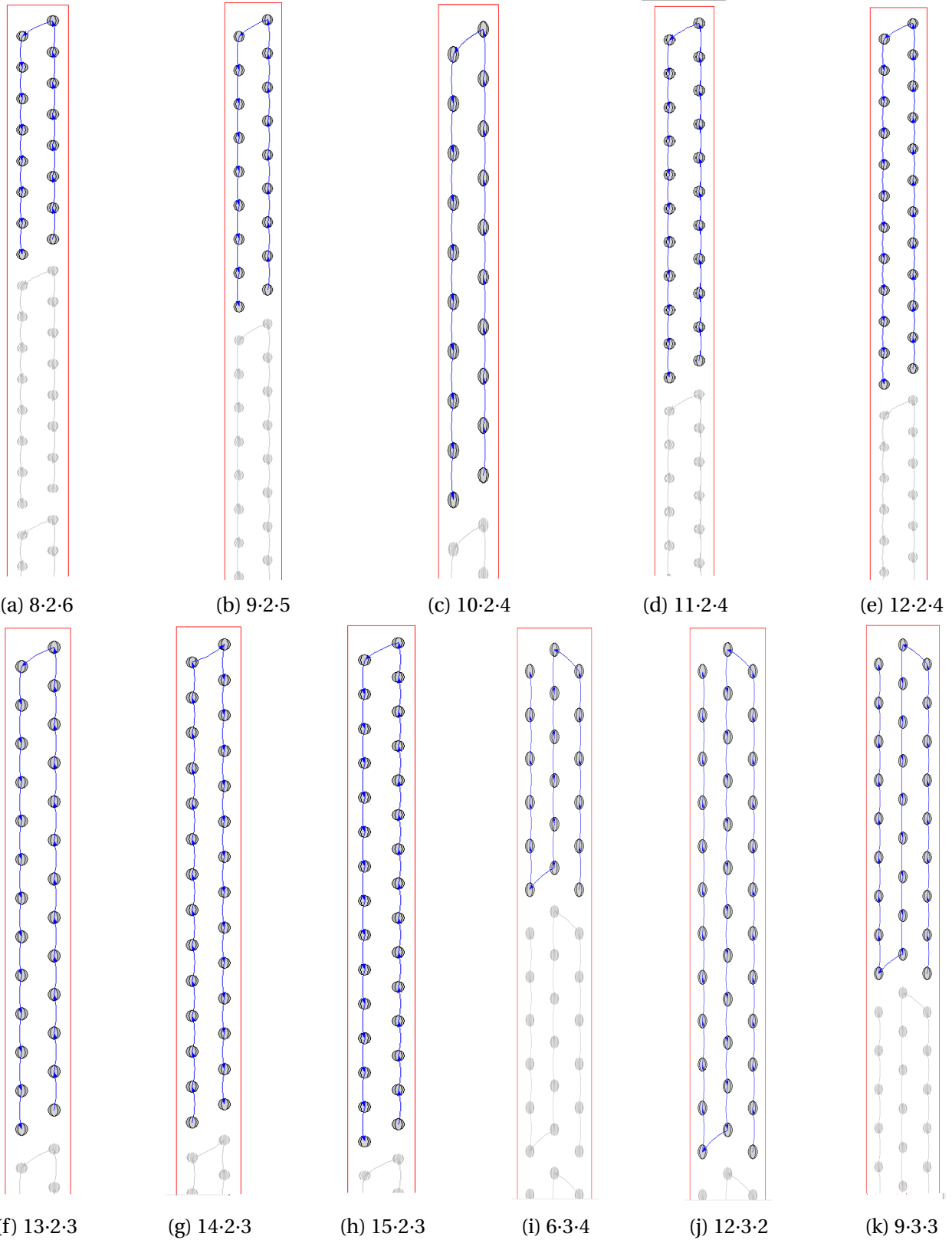


Figure A.3: CO₂ condenser configurations with two/ three rows and different vertical duplications.

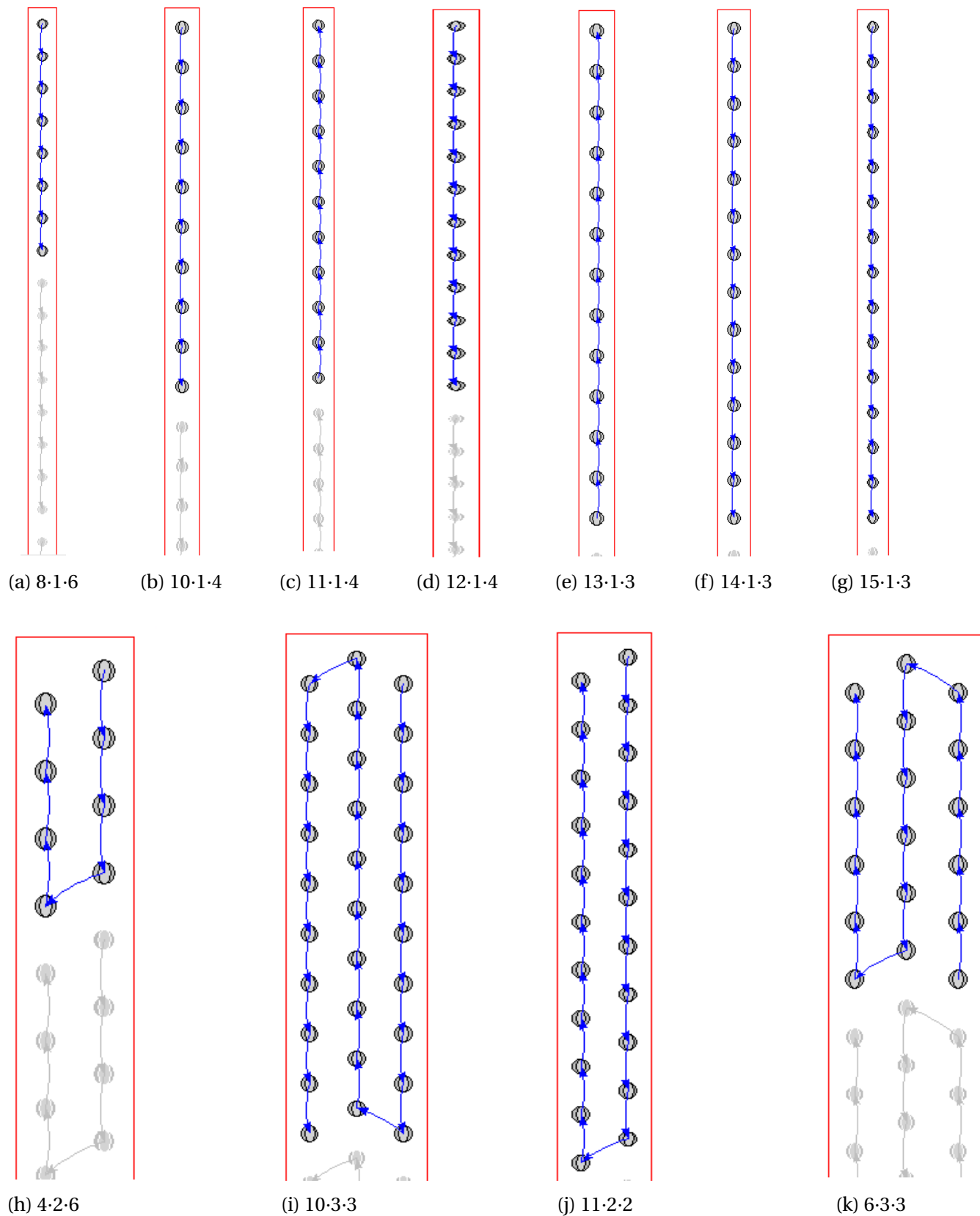


Figure A.4: Propane condenser configurations with different vertical duplications.

A.5 System operation in European capitals

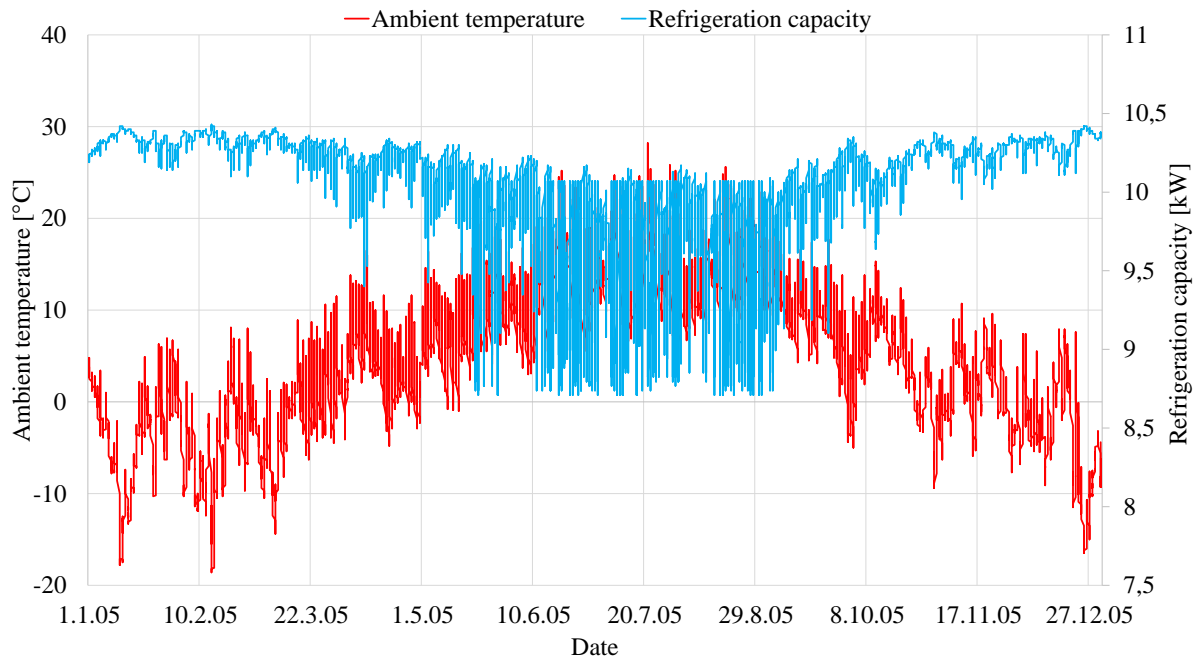


Figure A.5: Ambient temperature versus refrigeration capacity in Oslo 2005.

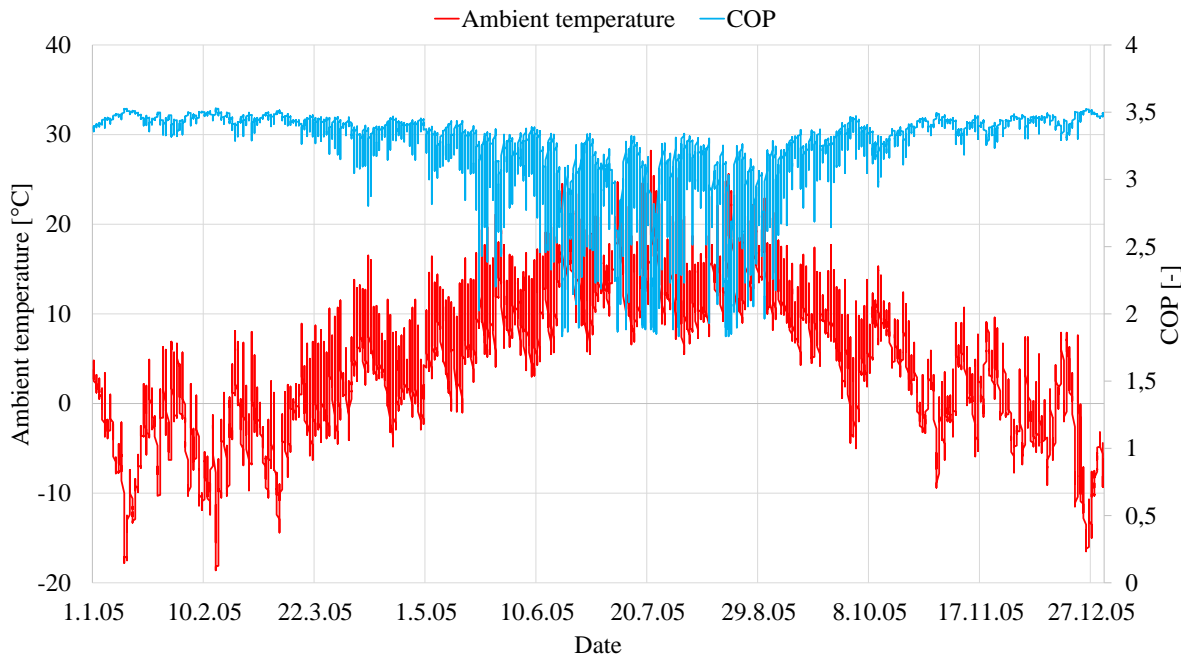


Figure A.6: Ambient temperature versus COP in Oslo 2005.

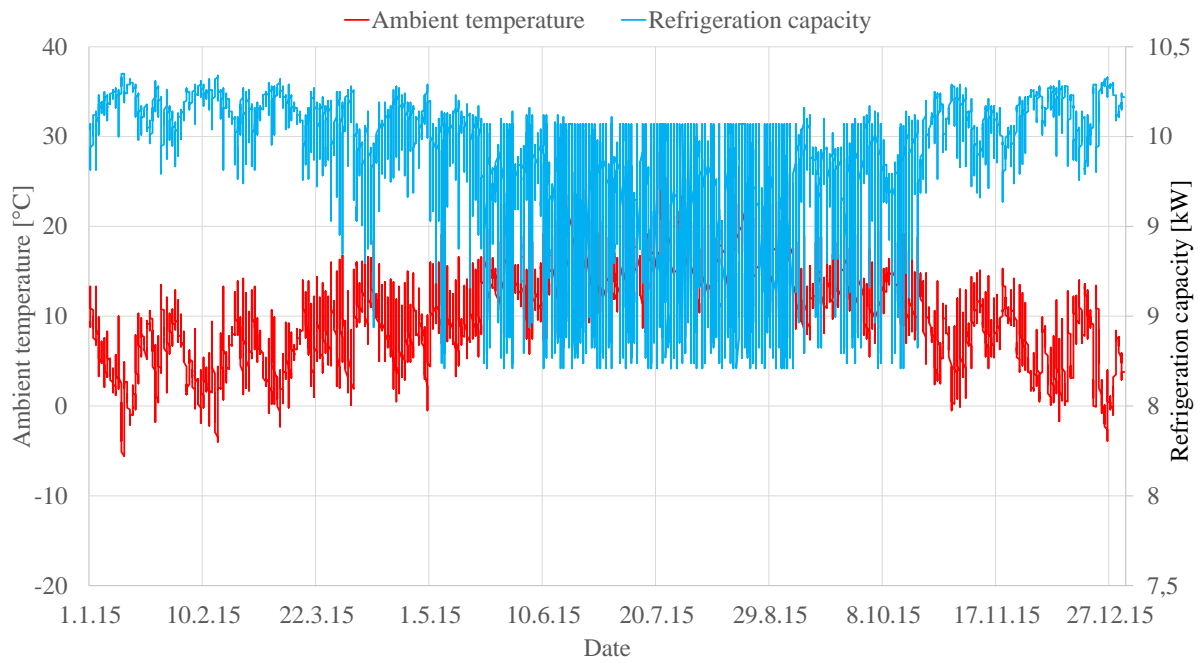


Figure A.7: Ambient temperature versus refrigeration capacity in London 2005.

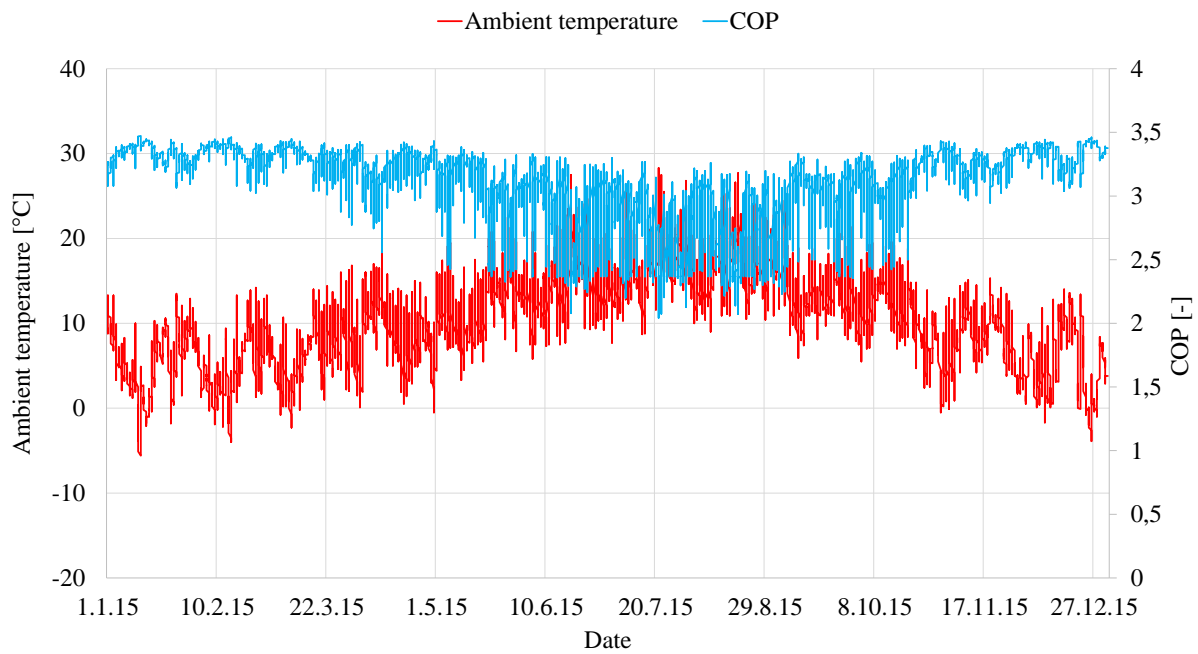


Figure A.8: Ambient temperature versus COP in London 2005.

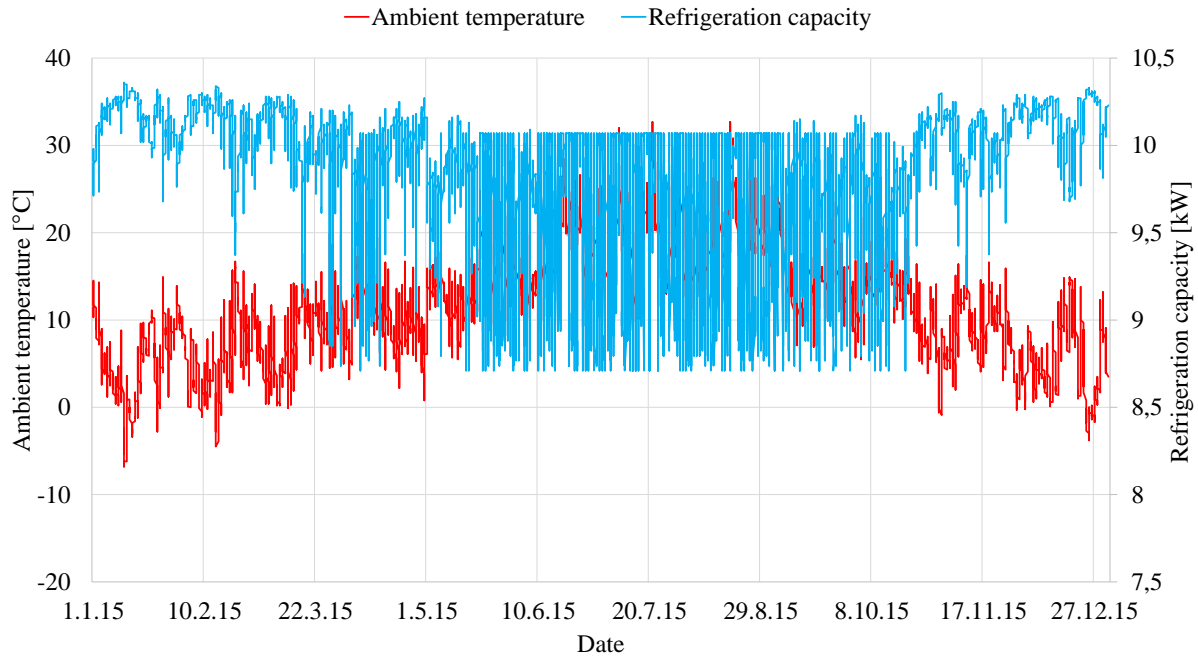


Figure A.9: Ambient temperature versus refrigeration capacity in Paris 2005.

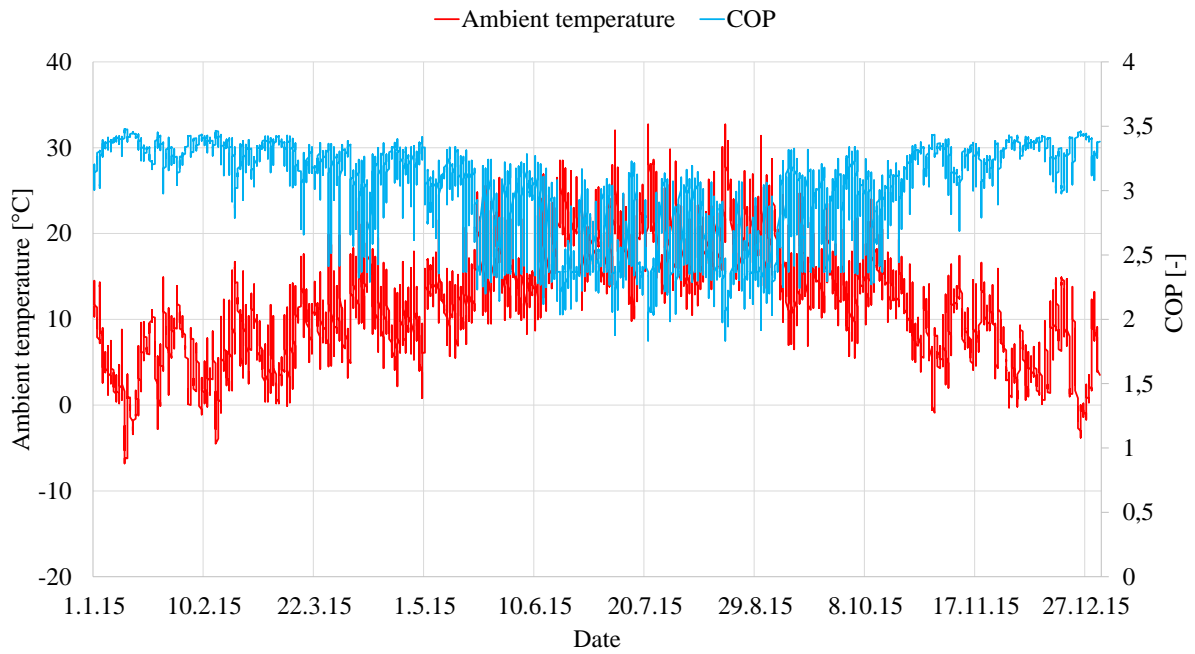


Figure A.10: Ambient temperature versus COP in Paris 2005.

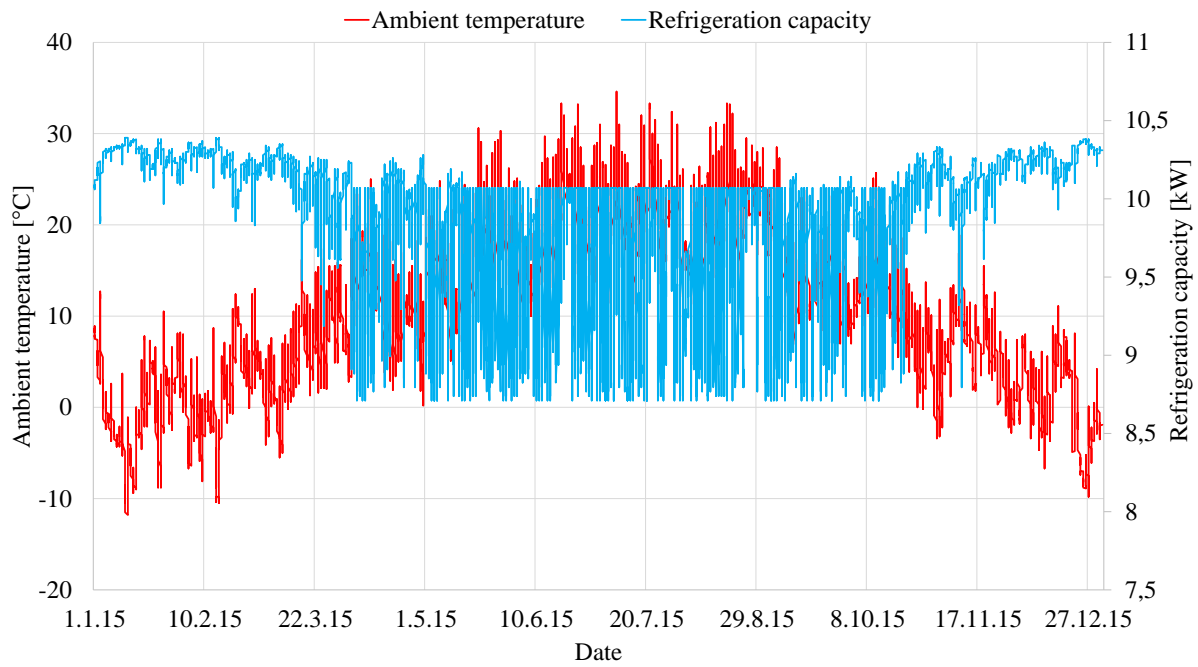


Figure A.11: Ambient temperature versus refrigeration capacity in Budapest 2005.

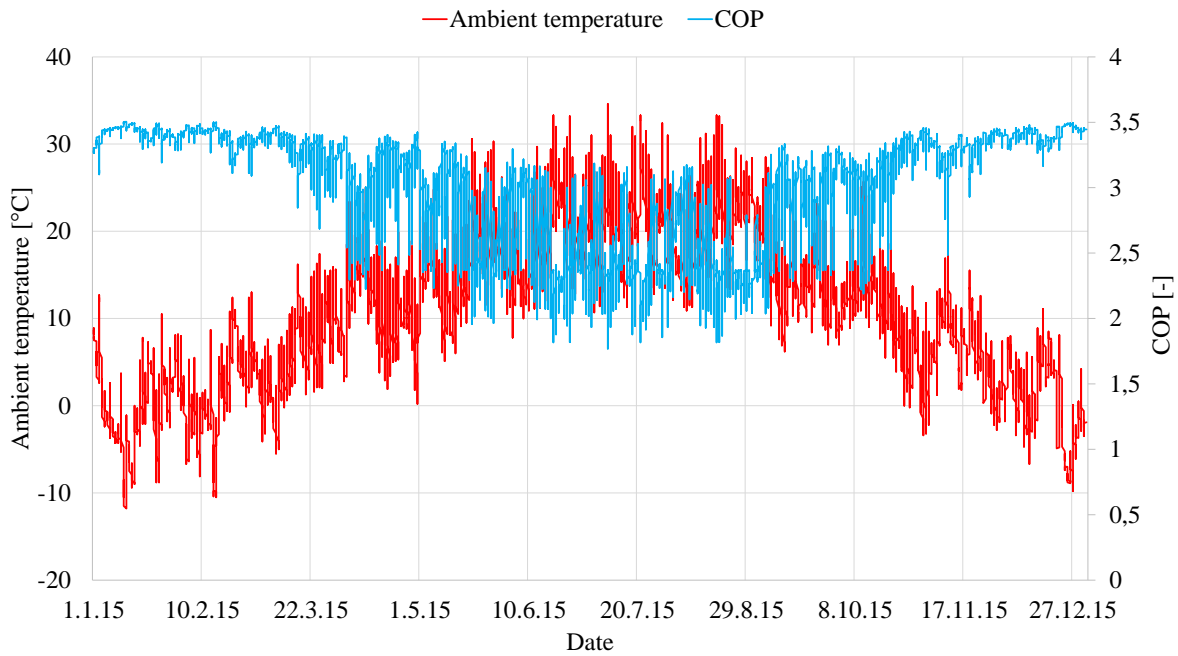


Figure A.12: Ambient temperature versus COP in Budapest 2005.

A.6 EES scripts

\$ARRAYS ON

"Fundamental simulation model"

PROCEDURE test(T_4;T_amb;ON;Q_o;COP;P_2;h_2;h_3;h_4;h_5;P_1p;P_2p;h_1p;h_2p;h_3p)

Q_o:=-1

COP:=-1

If(ON<1) Then

T_s:=10[C]

T_0:=-10[C]

T_1:=T_0+T_s

Q_heatloss=0,10

P_1:=P_sat(R744;T=T_0)

h_1:=enthalpy(R744;T=T_1;P=P_1)

v_1:=Volume(R744;T=T_1;P=P_1)

s_1:=entropy(R744;T=T_1;P=P_1)

if (T_amb<14) Then

cooler from Hxsim simulations"

T_diffgc:=9,61[C]

Else

T_diffgc:=7,63[C]

endif

"Get results with temperature difference in gas

If (T_amb<-4,7) Then

pressure is set at minimum of 37bar"

T_3=2,3[C]

else

T_3:=T_amb+T_diffgc

endif

"When the ambient temperature is low, discharge

If (T_3>18,27) and (T_3<21,98) Then

V_air:=0,4717*T_3-8,4233

else

if(T_3>=21,98) Then

V_air:=1,9444 [m^3/s]

else

V_air:=0,19444[m^3/s]

endif

endif

rho_air:=1,225 [kg/m^3]

m_air=rho_air*V_air

dp_air:= (3,6582*V_air^2 + 3,2504*V_air - 0,3654)/10^3 "[kPa]"

eta_fan:=0,5

W_fan:=(V_air*dp_air)/eta_fan

```

x_3:=0
P_3:=P_sat(R744;T=T_3)
h_3:=enthalpy(R744;T=T_3;x=x_3)
h_4:=h_3
h_5:=h_4
T_4corr:=T_3

phi:=P_3/P_1
lambda_c:= 0,0181*phi^2 - 0,1746*phi + 1,1078
Vs_c:=3[m^3/h]
m_c:=((Vs_c/3600[s/h])*lambda_c/v_1)*1,18

P_2:=P_3
h_2s:=Enthalpy(R744;s=s_1;P=P_2)
eta_c = -0,0832*(phi^2) + 0,3904*phi + 0,1247
h_2:=h_1+((h_2s-h_1)/eta_c)*(1-Q_heatloss)
T_2:=Temperature(R744;h=h_2;P=P_2)
m_c:=((Vs_c/3600[s/h])*lambda_c/v_1)*1,18
W:=(m_c*(h_2-h_1))/(1-Q_heatloss)

Q_rej:=m_c*(h_2-h_3)

Q_o:=m_c*(h_1-h_3)
COP:=Q_o/(W+W_fan)

P_1p:=0
P_2p:=0
h_1p:=0
h_2p:=0
h_3p:=0

Else

A:=-1
B:=-1

Repeat
T_4:=T_4+0,01[C]
value:=T_4-9,9[C]

T_sp:=7[C]
T_1p:=value+T_sp
P_1p:=P_sat(R290;T=value)
v_1p:=volume(R290;T=T_1p;P=P_1p)
Vs_p=9,7788[m^3/h]
lambda_p=0,8
m_p:=((Vs_p/3600[s/h])*lambda_p/v_1p)
h_1p:=enthalpy(R290;T=T_1p;P=P_1p)
T_diffcond:=15,75[C]
T_3p:=T_amb+T_diffcond
x_3p:=0
P_3p:=P_sat(R290;T=T_3p)
h_3p:=Enthalpy(R290;T=T_3p;x=x_3p)
Q_evap:=m_p*(h_1p-h_3p)

```

```
x_4:=0
P_4:=P_sat(R744;T=T_4)
h_4:=Enthalpy(R744;T=T_4;x=x_4)
h_5:=h_4
```

```
T_diffgc:=5[C]
T_3:=T_amb+T_diffgc
P_3:=P_4
h_3:=Enthalpy(R744;T=T_3;P=P_3)
```

```
T_s:=10[C]
T_0:=-10[C]
T_1:=T_0+T_s
P_1:=P_sat(R744;T=T_0)
h_1:=enthalpy(R744;T=T_1;P=P_1)
v_1:=Volume(R744;T=T_1;P=P_1)
phi:=P_3/P_1
lambda_c:= 0,0181*phi^2 - 0,1746*phi + 1,1078
Vs_c:=3[m^3/h]
m_c:=((Vs_c/3600[s/h])*lambda_c/v_1)*1,18
Q_sub:=m_c*(h_3-h_4)
```

```
Repeat
If (Q_sub>0,999*Q_evap) and (Q_sub<1,001*Q_evap) Then
A:=value
B:=T_4
value:=10
T_4:=29
value:=10
else
value:=value-0,01[C]
endif
until(value=10)
```

```
Until(T_4=29)
```

```
T_0pcorr:=A
T_4corr:=B
```

```
x_4:=0
P_4:=P_sat(R744;T=T_4corr)
h_4:=Enthalpy(R744;T=T_4corr;x=x_4)
```

```
P_2:=P_4
s_1:=entropy(R744;T=T_1;P=P_1)
eta_c = -0,0832*(phi^2) + 0,3904*phi + 0,1247
Q_heatloss=0,10
h_2s:=Enthalpy(R744;s=s_1;P=P_2)
h_2:=h_1+((h_2s-h_1)/eta_c)*(1-Q_heatloss)
T_2:=Temperature(R744;h=h_2;P=P_2)
m_c:=((Vs_c/3600[s/h])*lambda_c/v_1)*1,18
```

```
T_3p:=T_amb+T_diffcond
x_3p:=0
```

```
P_3p:=P_sat(R290;T=T_3p)
h_3p:=Enthalpy(R290;T=T_3p;x=x_3p)
```

```
W:=(m_c*(h_2-h_1))/(1-Q_heatloss)
```

```
T_1p:=T_0pcorr+T_sp
P_1p:=P_sat(R290;T=T_0pcorr)
s_1p:=entropy(R290;T=T_1p;P=P_1p)
```

```
P_2p:=P_3p
h_2sp:=enthalpy(R290;s=s_1p;P=P_2p)
eta_p=0,7
h_2p:=h_1p+((h_2sp-h_1p)/eta_p)*(1-Q_heatloss)
T_2p:=temperature(R290;P=P_2p;h=h_2p)
m_p:=((Vs_p/3600[s/h])*lambda_p/v_1p)
W_p:=(m_p*(h_2p-h_1p))/(1-Q_heatloss)
```

```
Q_o:=m_c*(h_1-h_4)
COP:=Q_o/(W+W_p)
```

```
endif
```

```
end
```

```
"Test CO2 refrigeration system"
```

```
T_4=19,9[C]
T_amb=21,98[C]
ON=2
```

```
"Tells if the propane system is on/off"
```

```
CALL test(T_4;T_amb;ON;Q_o;COP;P_2;h_2;h_3;h_4;h_5;P_1p;P_2p;h_1p;h_2p;h_3p)
```

```
T_s=10[C]
T_0=-10[C]
T_1=T_0+T_s
Q_heatloss=0,10
P_1=P_sat(R744;T=T_0)
h_1=enthalpy(R744;T=T_1;P=P_1)
v_1=Volume(R744;T=T_1;P=P_1)
s_1=entropy(R744;T=T_1;P=P_1)
```

\$ARRAYS ON

"Prototype simulation model"

PROCEDURE test(T_amb;ON:Q_o;COP;P_2;h_2;h_3;h_4;h_5;P_1p;P_2p;h_1p;h_2p;h_3p;W)

```
P_2 := 0
h_2 := 0
h_3 := 0
h_4 := 0
h_5 := 0
P_2p := 0
P_1p := 0
h_2p := 0
h_1p := 0
h_3p := 0
```

If ON = 0 Then
operating"

"ON=0, means that the propane system is not

```
T_s := 10[C]
T_0 := -10[C]
T_1 := T_0 + T_s
Q_heatloss = 0,10
P_1 := P_sat(R744;T=T_0)
h_1 := enthalpy(R744;T=T_1;P=P_1)
v_1 := Volume(R744;T=T_1;P=P_1)
s_1 := entropy(R744;T=T_1;P=P_1)
c_p := 1,005 [kJ/kg*K]
A := 40,957[m^2]
```

if (T_amb >= 0[C]) Then

```
U := (-0,0391*T_amb^2 + 1,6544*T_amb + 33,985)/1000 "Correlation for U-value CO2 condenser"
else
U := 0,035 [kW/m^2*C]
endif
```

```
T_exitcorr := 0
T_3corr := 0
```

```
If (T_amb >= 0) Then
T_3 := T_amb + 3[C]
else
T_3 := 2,279[C]
endif
```

```
Repeat
T_3 := T_3 + 0,01[C]
temperatures"
```

"Iterates between different condensing

```
if (T_amb>=0) Then
T_exit:=T_amb+2[C]
else
T_exit:=0[C]
endif
```

```
If (T_3>18,27) and (T_3<21,98) Then
V_air:=0,4717*T_3-8,4233
else
```

```
if(T_3>=21,98) Then
V_air:=1,9444 [m^3/s]
else
V_air:=0,19444[m^3/s]
endif
```

```
endif
```

```
rho_air:=1,225 [kg/m^3]
m_air=rho_air*V_air
```

```
dp_air:= (3,6582*V_air^2 + 3,2504*V_air - 0,3654)/10^3 "[kPa]"
```

```
eta_fan:=0,5
W_fan:=(V_air*dp_air)/eta_fan
```

```
if (T_amb>=6[C]) Then
LMTD := 0,0448*T_3^2 - 2,4286*T_3 + 38,196
else
LMTD := -1,3677*T_3 + 35,041
```

```
endif
```

```
Q_LMTD:= U*A*LMTD
```

```
Q_air:=m_air*c_p*(T_exit-T_amb)
```

```
x_3:=0
P_3t:=P_sat(R744;T=T_3)
h_3:=enthalpy(R744;T=T_3;x=x_3)
```

```
phi:=P_3t/P_1
lambda_c:= 0,0181*phi^2 - 0,1746*phi + 1,1078
Vs_c:=3[m^3/h]
m_c:=((Vs_c/3600[s/h])*lambda_c/v_1)*1,18
```

```
h_2s:=Enthalpy(R744;s=s_1;P=P_3t)
```

```
eta_c = -0,0832*(phi^2) + 0,3904*phi + 0,1247
h_2dis:=h_1+((h_2s-h_1)/eta_c)
h_2:=h_1+((h_2s-h_1)/eta_c)*(1-Q_heatloss)
calculated with the heat loss from the compressor"
```

"Temperature at the inlet of the condenser is

T_2:=Temperature(R744;h=h_2;P=P_3t)

Q_cond:=m_c*(h_2-h_3)

Repeat

If (Q_LMTD>0,90*Q_air) and (Q_LMTD<1,1*Q_air) and (Q_air>0,99*Q_cond) and (Q_air<1,01*Q_cond) and (Q_LMTD>0,90*Q_cond) and (Q_LMTD<1,1*Q_cond) Then

T_exitcorr:=T_exit

T_3corr:=T_3

T_exit:=0,97*T_3

T_3:=30

else

if(T_exit>0,95*T_3) Then

T_exit:=0,97*T_3

else

T_exit:=T_exit+0,1[C]

endif

endif

if (T_amb>=6[C]) Then

LMTD := 0,0448*T_3^2 - 2,4286*T_3 + 38,196

else

LMTD := -1,3677*T_3 + 35,041

endif

Q_LMTD:= U*A*LMTD

Q_air:=m_air*c_p*(T_exit-T_amb)

Until(T_exit=0,97*T_3)

Until(T_3=30)

T_3corr:=18[C]

T_diffgc:=T_3corr-T_amb

if (T_amb>=6[C]) Then

LMTDcorr := 0,0448*T_3corr^2 - 2,4286*T_3corr + 38,196

else

LMTDcorr := -1,3677*T_3corr + 35,041

endif

Q_LMTDcorr:= U*A*LMTDcorr

Q_aircorr:=m_air*c_p*(T_exitcorr-T_amb)

x_3:=0

P_3:=P_sat(R744;T=T_3corr)

h_3:=enthalpy(R744;T=T_3corr;x=x_3)

P_2:=P_3

phi:=P_3/P_1

```
lambda_c := 0,0181*phi^2 - 0,1746*phi + 1,1078
Vs_c:=3[m^3/h]
m_c:=(Vs_c/3600[s/h])*lambda_c/v_1)*1,18
```

"Multiply with 1,18 for 60hz"

```
h_2s:=Enthalpy(R744;s=s_1;P=P_3)
eta_c = -0,0832*(phi^2) + 0,3904*phi + 0,1247
h_2dis:=h_1+((h_2s-h_1)/eta_c)
h_2:=h_1+((h_2s-h_1)/eta_c)*(1-Q_heatloss)
T_2:=Temperature(R744;h=h_2;P=P_3)
```

"Outlet enthalpy compressor"
"Inlet enthalpy condenser"

```
h_4:=h_3
```

```
h_5:=h_1
```

```
Q_condcorr:=m_c*(h_2-h_3)
```

```
Q_o:=m_c*(h_1-h_3)
W:=(m_c*(h_2dis-h_1))
COP:=Q_o/(W+W_fan)
```

```
endif
```

```
if ON=2 Then
```

"Propane unit is operating"

```
T_4 := 19,9[C]
```

```
V_air := 1,9444 [m^3/s]
rho_air:=1,225 [kg/m^3]
m_air=rho_air*V_air
c_p:=1,005 [kJ/kg*K]
x_3:=0
x_3p:= 0
Vs_p=9,7788[m^3/h]
lambda_p=0,8
eta_p=0,6
A_p:=21,1795
U_p := (-0,0004*T_amb^2 + 0,0322*T_amb + 67,814)/1000
```

```
Q_heatloss=0,10
```

```
T_s:=10[C]
T_0:=-10[C]
T_1:=T_0+T_s
P_1:=P_sat(R744;T=T_0)
h_1:=enthalpy(R744;T=T_1;P=P_1)
v_1:=Volume(R744;T=T_1;P=P_1)
s_1:=entropy(R744;T=T_1;P=P_1)
Vs_c:=3[m^3/h]
T_exitcorr:=0
T_3corr:=1
A:=40,9573[m^2]
```

dp_airp:=(-0,21*T_amb + 16,75)/10^3
eta_fan:=0,5
W_fanp:=(V_air*dp_airp)/eta_fan

dp_air := (0,0002*T_amb^2 - 0,040*T_amb + 20,447)/10^3
W_fan:=((V_air*dp_air)/eta_fan)+W_fanp

Repeat
temperatures"

"Iterates between different CO2 condensing

T_4:=T_4+0,1[C]
T_3p := T_amb+3[C]
T_op:=T_4-9,9[C]

Repeat
temperatures"

"Iterates between different propane evaporating

T_op := T_op - 0,1[C]

Repeat
T_opcorr:=-1
T_4corr:=-1
T_exitpcorr:=T_amb +2[C]
T_3pcorr:=-1

T_3p := T_3p + 0,01[C]
T_exitp := T_amb + 2 [C]

LMTD_p:= -0,0004*T_3p^2 + 0,0596*T_3p + 5,4147
Q_LMTDP := LMTD_p * A_p *U_p

T_sp:=7[C]
T_1p:=T_op+T_sp
P_1p:=P_sat(R290;T=T_op)
v_1p:=volume(R290;T=T_1p;P=P_1p)
m_p:=((Vs_p/3600[s/h])*lambda_p/v_1p)
s_1p:=entropy(R290;T=T_1p;P=P_1p)

P_2p := P_sat(R290;T=T_3p)
h_3p := enthalpy(R290;T=T_3p;x=x_3p)

h_1p:=enthalpy(R290;T=T_1p;P=P_1p)
h_4p := h_3p
h_2sp:=enthalpy(R290;s=s_1p;P=P_2p)

```
h_2p:=h_1p+((h_2sp-h_1p)/eta_p)*(1-Q_heatloss)
h_2pdis:=h_1p+((h_2sp-h_1p)/eta_p)
T_2p=temperature(R290;P=P_2p;h=h_2p)
W_p:=(m_p*(h_2pdis-h_1p))
P_3p := P_2p
```

```
Q_airp:=m_air*c_p*(T_exitp-T_amb)
Q_condp := m_p*(h_2p - h_3p)
```

Repeat

```
If (Q_LMTDP>0,9*Q_airp) and (Q_LMTDP<1,1*Q_airp) and (Q_airp>0,99*Q_condp) and
(Q_airp<1,01*Q_condp) and (Q_LMTDP>0,9*Q_condp) and (Q_LMTDP<1,1*Q_condp) Then
```

```
    T_exitpcorr:=T_exitp
    T_3pcorr:=T_3p
    T_exitp:=0,95*T_3p
    T_3p:=60
```

else

```
if(T_exitp>0,94*T_3p) Then
```

```
    T_exitp:=0,95*T_3p
```

else

```
    T_exitp:=T_exitp+0,1[C]
```

```
endif
```

endif

```
LMTD_p:= -0,0004*T_3p^2 + 0,0596*T_3p + 5,4147
```

```
Q_LMTDP := LMTD_p * A_p *U_p
```

```
Q_airp:=m_air*c_p*(T_exitp-T_amb)
```

```
Until(T_exitp=0,95*T_3p)
```

```
Until(T_3p=60)
```

```
P_3p:=P_sat(R290;T=T_3pcorr)
```

```
with the corrected values for T_exit and T_3
```

```
h_3p:=enthalpy(R290;T=T_3pcorr;x=x_3)
```

"Need to redefine the state values for propane

```
P_2p := P_sat(R290;T=T_3pcorr)
```

```
h_4p := h_3p
```

```
h_2sp:=enthalpy(R290;s=s_1p;P=P_2p)
```

```
h_2p:=h_1p+((h_2sp-h_1p)/eta_p)*(1-Q_heatloss)
```

```
h_2pdis:=h_1p+((h_2sp-h_1p)/eta_p)
```

```
T_2p=temperature(R290;P=P_2p;h=h_2p)
```

```
W_p:=(m_p*(h_2pdis-h_1p))
```

```
T_3p :=T_3pcorr
```

```
Q_airpcorr:=m_air*c_p*(T_exitpcorr-T_amb)
```

```
Q_condpcorr:=m_p*(h_2p-h_3p)
Q_evap:=m_p*(h_1p-h_3p)
```

```
LMTD_pcorr:=-0,0004*T_3pcorr^2 + 0,0596*T_3pcorr + 5,4147
Q_LMTDPCorr := LMTD_p * A_p * U_p
```

```
T_3:=T_exitpcorr + 1,5[C]           "Set an initial guess of the CO2 temperature
leaving the gas cooler"
```

```
Repeat                               "Iterated between different CO2 gas cooler exit
temperatures"
```

```
T_3:=T_3+0,1[C]
T_exit:=T_exitpcorr + 1[C]
```

```
x_4:=0
P_4:=P_sat(R744;T=T_4)
P_3:=P_4
```

```
If (T_3<=T_4) Then
T_3=T_4+0,5 [C]
endif
```

```
h_3:=enthalpy(R744;T=T_3;P=P_3)
```

```
phi:=P_3/P_1
lambda_c := 0,0181*phi^2 - 0,1746*phi + 1,1078
m_c:=(Vs_c/3600[s/h])*lambda_c/v_1*1,18
```

```
h_2s:=Enthalpy(R744;s=s_1;P=P_3)
eta_c = -0,0832*(phi^2) + 0,3904*phi + 0,1247
h_2:=h_1+((h_2s-h_1)/eta_c)*(1-Q_heatloss)
h_2dis:=h_1+((h_2s-h_1)/eta_c)
T_2:=Temperature(R744;h=h_2;P=P_3)
```

```
Q_air:=m_air*c_p*(T_exit-T_exitpcorr)
Q_cond:=m_c*(h_2-h_3)
```

```
Repeat
If (Q_air>0,99*Q_cond) and (Q_air<1,01*Q_cond) Then
    T_exitcorr:=T_exit
    T_3corr:=T_3
    T_exit:=0,95*T_3
    T_3:=60
else
```

```
if(T_exit>0,94*T_3) Then
T_exit:=0,95*T_3
else
T_exit:=T_exit+0,1[C]
endif
endif
```

```
Q_air:=m_air*c_p*(T_exit-T_exitpcorr)
```

Until(T_exit=0,95*T_3)

Until(T_3=60)

T_diffgc:=T_3corr-T_exitpcorr
the corrected values for T_exit and T_3"

"Need to redefine the state values for CO2 with

Q_aircorr:=m_air*c_p*(T_exitcorr-T_exitpcorr)

P_4:=P_sat(R744;T=T_4)

P_3 := P_4

P_2 :=P_3

phi:=P_3/P_1

lambda_c := 0,0181*phi^2 - 0,1746*phi + 1,1078

m_c:=((Vs_c/3600[s/h])*lambda_c/v_1)*1,18

h_4 := enthalpy(R744;T=T_4;x=x_4)

s_1:=entropy(R744;T=T_1;P=P_1)

eta_c = -0,0832*(phi^2) + 0,3904*phi + 0,1247

h_2s:=Enthalpy(R744;s=s_1;P=P_2)

h_2:=h_1+((h_2s-h_1)/eta_c)*(1-Q_heatloss)

h_2dis:=h_1+((h_2s-h_1)/eta_c)

T_2:=Temperature(R744;h=h_2;P=P_2)

h_3 := Enthalpy(R744;T=T_3corr;P=P_2)

Q_condcorr:=m_c*(h_2-h_3)

Q_sub:=m_c*(h_3-h_4)

If (Q_sub>0,95*Q_evap) and (Q_sub<1,05*Q_evap) Then

T_opcorr = T_op

T_4corr:=T_4

T_4:=29

T_op :=10

endif

Until (T_op =10)

until (T_4 = 29)

T_op := T_opcorr

x_4:=0

P_4:=P_sat(R744;T=T_4corr)

h_4:=Enthalpy(R744;T=T_4corr;x=x_4)

h_5:=h_4

P_2:=P_4

s_1=entropy(R744;T=T_1;P=P_1)

```
eta_c = -0,0832*(phi^2) + 0,3904*phi + 0,1247
lambda_c := 0,0181*phi^2 - 0,1746*phi + 1,1078
h_2s:=Enthalpy(R744;s=s_1;P=P_2)
h_2:=h_1+((h_2s-h_1)/eta_c)*(1-Q_heatloss)
h_2dis:=h_1+((h_2s-h_1)/eta_c)
T_2:=Temperature(R744;h=h_2;P=P_2)
m_c:=((Vs_c/3600[s/h])*lambda_c/v_1)*1,18
```

```
W:=(m_c*(h_2dis-h_1))
```

```
T_1p:=T_op+T_sp
P_1p:=P_sat(R290;T=T_op)
s_1p:=entropy(R290;T=T_1p;P=P_1p)
```

```
h_2sp:=enthalpy(R290;s=s_1p;P=P_2p)
h_2p:=h_1p+((h_2sp-h_1p)/eta_p)*(1-Q_heatloss)
h_2pdis:=h_1p+((h_2sp-h_1p)/eta_p)
T_2p=temperature(R290;P=P_2p;h=h_2p)
m_p:=((Vs_p/3600[s/h])*lambda_p/v_1p)
W_p:=(m_p*(h_2pdis-h_1p))
```

```
Q_o:=m_c*(h_1-h_5)
W_total := W + W_p + W_fan
COP:=Q_o/(W_total)
```

```
endif
```

```
end
```

```
"Test CO2 refrigeration system"
```

```
T_amb=35[C]
```

```
ON=2
```

```
"Tells if the propane system is on/off"
```

```
CALL test(T_amb;ON;Q_o;COP;P_2;h_2;h_3;h_4;h_5;P_1p;P_2p;h_1p;h_2p;h_3p;W)
```

```
T_s=10[C]
T_0=-10[C]
T_1=T_0+T_s
P_1=P_sat(R744;T=T_0)
h_1=enthalpy(R744;T=T_1;P=P_1)
v_1=Volume(R744;T=T_1;P=P_1)
s_1=entropy(R744;T=T_1;P=P_1)
```

```
"ARRAY table"
```

```
P[1]=P_1
P[2]=P_2
P[3]=P_2
P[4]=P_2
P[5]=P_1
```

$P[6]=P_1$

$h[1]=h_1$

$h[2]=h_2$

$h[3]=h_3$

$h[4]=h_4$

$h[5]=h_5$

$h[6]=h_1$

$P_p[1]=P_1p$

$P_p[2]=P_2p$

$P_p[3]=P_2p$

$P_p[4]=P_1p$

$P_p[5]=P_1p$

$h_p[1]=h_1p$

$h_p[2]=h_2p$

$h_p[3]=h_3p$

$h_p[4]=h_3p$

$h_p[5]=h_1p$

\$ARRAYs ON

"Simple transcritical operation"

PROCEDURE trans2(T_amb :Q_o;COP;P_1;P_2;h_1;h_2;h_3)

P_1p:=0
P_2p:=0
Q_o:=-1
COP:=-1
P_2t:=0

T_diffgc=5[C]
T_3=T_amb+T_diffgc

If(T_amb>18,85) Then
operate transcritical above this limit"

"Design point for system, T_3=25C. System will

DUPLICATE P_2t = 75;135
optimum pressure is set in the loop, P_2 is the same as the temporary value"

"P_2t is the temporary value of P_2. When the

P_3t = P_2t

h_3t=enthalpy(R744; T=T_3;P=P_3t)

T_0=-10[C]
T_s=10[C]
T_1=T_0+T_s

Q_heatloss=0,1
V_air:=1,9444 [m^3/s] "Maximum volume flow air"
dp_air:= (3,6582*V_air^2 + 3,2504*V_air - 0,3654)/10^3 [kPa]
eta_fan:=0,5
W_fan:=(V_air*dp_air)/eta_fan

Vs_c=3[m^3/h]
T_1=T_0+T_s
P_1t=P_sat(R744;T=T_0)
h_1t=enthalpy(R744;T=T_1;P=P_1t)
v_1=Volume(R744;T=T_1;P=P_1t)
s_1=entropy(R744;T=T_1;P=P_1t)

phi=P_2t/P_1t
lambda_c := 0,0207*phi^2 -0,2163*phi + 1,2054
eta_c = 0,0076*(phi^2) -0,0438*phi + 0,6542

h_2st=Enthalpy(R744;s=s_1;P=P_2t)
h_2t=h_1t+((h_2st-h_1t)/eta_c)*(1-Q_heatloss)
h_2dist=h_1t+((h_2st-h_1t)/eta_c)

```
T_2=Temperature(R744;h=h_2t;P=P_2t)
m_c=((Vs_c/3600[s/h])*lambda_c/v_1)*1,18
Wt=(m_c*(h_2dist-h_1t))
```

```
Q_ot=m_c*(h_1t-h_3t)
COPmat[P_2t]=Q_ot/(Wt+W_fan)
```

```
if COPmat[P_2t] > COP Then
finding the maximum COP"
```

"Loop that determine the optimal pressure, by

```
COP = COPmat[P_2t]
```

```
P_1 = P_1t
P_2 = P_2t
h_1 = h_1t
h_2 = h_2t
h_2dis= h_2dist
h_3 = h_3t
W=Wt
Q_o=Q_ot
```

```
endif
```

```
end
```

```
else
```

"Subcritical operation"

```
T_s:=10[C]
T_0:=-10[C]
T_1:=T_0+T_s
Q_heatloss=0,10
P_1:=P_sat(R744;T=T_0)
h_1:=enthalpy(R744;T=T_1;P=P_1)
v_1:=Volume(R744;T=T_1;P=P_1)
s_1:=entropy(R744;T=T_1;P=P_1)
c_p:=1,005 [kJ/kg*K]
A:=40,957[m^2]
```

```
if (T_amb>=0[C]) Then
```

```
U:= (-0,0391*T_amb^2 + 1,6544*T_amb + 33,985)/1000
```

```
else
```

```
U:=0,035 [kW/m^2*C]
```

```
endif
```

```
T_exitcorr:=0
```

```
T_3corr:=0
```

```
If (T_amb>=0) Then
```

```
T_3:=T_amb+3[C]
```

```

else
T_3:=2,279[C]
endif

Repeat
T_3:=T_3+0,01[C]

if (T_amb>=0) Then
T_exit:=T_amb+2[C]
else
T_exit:=0[C]
endif

If (T_3>18,27) and (T_3<21,98) Then
V_air:=0,4717*T_3-8,4233
else

if(T_3>=21,98) Then
V_air:=1,9444 [m^3/s]
else
V_air:=0,19444[m^3/s]
endif

endif

rho_air:=1,225 [kg/m^3]
m_air=rho_air*V_air

dp_air:= (3,6582*V_air^2 + 3,2504*V_air - 0,3654)/10^3 "[kPa]"

eta_fan:=0,5
W_fan:=(V_air*dp_air)/eta_fan

if (T_amb>=6[C]) Then
LMTD := 0,0448*T_3^2 - 2,4286*T_3 + 38,196
else
LMTD := -1,3677*T_3 + 35,041
endif

Q_LMTD:= U*A*LMTD

Q_air:=m_air*c_p*(T_exit-T_amb)

x_3:=0
P_3t:=P_sat(R744;T=T_3)
h_3:=enthalpy(R744;T=T_3;x=x_3)

phi:=P_3t/P_1
lambda_c:= 0,0181*phi^2 - 0,1746*phi + 1,1078
Vs_c:=3[m^3/h]
m_c:=((Vs_c/3600[s/h])*lambda_c/v_1)*1,18

```

$h_{2s} := \text{Enthalpy}(\text{R744}; s = s_1; P = P_{3t})$

$\eta_{c} = -0,0832 * (\phi^2) + 0,3904 * \phi + 0,1247$

$h_{2dis} := h_1 + ((h_{2s} - h_1) / \eta_c)$

$h_2 := h_1 + ((h_{2s} - h_1) / \eta_c) * (1 - Q_{\text{heatloss}})$
calculated with the heat loss from the compressor"

"Temperature at the inlet of the condenser is

$T_2 := \text{Temperature}(\text{R744}; h = h_2; P = P_{3t})$

$Q_{\text{cond}} := m_c * (h_2 - h_3)$

Repeat

"Energy balance condenser"

If $(Q_{\text{LMTD}} > 0,90 * Q_{\text{air}})$ and $(Q_{\text{LMTD}} < 1,1 * Q_{\text{air}})$ and $(Q_{\text{air}} > 0,99 * Q_{\text{cond}})$ and $(Q_{\text{air}} < 1,01 * Q_{\text{cond}})$ and $(Q_{\text{LMTD}} > 0,90 * Q_{\text{cond}})$ and $(Q_{\text{LMTD}} < 1,1 * Q_{\text{cond}})$ Then

$T_{\text{exitcorr}} := T_{\text{exit}}$

$T_{3\text{corr}} := T_3$

$T_{\text{exit}} := 0,97 * T_3$

$T_3 := 30$

else

if $(T_{\text{exit}} > 0,95 * T_3)$ Then

$T_{\text{exit}} := 0,97 * T_3$

else

$T_{\text{exit}} := T_{\text{exit}} + 0,1[\text{C}]$

endif

endif

if $(T_{\text{amb}} \geq 6[\text{C}])$ Then

$\text{LMTD} := 0,0448 * T_3^2 - 2,4286 * T_3 + 38,196$

else

$\text{LMTD} := -1,3677 * T_3 + 35,041$

endif

$Q_{\text{LMTD}} := U * A * \text{LMTD}$

$Q_{\text{air}} := m_{\text{air}} * c_p * (T_{\text{exit}} - T_{\text{amb}})$

Until $(T_{\text{exit}} = 0,97 * T_3)$

Until $(T_3 = 30)$

$T_{\text{diffgc}} := T_{3\text{corr}} - T_{\text{amb}}$

if $(T_{\text{amb}} \geq 6[\text{C}])$ Then

$\text{LMTDcorr} := 0,0448 * T_{3\text{corr}}^2 - 2,4286 * T_{3\text{corr}} + 38,196$

else

$\text{LMTDcorr} := -1,3677 * T_{3\text{corr}} + 35,041$

endif

$Q_{\text{LMTDcorr}} := U * A * \text{LMTDcorr}$

$Q_{\text{aircorr}} := m_{\text{air}} * c_p * (T_{\text{exitcorr}} - T_{\text{amb}})$

$x_3 := 0$

$P_3 := P_{\text{sat}}(\text{R744}; T = T_{3\text{corr}})$

h_3:=enthalpy(R744;T=T_3corr;x=x_3)
P_2:=P_3

phi:=P_3/P_1
lambda_c := 0,0181*phi^2 - 0,1746*phi + 1,1078
Vs_c:=3[m^3/h]
m_c:=((Vs_c/3600[s/h])*lambda_c/v_1)*1,18

"Multiply with 1,18 for 60hz"

h_2s:=Enthalpy(R744;s=s_1;P=P_3)
eta_c = -0,0832*(phi^2) + 0,3904*phi + 0,1247
h_2dis:=h_1+((h_2s-h_1)/eta_c)
h_2:=h_1+((h_2s-h_1)/eta_c)*(1-Q_heatloss)
T_2:=Temperature(R744;h=h_2;P=P_3)

"Outlet enthalpy compressor"
"Inlet enthalpy condenser"

h_4:=h_3
h_5:=h_1

Q_condcorr:=m_c*(h_2-h_3)

Q_o:=m_c*(h_1-h_3)
W:=(m_c*(h_2dis-h_1))
COP:=Q_o/(W+W_fan)

endif

end

"Test CO2 refrigeration system"

T_amb =35 [C]

Call trans2(T_amb :Q_o;COP;P_1;P_2;h_1;h_2;h_3)

P[1]=P_1
P[2]=P_2
P[3]=P_2
P[4]=P_1
P[5]=P_1

h[1]=h_1
h[2]=h_2
h[3]=h_3
h[4]=h_3
h[5]=h_1

\$ARRAYs ON

"Transcritical system with internal heat exchanger"

PROCEDURE trans2(T_amb :Q_o;COP;P_1;P_3;h_1;h_2;h_3;h_4;h_5)

Q_o:=-1
COP:=-1
P_3t:=0

T_diffgc=5[C]
T_4t=T_amb+T_diffgc

If(T_amb>18,5) Then
operate transcritical above this limit"

"Design point for system, T_4=25C. System will

DUPLICATE P_3t = 75;135
optimum pressure is set in the loop, P_3 is the same as the temporary value"

"P_3t is the temporary value of P_3. When the

T_0=-
10[C]

Q_heatloss=0,1
V_air=1,9444 [m^3/s]
dp_air=(3,6582*V_air^2 + 3,2504*V_air - 0,3654)/10^3 [kPa]
eta_fan=0,5
W_fan=(V_air*dp_air)/eta_fan

"Maximum volume flow air"

Vs_c=3[m^3/h]
P_1t=P_sat(R744;T=T_0)
h_1t=enthalpy(R744;P=P_1t;x=1)
v_1t=Volume(R744;P=P_1t;x=1)
s_1t=entropy(R744;P=P_1t;x=1)

h_4design=enthalpy(R744;T=25;x=0)
dh_design=(h_1t-h_4design)

"Specific refrigeration capacity at design point"

dh_slhe=0,05*dh_design
exchanger is 5% of the specific refrigeration capacity"
h_2t=h_1t+dh_slhe
T_2t=temperature(R744;h=h_2t;P=P_1t)
s_2t=entropy(R744;T=T_2t;P=P_1t)

"Enthalpy difference in suction line heat

phi=P_3t/P_1t
lambda_c := 0,0207*phi^2 -0,2163*phi + 1,2054
eta_c = 0,0076*(phi^2) -0,0438*phi + 0,6542

h_3st=Enthalpy(R744;s=s_2t;P=P_3t)
h_3t=h_2t+((h_3st-h_2t)/eta_c)*(1-Q_heatloss)
h_3dist=h_2t+((h_3st-h_2t)/eta_c)
T_3t=Temperature(R744;h=h_3t;P=P_3t)
m_c=((Vs_c/3600[s/h])*lambda_c/v_1t)*1,18

```
W_t=(m_c*(h_3dist-h_2t))
```

```
h_4t=enthalpy(R744;T=T_4t;P=P_3t)
```

"enthalpy after gas cooler"

```
h_5t= h_4t-  
dh_slhe
```

```
T_5t=temperature(R744;P=P_3t;h=h_5t)  
exchanger"
```

"CO2 temperature after suction line heat exchanger"

```
Q_ot:=m_c*(h_1t-h_5t)
```

```
COPmat[P_3t] =Q_ot/(W_t+W_fan)
```

```
if COPmat[P_3t] > COP Then  
maximum COP"
```

"Loop that find the Optimal pressure by finding the maximum COP"

```
COP = COPmat[P_3t]
```

```
P_1 = P_1t  
P_3:= P_3t  
h_1 = h_1t  
h_2 = h_2t  
h_3 = h_3t  
h_3dis=h_3dist  
h_4 =h_4t  
h_5 =h_5t  
W=W_t  
Q_o=Q_ot  
T_5=T_5t  
T_2=T_2t  
endif
```

```
end
```

```
else
```

"Subcritical operation, only CO2 in operation"

```
T_0:=-10[C]  
Q_heatloss=0,10  
P_1:=P_sat(R744;T=T_0)  
h_1:=enthalpy(R744;P=P_1;x=1)  
v_1:=Volume(R744;P=P_1;x=1)  
c_p:=1,005 [kJ/kg*K]  
A:=40,957[m^2]
```

```
if (T_amb>=0[C]) Then
```

```
U:= (-0,0391*T_amb^2 + 1,6544*T_amb + 33,985)/1000
```

```
else
```

```
U:=0,035 [kW/m^2*C]
```

```
endif
```

T_exitcorr:=0
T_4corr:=0

If (T_amb>=0) Then
T_4=T_amb+3[C]
else
T_4:=2,279[C]
endif

Repeat
T_4=T_4+0,01[C]

if (T_amb>=0) Then
T_exit:=T_amb+2[C]
else
T_exit:=0[C]
endif

If (T_4>18,27) and (T_4<21,98) Then
V_air:=0,4717*T_4-8,4233
else

if(T_4>=21,98) Then
V_air:=1,9444 [m^3/s]
else
V_air:=0,19444[m^3/s]
endif

endif

rho_air:=1,225 [kg/m^3]
m_air=rho_air*V_air

dp_air:= (3,6582*V_air^2 + 3,2504*V_air - 0,3654)/10^3 "[kPa]"

eta_fan:=0,5
W_fan:=(V_air*dp_air)/eta_fan

if (T_amb>=6[C]) Then
LMTD := 0,0448*T_4^2 - 2,4286*T_4 + 38,196
else
LMTD := -1,3677*T_4 + 35,041

endif

Q_LMTD:= U*A*LMTD

Q_air:=m_air*c_p*(T_exit-T_amb)

x_4:=0
P_4t:=P_sat(R744;T=T_4)
h_4:=enthalpy(R744;T=T_4;x=x_4)


```

phi:=P_4t/P_1
lambda_c:= 0,0181*phi^2 - 0,1746*phi + 1,1078
Vs_c:=3[m^3/h]
m_c:=(Vs_c/3600[s/h])*lambda_c/v_1)*1,18

```

```

h_3design=enthalpy(R744;T=25;x=0)
dh_design=(h_1-h_3design)

```

"Specific refrigeration capacity at design point"

```

dh_slhe=0,05*dh_design
exchanger is 5% of the specific refrigeration capacity"

```

"Enthalpy difference in suction line heat

```

h_2=h_1+dh_slhe
T_2=temperature(R744;h=h_2;P=P_1)
s_2=entropy(R744;T=T_2;P=P_1)

```

```

h_3s:=Enthalpy(R744;s=s_2;P=P_4t)

```

```

eta_c = -0,0832*(phi^2) + 0,3904*phi + 0,1247
h_3dis:=h_2+((h_3s-h_2)/eta_c)
h_3:=h_2+((h_3s-h_2)/eta_c)*(1-Q_heatloss)
T_3:=Temperature(R744;h=h_3;P=P_4t)

```

"Temperature at the inlet of the condenser is calculated with the heat loss from the compressor"

```

h_4=enthalpy(R744;T=T_4;x=0)
Q_cond:=m_c*(h_3-h_4)

```

```

h_5=h_4-dh_slhe
T_5=temperature(R744;P=P_4t;h=h_5)

```

Repeat

```

if (Q_LMTD>0,90*Q_air) and (Q_LMTD<1,1*Q_air) and (Q_air>0,99*Q_cond) and (Q_air<1,01*Q_cond)
and (Q_LMTD>0,90*Q_cond) and (Q_LMTD<1,1*Q_cond) Then

```

```

    T_exitcorr:=T_exit
    T_4corr:=T_4
    T_exit:=0,97*T_4
    T_4:=30

```

else

```

if(T_exit>0,95*T_4) Then

```

```

    T_exit:=0,97*T_4

```

else

```

    T_exit:=T_exit+0,1[C]

```

endif

endif

```

if (T_amb>=6[C]) Then

```

```

    LMTD := 0,0448*T_4^2 - 2,4286*T_4 + 38,196

```

else

```

    LMTD := -1,3677*T_4 + 35,041

```

endif

```

Q_LMTD:= U*A*LMTD

```

```

Q_air:=m_air*c_p*(T_exit-T_amb)

```

Until(T_exit=0,97*T_4)

Until(T_4=30)

T_diffgc:=T_4corr-T_amb

if (T_amb>=6[C]) Then

LMTDcorr := 0,0448*T_4corr^2 - 2,4286*T_4corr + 38,196

else

LMTDcorr := -1,3677*T_4corr + 35,041

endif

Q_LMTDcorr:= U*A*LMTDcorr

Q_aircorr:=m_air*c_p*(T_exitcorr-T_amb)

x_4:=0

P_4:=P_sat(R744;T=T_4corr)

h_4:=enthalpy(R744;T=T_4corr;x=x_4)

P_3=P_4

phi:=P_4/P_1

lambda_c := 0,0181*phi^2 - 0,1746*phi + 1,1078

Vs_c:=3[m^3/h]

m_c:=(Vs_c/3600[s/h])*lambda_c/v_1*1,18

"Multiply with 1,18 for 60hz"

h_4design=enthalpy(R744;T=25;x=0)

dh_design=(h_1-h_4design)

"Specific refrigeration capacity at design point"

dh_slhe=0,05*dh_design

exchanger is 5% of the specific refrigeration capacity"

"Enthalpy difference in suction line heat

h_2=h_1+dh_slhe

T_2=temperature(R744;h=h_2;P=P_1)

s_2=entropy(R744;T=T_2;P=P_1)

h_3s:=Enthalpy(R744;s=s_2;P=P_4)

eta_c = -0,0832*(phi^2) + 0,3904*phi + 0,1247

h_3dis:=h_2+((h_3s-h_2)/eta_c)

h_3:=h_2+((h_3s-h_2)/eta_c)*(1-Q_heatloss)
calculated with the heat loss from the compressor"

"Temperature at the inlet of the condenser is

T_3:=Temperature(R744;h=h_3;P=P_4)

h_4=enthalpy(R744;T=T_4corr;x=0)

Q_cond:=m_c*(h_3-h_4)

h_5=h_4-dh_slhe

T_5=temperature(R744;P=P_4;h=h_5)

Q_condcorr:=m_c*(h_3-h_4)

"Corrected heat of condensation"

Q_o:=m_c*(h_1-h_5)

```
W:=(m_c*(h_3dis-h_2))  
COP:=Q_o/(W+W_fan)
```

```
endif
```

```
end
```

```
"Test CO2 refrigeration system"
```

```
T_amb = 35[C]
```

```
Call trans2(T_amb :Q_o;COP;P_1;P_3;h_1;h_2;h_3;h_4;h_5)
```

```
P[1]=P_1  
P[2]=P_1  
P[3]=P_3  
P[4]=P_3  
P[5]=P_3  
P[6]=P_1  
P[7]=P_1
```

```
h[1]=h_1  
h[2]=h_2  
h[3]=h_3  
h[4]=h_4  
h[5]=h_5  
h[6]=h_5  
h[7]=h_1
```

\$ARRAYs ON

"Mechanical subcooling system"

PROCEDURE modification3(T_amb
:Q_o;COP;P_1p;P_2p;h_1p;h_2p;h_3p;P_1;P_2;h_1;h_2;h_3;h_4;dT_sub)

Q_o=0
COP=0

P_1p=0
P_2p=0
h_1p=0
h_2p=0
h_3p=0
P_1=0
P_2=0
h_1=0
h_2=0
h_3=0
h_4=0
T_1p=0
T_4=0
dT_sub=0

P_1pt=3,9 [bar]

T_diffgc=5[C]
T_3=T_amb+T_diffgc

If(T_amb>18,85) Then "Design point for system, T_cond=25C. System
will operate transcritical above this limit, with a minimum refrigeration capacity equal to design
point"

Repeat
P_1pt:=P_1pt+0,1[bar]

"DUPLICATE P_1pt = 3;8 " "P_1pt is the temporary value of P_1p. When the
optimum pressure is set in the loop, P_1p is the same as the temporary value"

DUPLICATE P_2t = 75;135

P_3t = P_2t
P_4t = P_2t

T_0=-10[C]
T_s=10[C]

Q_heatloss=0,1
V_air:=1,9444
[m^3/s]

"Maximum volume flow air"

dp_air:=(3,6582*V_air^2 + 3,2504*V_air - 0,3654)/10^3 "[kPa]"
eta_fan:=0,5

$$W_{fan} := (V_{air} * dp_{air}) / \eta_{fan}$$

$$V_{s_c} = 3 [m^3/h]$$

$$T_{1t} = T_{0t} + T_{st}$$

$$P_{1t} = P_{sat}(R744; T = T_{0t})$$

$$h_{1t} = \text{enthalpy}(R744; T = T_{1t}; P = P_{1t})$$

$$v_{1t} = \text{Volume}(R744; T = T_{1t}; P = P_{1t})$$

$$s_{1t} = \text{entropy}(R744; T = T_{1t}; P = P_{1t})$$

$$\phi = P_{2t} / P_{1t}$$

$$\lambda_c := 0,0207 * \phi^2 - 0,2163 * \phi + 1,2054$$

$$\eta_c = 0,0076 * (\phi^2) - 0,0438 * \phi + 0,6542$$

$$h_{2st} = \text{Enthalpy}(R744; s = s_{1t}; P = P_{2t})$$

$$h_{2t} = h_{1t} + ((h_{2st} - h_{1t}) / \eta_c) * (1 - Q_{heatloss})$$

$$h_{2dist} = h_{1t} + ((h_{2st} - h_{1t}) / \eta_c)$$

$$T_{2t} = \text{Temperature}(R744; h = h_{2t}; P = P_{2t})$$

$$m_{ct} = ((V_{s_c} / 3600 [s/h]) * \lambda_c / v_{1t}) * 1,18$$

$$W_{t} = (m_{ct} * (h_{2dist} - h_{1t}))$$

$$h_{3t} = \text{enthalpy}(R744; T = T_{3t}; P = P_{3t})$$

$$Q_{odesign} = 8,812 [kW]$$

$$h_{3design} = h_{1t} - (Q_{odesign} / m_{ct})$$

$$T_{opt} := T_{sat}(R290; P = P_{1pt})$$

$$T_{sp} := 7 [C]$$

$$v_{1p} := \text{volume}(R290; P = P_{1pt}; x = 1)$$

$$V_{s_p} = 6 [m^3/h]$$

$$\lambda_p = 0,60$$

$$m_p := ((V_{s_p} / 3600 [s/h]) * \lambda_p / v_{1p})$$

$$h_{1pt} := \text{enthalpy}(R290; P = P_{1pt}; x = 1)$$

$$T_{diffcond} := 15 [C]$$

$$T_{3p} := T_{amb} + T_{diffcond}$$

$$x_{3p} = 0$$

$$P_{3pt} := P_{sat}(R290; T = T_{3p})$$

$$h_{3pt} := \text{Enthalpy}(R290; T = T_{3p}; x = x_{3p})$$

$$Q_{evap} := m_p * (h_{1pt} - h_{3pt})$$

$$s_{1p} := \text{entropy}(R290; P = P_{1pt}; x = 1)$$

$$Q_{evap} = m_p * (h_{1pt} - h_{3pt})$$

$$P_{2pt} := P_{3pt}$$

$$h_{2sp} := \text{enthalpy}(R290; s = s_{1p}; P = P_{2pt})$$

$$\eta_p = 0,6$$

$$h_{2pt} := h_{1pt} + ((h_{2sp} - h_{1pt}) / \eta_p) * (1 - Q_{heatloss})$$

$$h_{2pdis} := h_{1pt} + ((h_{2sp} - h_{1pt}) / \eta_p)$$

$$W_p := m_p * (h_{2pdis} - h_{1pt})$$

$$h_{4t} = h_{3t} - (Q_{evap} / m_{ct})$$

$$T_{4t} = \text{temperature}(R744; P = P_{2t}; h = h_{4t})$$

$$Q_{gc} = m_{ct} * (h_{2t} - h_{3t})$$

$Q_{ot} = m_{ct} \cdot (h_{1t} - h_{4t})$

$dT_{subt} = T_{4t} - T_{opt}$
subcooler"

"Temperature difference R290 and R744 in

$COP_{mat}[P_{1pt}; P_{2t}] = Q_{ot} / (W_t + W_p + W_{fan})$

if ($dT_{subt} < 5$) Then
subcooler is set to 5K"
 $COP_{mat}[P_{1pt}; P_{2t}] = 0$
endif

"Minimum value temperature difference in

if $COP_{mat}[P_{1pt}; P_{2t}] > COP$ Then
evaporating pressure for R290"

"Find the optimal high side pressure for CO2 and

$COP = COP_{mat}[P_{1pt}; P_{2t}]$

$T_{op} = T_{opt}$
 $T_{4t} = T_{4t}$
 $P_{1p} = P_{1pt}$
 $P_{2p} = P_{2pt}$
 $h_{1p} = h_{1pt}$
 $h_{2p} = h_{2pt}$
 $h_{3p} = h_{3pt}$
 $P_{1t} = P_{1t}$
 $P_{2t} = P_{2t}$
 $h_{1t} = h_{1t}$
 $h_{2t} = h_{2t}$
 $h_{3t} = h_{3t}$
 $h_{4t} = h_{4t}$
 $Q_o = Q_{ot}$
 $W = W_t$
 $m_c = m_{ct}$
 $dT_{sub} = dT_{subt}$
endif

end
Until ($P_{1pt} = 8$)

else

"Subcritical operation"

$T_s = 10[C]$
 $T_0 = -10[C]$
 $T_1 = T_0 + T_s$
 $Q_{heatloss} = 0,10$
 $P_1 = P_{sat}(R744; T=T_0)$
 $h_1 = \text{enthalpy}(R744; T=T_1; P=P_1)$
 $v_1 = \text{Volume}(R744; T=T_1; P=P_1)$
 $s_1 = \text{entropy}(R744; T=T_1; P=P_1)$
 $c_p = 1,005 [kJ/kg \cdot K]$
 $A = 40,957 [m^2]$

if ($T_{amb} >= 0[C]$) Then

```
U:= (-0,0391*T_amb^2 + 1,6544*T_amb + 33,985)/1000
else
U:=0,035 [kW/m^2*C]
endif
```

```
T_exitcorr:=0
T_3corr:=0
```

```
If (T_amb>=0) Then
T_3:=T_amb+3[C]
else
T_3:=2,279[C]
endif
```

```
Repeat
T_3:=T_3+0,01[C]
```

```
if (T_amb>=0) Then
T_exit:=T_amb+2[C]
else
T_exit:=0[C]
endif
```

```
If (T_3>18,27) and (T_3<21,98) Then
V_air:=0,4717*T_3-8,4233
else
```

```
if(T_3>=21,98) Then
V_air:=1,9444 [m^3/s]
else
V_air:=0,19444[m^3/s]
endif
```

```
endif
```

```
rho_air:=1,225 [kg/m^3]
m_air=rho_air*V_air
```

```
dp_air:= (3,6582*V_air^2 + 3,2504*V_air - 0,3654)/10^3 "[kPa]"
```

```
eta_fan:=0,5
W_fan:=(V_air*dp_air)/eta_fan
```

```
if (T_amb>=6[C]) Then
LMTD := 0,0448*T_3^2 - 2,4286*T_3 + 38,196
else
LMTD := -1,3677*T_3 + 35,041
endif
```

```
Q_LMTD:= U*A*LMTD
```

$Q_{air} = m_{air} \cdot c_p \cdot (T_{exit} - T_{amb})$

$x_3 = 0$

$P_{3t} = P_{sat}(R744; T = T_3)$

$h_3 = \text{enthalpy}(R744; T = T_3; x = x_3)$

$\phi = P_{3t} / P_1$

$\lambda_c = 0,0181 \cdot \phi^2 - 0,1746 \cdot \phi + 1,1078$

$V_{s_c} = 3 \text{ [m}^3/\text{h]}$

$m_c = (V_{s_c} / 3600 \text{ [s/h]}) \cdot \lambda_c / v_1 \cdot 1,18$

$h_{2s} = \text{Enthalpy}(R744; s = s_1; P = P_{3t})$

$\eta_c = -0,0832 \cdot (\phi^2) + 0,3904 \cdot \phi + 0,1247$

$h_{2dis} = h_1 + ((h_{2s} - h_1) / \eta_c)$

$h_2 = h_1 + ((h_{2s} - h_1) / \eta_c) \cdot (1 - Q_{heatloss})$
"Temperature at the inlet of the condenser is calculated with the heat loss from the compressor"

"Temperature at the inlet of the condenser is calculated with the heat loss from the compressor"

$T_2 = \text{Temperature}(R744; h = h_2; P = P_{3t})$

$Q_{cond} = m_c \cdot (h_2 - h_3)$

Repeat

If $(Q_{LMTD} > 0,90 \cdot Q_{air})$ and $(Q_{LMTD} < 1,1 \cdot Q_{air})$ and $(Q_{air} > 0,99 \cdot Q_{cond})$ and $(Q_{air} < 1,01 \cdot Q_{cond})$ and $(Q_{LMTD} > 0,90 \cdot Q_{cond})$ and $(Q_{LMTD} < 1,1 \cdot Q_{cond})$ Then

$T_{exitcorr} = T_{exit}$

$T_{3corr} = T_3$

$T_{exit} = 0,97 \cdot T_3$

$T_3 = 30$

else

if $(T_{exit} > 0,95 \cdot T_3)$ Then

$T_{exit} = 0,97 \cdot T_3$

else

$T_{exit} = T_{exit} + 0,1 \text{ [C]}$

endif

endif

if $(T_{amb} \geq 6 \text{ [C]})$ Then

$LMTD := 0,0448 \cdot T_3^2 - 2,4286 \cdot T_3 + 38,196$

else

$LMTD := -1,3677 \cdot T_3 + 35,041$

endif

$Q_{LMTD} = U \cdot A \cdot LMTD$

$Q_{air} = m_{air} \cdot c_p \cdot (T_{exit} - T_{amb})$

Until $(T_{exit} = 0,97 \cdot T_3)$

Until $(T_3 = 30)$

$T_{diffgc} = T_{3corr} - T_{amb}$


```

if (T_amb>=6[C]) Then
LMTDcorr := 0,0448*T_3corr^2 - 2,4286*T_3corr + 38,196
else
LMTDcorr := -1,3677*T_3corr + 35,041
endif

```

```

Q_LMTDcorr:= U*A*LMTDcorr

```

```

Q_aircorr:=m_air*c_p*(T_exitcorr-T_amb)

```

```

x_3:=0
P_3:=P_sat(R744;T=T_3corr)
h_3:=enthalpy(R744;T=T_3corr;x=x_3)
P_2:=P_3

```

```

phi:=P_3/P_1
lambda_c := 0,0181*phi^2 - 0,1746*phi + 1,1078
Vs_c:=3[m^3/h]
m_c:=((Vs_c/3600[s/h])*lambda_c/v_1)*1,18

```

"Multiply with 1,18 for 60hz"

```

h_2s:=Enthalpy(R744;s=s_1;P=P_3)
eta_c = -0,0832*(phi^2) + 0,3904*phi + 0,1247
h_2dis:=h_1+((h_2s-h_1)/eta_c)
h_2:=h_1+((h_2s-h_1)/eta_c)*(1-Q_heatloss)
T_2:=Temperature(R744;h=h_2;P=P_3)

```

"Outlet enthalpy compressor"

"Inlet enthalpy condenser"

```

h_4:=h_3
h_5:=h_1

```

```

Q_condcorr:=m_c*(h_2-h_3)

```

```

Q_o:=m_c*(h_1-h_3)
W:=(m_c*(h_2dis-h_1))
COP:=Q_o/(W+W_fan)

```

```

endif
end

```

"Test CO2 refrigeration system"

```

T_amb = 35[C]

```

```

Call modification3(T_amb :Q_o;COP;P_1p;P_2p;h_1p;h_2p;h_3p;P_1;P_2;h_1;h_2;h_3;h_4;dT_sub)

```